Doctoral Dissertation

博士論文

Molecular biological studies on the bioactive substances related to bone inflammation

（骨の炎症機構に関わる生理活性物質の分子生物学的研究）

Hisako Hikiji

引地　尚子

CONTENTS

List of abbreviations

ALPase, alkaline phosphatase

BMC/TV, bone mineral content per tissue volume

BMD, bone mineral density

BV/TV, bone volume per tissue volume

cAMP, cyclic adenosine monophosphate

cGMP, cyclic guanosine monophosphate

COX, cyclooxygenase

cPLA$_2\alpha$, cytosolic phospholipase A$_2\alpha$

dNO, Ethanamine, *N*-ethyl-, compound with l,l-diethyl-2-hydroxy-2-nitrosohydrazine

DXA, dual X-ray absorptiometry

ecNOS, endothelial cell nitric oxide synthase,

EIA, enzyme immunoassay

GFP, green fluorescent protein

GPCRs, G-protein coupled receptors

gt, gene trap

GTP, guanosine triphosphate

12-HHT, 12(*S*)-hydroxyheptadeca-5*Z*, 8*E*, 10E-trienoic acid

IL-1ß, Interleukin-1ß

iNOS, inducible nitric oxide synthase

L-NMMA, NG-monomethyl-l-arginine

LTB_4, leukotriene B_4

M-CSF, macrophage colony-stimulating factor

µCT, microcomputed tomography

nNOS, neuronal nitric oxide synthase

NO, nitric oxide

NOS, nitric oxide synthase

O_2^-, superoxide

OGR1, ovarian cancer G-protein-coupled receptor 1

$ONOO^-$, peroxynitrite

PAF, platelet-activating factor

PGE_2, prostaglandin E_2

Pgl, pyrogallol

PLA_2, phospholipase A_2

PTX, pertussis toxin

RANKL, receptor activator of NF-κB ligand

RT-PCR, reverse transcription-polymerase chain reaction

SNAP, *S*-nitroso-acetyl-penicillamine

SNP, sodium nitroprusside

SOD, superoxide dismutase

Tb.N, trabecular number

Tb.Sp, trabecular separation

TDAG8, T-cell death-associated gene 8

TNF-α, tumor necrosis factor-α.

TRAP, tartrate-resistant acid phosphatase

WT, wild-type

Abstract

Bone is a living hard tissue. Bone tissue is constantly remodeled to maintain bone homeostasis. I have investigated and elucidated some inflammatory mechanisms of bone. The results of this investigation are divided into three chapters, as follows:

Chapter 1: Nitric oxide and bone

I have examined the effects of nitric oxide (NO) on osteoblastic differentiation in mouse osteoblast-like cells (Part 1).

The results showed that gene expression of inducible NO synthase (NOS) is increased in response to inflammatory cytokines, TNF-α and IL-1β. However, the expression of constitutive NOS was not increased. NO production was increased in response to TNF-α and IL-1β, and suppressed by the NOS inhibitor, NG-monomethyl-l-arginine (L-NMMA). Conversely, alkaline phosphatase (ALP) activity decreased in response to tumor necrosis factor-α (TNF-α) and Interleukin-1β (IL-1β), and their gene expression was not restored by L-NMMA treatment. Furthermore, ALP activity and osteocalcin gene expression were increased in response to NO donors, nitroprusside sodium or ethanamine, and N-ethyl-, compound with 1,1-diethyl-2-hydroxy-2-nitrosohydrazine. These results suggest that osteoblastic differentiation is promoted by

NO, but the inhibition of ALP by cytokines does not occur via NO. This is the first study to show that NO itself promotes osteoblastic differentiation (Part 1).

Next, I sought to demonstrate that peroxynitrite ($ONOO^-$), when both NO and superoxide are simultaneously generated, would exceed the stimulatory effect of NO on the osteoblastic activity and inhibit osteoblastic differentiation (Part 2).

Chapter 2: Bone and bioactive lipids

Prostaglandins (PG) and NO are well-known inflammatory, bioactive molecules, and the synthetases of these molecules are cyclooxygenase (COX) and NOS, respectively. NOS regulates the expression of COX by producing NO. Generally, bioactive lipids, including PGs, are inflammatory molecules. However, the role of these molecules, apart from PGE_2, has not been studied in the context of bone metabolism. Herein, I have demonstrated that leukotriene B_4 (LTB_4) increases bone resorption through BLT1, the LTB_4 receptor.

Using bone morphometry, I have shown that bone resorption is remarkably attenuated in BLT1-deficient mice. Furthermore, bone resorption is attenuated in osteoclasts derived from BLT1-deficient mice compared with those from the wild-type mice. Moreover, I have demonstrated that LTB_4 changes the morphology of osteoclasts

derived from wild-type mice via the BLT1-Gi protein-Rac1 signaling pathway. These results suggest that osteoclasts are activated and bone resorption is enhanced, largely because of LTB_4/BLTI binding.

Chapter 3: Bone and G-protein coupled receptors

Osteoclasts produce acids that dissolve the bone matrix. However, the function of proton-sensing receptors in bone metabolism is not well understood. Most bioactive lipid receptors are G-protein coupled receptors (GPCRs). Performing phylogenetic analysis of GPCRs, I found that the T-cell death-associated gene 8 (TDAG8), a proton-sensing GPCR, participates in bone resorption.

I have shown, using bone morphometry, that bone resorption is exacerbated in TDAG8-deficient mice. In addition, calcium absorption is higher in osteoclasts derived from TDAG8-deficient mice than in those from the wild-type mice. TDAG8-Rho signal-dependent morphological changes in an acidic environment did not occur in osteoclasts derived from TDAG8-deficient mice. These results suggest that TDAG8 inhibits bone resorption caused by inflammation.

Taken together, I investigated several molecules which play certain roles in bone inflammation, and showed the stepping stone to treat inflammatory diseases.

General introduction

While bone is a hard and rigid tissue, it is not static. Bone tissue is constantly remodeled to maintain the skeletal structure of an organism (*1*). It is difficult to study hard tissue histologically because of its rigidity. However, bone as a living tissue is a fascinating subject for biological researchers to investigate; bone cells regulate bone metabolism and communicate with other bone cells and bone marrow immune cells (*2*). These cells share a variety of bioactive molecules and form the skeletal and immune systems (*3*). Among these common bioactive molecules, nitric oxide (NO) (*4*) and bioactive lipid molecules (*5*) play important roles in inflammation. I have investigated the role of these inflammatory molecules and molecules associated with these compounds in bone metabolism and present the results of these investigations.

NO, a gas that regulates intracellular signaling pathways in cells, is primarily recognized as an important component of the vasculature, which contributes to a short-term decrease in blood pressure (*6*). NO also plays various roles in many tissues other than vascular tissues (*7*). Herein, I present the role of NO in bone metabolism.

NO is endogenously produced from L-arginine by nitric oxide synthase (NOS). Three isoforms of NOS are isolated. Two constitutive isozymes; endothelial cell (ecNOS) and neuronal (nNOS) types which produce less amount of NO with several

physical/chemical stimuli. On the other hand, inducible isoform (iNOS) yields larger amount of NO through *de novo* synthesis of the enzyme stimulated by proinflammatory cytokines or bacterial endotoxin. I present the role of the constitutive isoform ecNOS, as well as iNOS that produces NO, in response to proinflammatory cytokines during bone metabolism.

Many lipids function as bioactive molecules, including prostanoids, leukotrienes (LTs), platelet-activating factor, and endocannabinoids. Arachidonic acid is an essential molecule, located among the fatty acids in the plasma membrane. Phospholipase A_2 (PLA_2) enzymes produce arachidonic acid by hydrolyzing membrane glycerophospholipids, which are then metabolized to prostanoids and LTs. Prostaglandin E_2 (PGE_2) is one of the most well-known prostanoids involved in bone remodeling, and it has been linked to many bone-resorptive diseases (*5*). However, little is known about the role of LTs in bone metabolism compared with prostanoids (*5*). I have investigated the role of LTB_4, one of the most important LTs in bone metabolism and present the results of the investigation.

Most bioactive lipid receptors are G-protein coupled receptors (GPCRs, (*8*). Among the many GPCRs, I examined the proton-sensing GPCR, T-cell death-associated gene 8 (TDAG8). Protons play a role in bone resorption, as osteoclasts actively excrete protons

to dissolve hydroxyapatite minerals in the bone matrix (*9*). I propose that TDAG8 inhibits bone resorption as a means of maintaining bone homeostasis.

Chapter 1

Nitric oxide and bone

Part 1

Direct action of nitric oxide on osteoblastic differentiation

Abstract

The effect of nitric oxide (NO) on osteoblastic differentiation was examined in cultured mouse osteoblasts. Interleukin-1β and tumor necrosis factor-α expressed inducible NO synthase gene with little effect on constitutive NO synthase gene. These cytokines increased NO production, which was inhibited by L-NMMA pretreatment, and decreased alkaline phosphatase (ALPase) activity, which was not restored by L-NMA. Furthermore, NO donors, sodium nitroprusside and dNO dose-dependently elevated ALPase activity and expression of osteocalcin gene. These results suggest that NO directly facilitates osteoblastic differentiation and the cytokine-induced inhibition of ALPase activity is mediated via mechanism other than NO.

Introduction

Nitric oxide (NO) is involved in various pathophysiological processes in many tissues (*7*) and is produced from L-arginine by nitric oxide synthase (NOS). So far, three isoforms of NOS are isolated. Two constitutive isozymes; endothelial cell (ecNOS) and neuronal (nNOS) types which produce less amount of NO with several physical/chemical stimuli, while inducible isoform (iNOS) yields larger amount of NO through *de novo* synthesis of the enzyme in response to proinflammatory cytokines or bacterial endotoxin (*7*).

Osteoblasts have been reported to produce NO after induction of iNOS gene by cytokines (*10, 11*), and NO may inhibit the bone-resorbing activity in adjacent osteoclasts (*11, 12*), suggesting a cross-talk between osteoblast and osteoclast via NO. Nevertheless, the role of NO in osteoblasts is still obscure. The purpose of the present study was addressed to examine whether (1) mouse osteoblast expresses constitutive (endothelial cell type) and/or inducible NOS gene, (2) these genes actually increase NO production and (3) NO actively affects the osteoblastic differentiation, with using four parameters, alkaline phosphatase (ALPase) activity and cGMP levels in osteoblasts, an expression of osteocalcin gene and PGE_2 synthesis in culture medium.

Materials and methods

Cell culture

Primary cultures of mouse osteoblasts were prepared from 1-day-old ddy mouse calvaria as described previously (*13*). Isolated cells were grown in αMEM (Gibco, Grand Island, NY, USA) containing 10% fetal bovine serum (Bioserum, Victoria, Australia), penicillin, streptomycin and amphotericin B (Sigma, St. Louis, MO, USA). When indicated, NG-monomethyl-l-arginine (L-NMMA, Wako, Osaka, Japan, 10^{-4} M) was applied to the culture medium 4 days before and throughout cytokine stimulation described below.

Reverse transcription-polymerase chain reaction

Each NOS message was detected using RT-PCR as described previously (*14*). Total RNA was extracted, and the reverse transcribed NA was used as a template for PCR. The primer sequences for NOS were: upper, 5' -GGCATCACCAGGAAGAAGAC (1516-1535); and lower, 5'-ACTGGACTCCTTCCTCTTCC (1953-1934) (*14*). The primer sequences for iNOS were: upper, 5' -GG A A AAGGA-C ATT A AC AACA A (244-264); and lower, 5'-ATGTACCAGC-CATTGAAGGGG (1287-1267) (*15*).

DNO (Cayman Chemical, Ann Arbor, MI, USA) was applied to osteoblasts for 48 h

and the total RNA was extracted and used for detection of osteocalcin message. The primer sequences for osteocalcin were: upper, 5' - AT GAGG ACCCT CT C-TCTGCT (49-69); and lower, 5 '-CCGTAGATGCGTTTGTAGGC (325-305) (*16*).

The denaturing, annealing and elongating conditions for the PCR reaction was 94, 56, and 72°C respectively for a total of 25 cycles, 94, 55, and 72°C for a total of 30 cycles, 94, 55, and 72°C for a total of 35 cycles with an initial 5 min denaturation and an additional 10min (7 mm for osteocalcin) extension step at 72°C for ecNOS, iNOS and osteocalcin, respectively. The reaction products were separated by gel electrophoresis and stained in ethidium bromide.

Assays of nitrate/nitrite, cGMP, ALPase and prostaglandin E_2 (PGE_2)

NO was measured as nitrate/nitrite products in medium 48 h after the incubation with or without recombinant tumor necrosis factor-α (TNF-α, 100 ng/ml, Dainippon Pharmaceutical, Tokyo, Japan) and/or interleukin-1ß (IL-1ß, Cambridge, MA, USA). Nitrate was converted to nitrite with nitrate reductase, then Griess reagent was applied for spectrophotometry measurement at 540 nm(*17*). Nitrite level was normalized with protein amount measured by Bradford's method (Bio-Rad, Germany).

NO action was verified with measurement of cGMP with or without addition of an

NO donor, sodium nitroprusside (SNP, Wako). For cGMP assay, confluent cells were preincubated at 37°C for 20 min then with 0.1 mM 3-isobutyl-1-methylxanthine (Wako) for 6 min. After 2 min of administration of SNP, incubation was terminated with ice-cold 10% trichloroacetic acid. cGMP levels were determined using a EIA kit (Cayman Chemical).

In bone tissues, the expression of ALPase is closely associated with osteoblastic differentiation (*18*). Osteoblasts applied SNP for 5 h or cytokines for 48 h were washed twice with phosphate-buffered saline and then lysed in 0.1% Triton X-100. An a aliquot of homogenate after three cycles of freezing and thawing was assayed for ALPase activity (Wako, Osaka). The content of PGE_2 in culture media of the osteoblasts were measured using a EIA kit (Cayman Chemical).

Statistics

All values were expressed as the mean ± SE. Statistical differences between the values were examined by one-way ANOVA for multiple comparisons followed by Fisher's test. The p values less than 0.05 were considered significant.

Results

Induction of mRNA of iNOS and ecNOS by cytokines

I used RT-PCR to define the isoforms of NOS specifically expressed in mouse osteoblasts (Fig. 1). iNOS mRNA was not detected in unstimulated cells or cells treated with TNF-α (100 ng/ml) alone. In contrast, IL-1ß (10 ng/ml) and combinations of two cytokines (TNF-α + IL-1ß) induced the iNOS mRNA expression (a 1044-bp PCR product in Fig.1). In contrast, ecNOS mRNA was detected in both unstimulated and stimulated osteoblasts (a 526-bp PCR product in Fig. 1). These data suggest that iNOS gene was exclusively induced by IL-1ß, but not by TNF-α alone, while ecNOS gene was constitutively expressed, irrespective of the stimulation with these cytokines.

Modulation of NO production and ALPase activity with cytokines

Without cytokine, mouse osteoblasts released a modest but steady amount of NO detected as nitrate/nitrite (25.7 ± 5. 5 nmol/mg protein, Fig. 2). TNF-α (100 ng/ml) alone had no effect on the basal release (25.0 ± 5.0 nmol/mg protein). In contrast, IL-1ß (10 ng/ml) increased the NO production to 46.6 ± 5.3 nmol/mg protein ($p < 0.02$, vs. control). Combination of TNF-α and IL-lß enhanced the NO production three folds over the control level (70.7 ± 7.2 nmol/mg protein, $p < 0.0001$, vs. control), indicating that

synergistically increased NO production with TNF-α via NOS induction. The increased NO production by combination of TNF-α plus IL-1ß was attenuated by a competitive NOS inhibitor, L-NMMA (10^{-4} M, Fig. 3A), and decreased from 75.9 ± 2.6 nmol/mg protein to 36.1 ± 2.6 nmol/mg protein ($p < 0.05$, vs. TNF-α + IL-1ß).

Combination of TNF-α and IL-1ß reduced ALPase activity in osteoblasts (77.4 ± 4.6 vs. 56.6 ± 2.7 nmol/min per mg protein). These results are compatible with the previous reports that TNF-α and/or IL-1ß possess bone-resorbing action(*19, 20*). However, L-NMMA did not restore the reduced level of ALPase by these cytokines at a11 (54.9 ± 2.6 nmol/min per mg protein, Fig. 3B). These results indicate that the bone-resorbing effect of cytokines is not mediated via NO, despite of cytokine induction of iNOS gene and the actual NO production.

Effect of NO donors on biosynthesis of cGMP, ALPase activity and PGE_2 production, and osteocalcin gene expression

To examine the direct effect of NO on osteoblasts, I used the NO donor, SNP or dNO (*21*), Two-minute incubation of SNP (> 10^{-4} M) increased intracellular cGMP level in concentration-dependent manner (Fig. 4A).

This result confirms my previous report that NO has an autocrine action on the NO

producing cells themselves, as well as adjacent cells via paracrine action(*22, 23*).

Osteoblasts treated with SNP for 5 h, did elevate ALPase activity in a concentration-dependent manner (Fig. 4B), exhibiting a clear contrast with the reduction of the activity in cytokine-stimulated osteoblasts (Fig. 3B). In response to SNP, the level of PGE_2 in culture medium decreased in a concentration-dependent manner (Fig. 4C). The SNP concentrations necessary for 50% increment for cGMP synthesis and ALPase activity were 10^{-4} M and 10^{-8} M, respectively.

The expression of osteocalcin mRNA was enhanced in osteoblasts when they were treated by a long-lasting NO donor, dNO, for 48 h more than untreated osteoblasts (a 276-bp PCR product in Fig. 5).

Discussion

Rat osteosarcoma cells have been reported to express nNOS (*24*). However, the expression of ecNOS in osteoblasts have not been reported thus far. I have found that mouse osteoblasts express ecNOS gene constitutively and iNOS gene only after cytokine stimulation. I have also found ecNOS and iNOS in human osteosarcoma cells (data not shown). Furthermore, homogeneous staining was observed in mouse-osteoblast culture with specific antibody against ecNOS (data not shown). These results show that ecNOS expresses in mouse osteoblasts at both mRNA and protein level. The cytokine-induced NO production was inhibited by L-NMMA. These cytokines also decreased osteoblastic differentiation in terms of reduction of ALPase activity without restoration by L-NMMA. Present results were totally different from the previous report by Hukkanen et al. (*10*) in the aspect of L-NMMA action on cytokine-induced ALPase activity and accordingly give rise to an argument against the scheme that NO facilitates osteoblastic differentiation.

The role of steady ecNOS gene expression and low but significant concentrations of NO produced in unstimulated cells (Fig. 2) has not been noticed so far. Low concentrations of NO produced by ecNOS may control the basal metabolism of osteoblasts. In addition to the basal synthesis of NO by ecNOS, large amount of NO

may have been produced by iNOS after the induction by IL-1ß and TNF-α+IL-lß (Figs. 2 and 3A). This situation will take place in the setting of inflammatory response of osteoblastic metabolism. iNOS is not an only gene induced by IL-1ß and/or TNF-α in osteoblasts. IL-1ß induces cyclic AMP production in human osteoblasts (*25*), TNF-α also promotes the expression of prostaglandin endoperoxide synthase-2 mRNA and synthesis of PGE_2 (*26*). In other tissues, such as vascular tissues, the condition which evokes NO simultaneously produces superoxide anion (O_2^-) to form peroxynitrite ($ONOO^-$) (*27*). There is no evidence that the cytokine-induced NO has direct action on bone resorption.

Accordingly, it is of a great significance to know the direct effect of NO on osteoblasts. An NO donor, SNP, increased the ALPase activity, which is the index of osteoblastic differentiation, in a concentration-dependent manner. It also increased the intracellular concentration of cGMP, which is the second messenger of NO as well as the activator of the osteoblastic differentiation(*28, 29*), The long-lasting NO donor, dNO, increased the gene expression of osteocalcin, which is the another index of osteoblastic differentiation(*30, 31*). On the contrary, it decreased the levels of PGE_2 in medium. Prostaglandins are multifunctional regulators with stimulatory and inhibitory effects on bone metabolism (*32*). At low concentrations, PGE_2 increased

collagen synthesis in cultured fetal rat calvaria, whereas at high concentrations, the major effect was inhibitory. However, as to the osteoblastic differentiation, PGE_2 is reported to be inhibitory (*33*). Present findings indicate that NO acts on osteoblastic differentiation and suggest that NO inhibits bone resorption through PGE_2 production by osteoblasts.

SNP below 10^{-4} M changed the levels of both ALPase activity and PGE_2 in medium, while the same agent above 10^{-4} M raised the intracellular concentration of cGMP, the second messenger of NO. These results suggest that the effect of NO on osteoblastic differentiation is mediated by both cGMP-dependent and independent mechanisms. Actually, NO action is not simply cGMP-dependent, and cGMP-independent pathway also plays significant role on platelets, fibroblasts and osteoclasts (*12, 34, 35*).

In conclusion, I have demonstrated that NO directly facilitates osteoblastic differentiation and that it is not responsible for the action of cytokine-induced bone resorption. I have also shown evidence that osteoblasts have ecNOS which may control the basal level of osteoblastic differentiation.

Legends

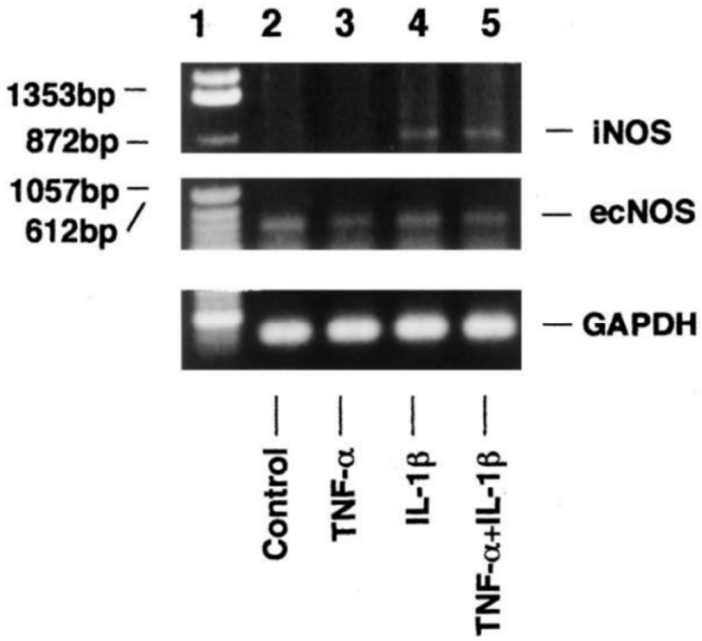

Fig. 1. Expression of iNOS, ecNOS and GAPDH mRNA in unstimulated cells or cells stimulated with several factors. Isolated mRNA was reverse transcribed and amplified by PCR. The PCR product showed the 526-bp and 1044-bp for ecNOS for iNOS of predicted size, respectively.

Lanes: 1, DNA size markers; 2, unstimulated osteoblasts; 3, TNF-α-treated cells; 4, IL-lß-treated cells; 5, TNF-α plus IL-lß-treated cells.

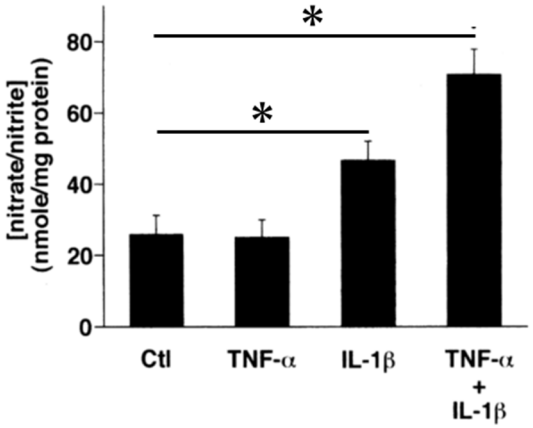

(*: p<0.02 vs Ctl, N=12)

Fig. 2. Stimulatory effects of TNF-α and IL-1ß on NO production, measured as nitrate/nitrite in osteoblasts (mean ± SE, n = 12). * indicates a significant difference ($p < 0.02$), compared with the control (Ctl).

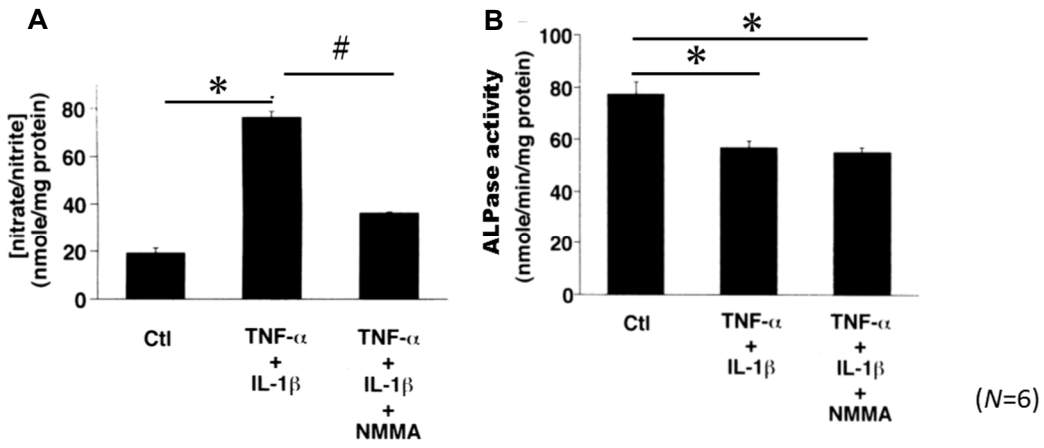

(*: p<0.001 vs control(Ctl), #: p<0.001 vs TNF-α+IL-1β)

Fig. 3. Inhibitory effect of L-NMMA on NO production (A) and alkaline phosphatase (ALP) activity in culture medium (B). * and # indicate a significant difference (p < 0.001), compared with the control and condition stimulated by TNF-α plus IL-1ß (5, respectively. Each value denotes the mean ± SE (n = 6).

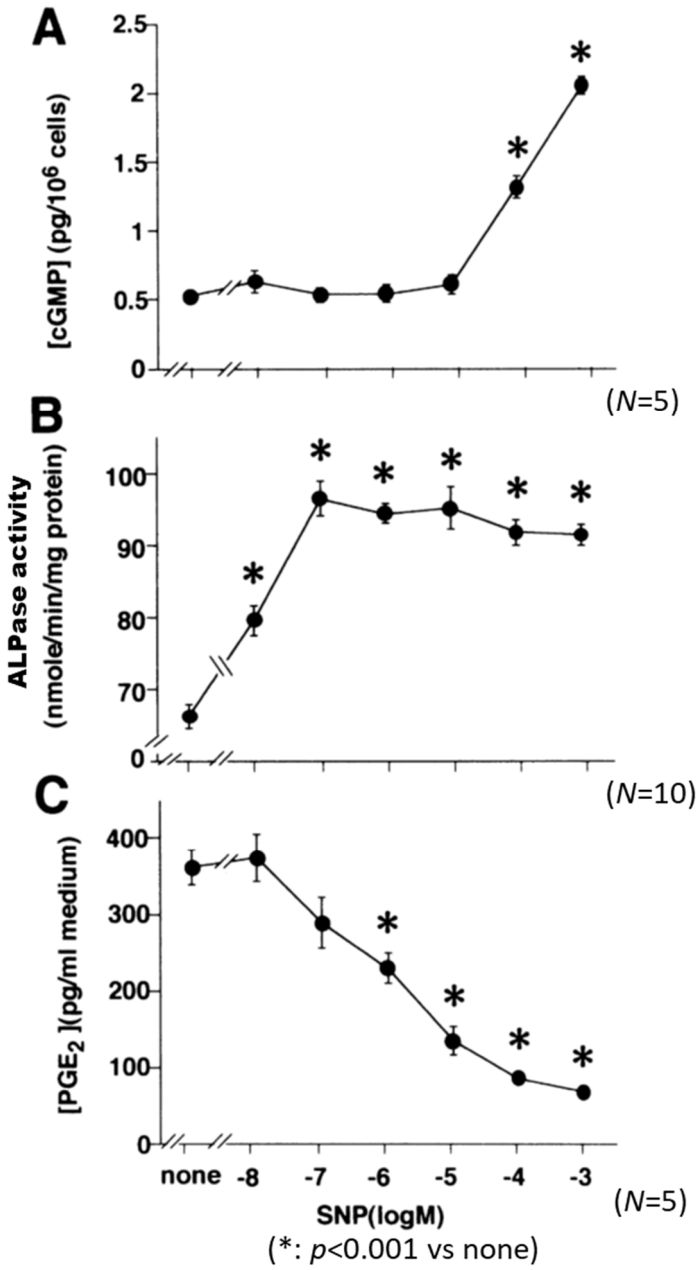

Fig. 4. Effects of SNP on cGMP levels (mean ± SE, n = 5) (A), alkaline phosphatase (ALP) activity (mean ± SE, n = 10) (B), and PGE_2 production (mean ± SE, n = 5) (C) in osteoblasts. * denotes a significant difference ($p < 0.001$), compared with the control.

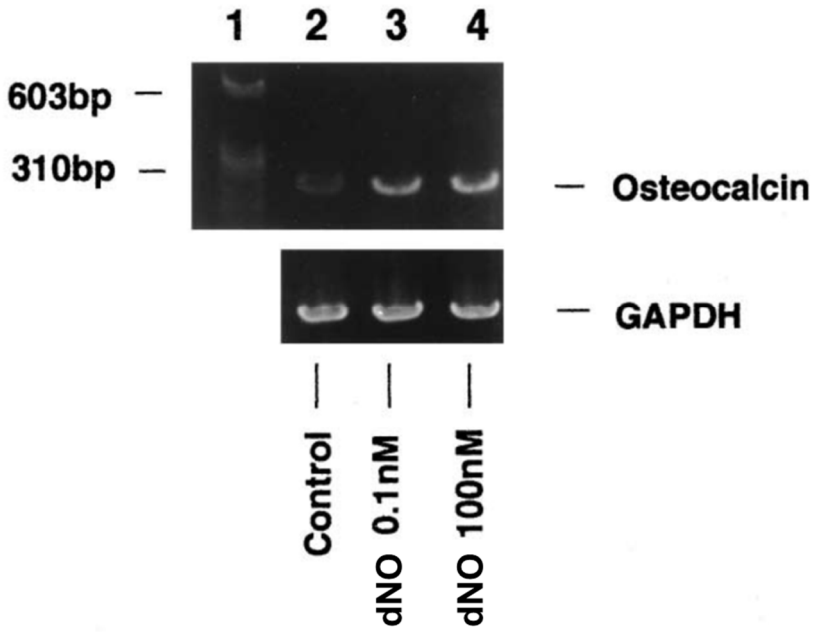

Fig. 5. Expression of osteocalcin and GAPDH mRNA in unstimulated cells or cells stimulated with dNO. Isolated mRNA was reverse transcribed and amplified by PCR. The PCR product was 276 bp. Lanes: 1, DNA size markers; 2, unstimulated osteoblasts; 3, 0.1 nM dNO-treated cells; 4, 100 nM dNO-treated cells.

Part 2

Peroxynitrite production by TNF-α and IL-1ß:

implication for suppression of osteoblastic differentiation

Abstract

To determine the roles of nitric oxide (NO) and its metabolite, peroxynitrite ($ONOO^-$), on osteoblastic activation, I investigated the effects of a NO donor [ethanamine, 2,2'-(hydroxynitrosohydrazono)bis-(dNO)], an O_2^- donor (pyrogallol), and an $ONOO^-$ scavenger (urate) on alkaline phosphatase (ALPase) activity and osteocalcin gene expression, which are indexes of osteoblastic differentiation. dNO elevated ALPase activity in the osteogenic MC3T3-E1 cell line. The combination of dNO and pyrogallol reduced both ALPase activity and osteocalcin gene expression. Because both indexes were recovered by urate, $ONOO^-$, unlike NO itself, inhibited the osteoblastic differentiation. Furthermore, treatment with a combination of the proinflammatory cytokines tumor necrosis factor-α (TNF-α) and interleukin-1ß (IL-1ß) was found to yield $ONOO^-$ as well as NO and O_2^-. The reductions in ALPase activity and osteocalcin gene expression were also restored by urate. I conclude that $ONOO^-$ produced by TNF-α and IL-1ß, but not NO per se, would overcome the stimulatory effect of NO on osteoblastic activity and inhibit osteoblastic differentiation.

Introduction

Peroxynitrite ($ONOO^-$), a potent oxidant produced by the rapid reaction between nitric oxide (NO) and superoxide (O_2^-), is formed in an inflammatory response and causes a variety of toxic effects, including lipid peroxidation and tyrosine nitration, on several biomolecules (*36*). Activated macrophages are reported to synthesize a significant amount of $ONOO^-$ when both NO and O_2^- are simultaneously generated (*37*). In vascular tissues, $ONOO^-$ may cause oxidant injury in endothelium (*27*).
In these tissues, NO and O_2^- themselves may react with other biomolecules, raising questions about their actual toxicities per se.

Little is known about the effects of NO, O_2^-, and $ONOO^-$ on bone-forming activity in osteoblasts. I have previously demonstrated that NO stimulates differentiation in primary osteoblasts (*38*). In brief, the NO donor sodium nitroprusside (SNP) elevated alkaline phosphatase (ALPase) activity, osteocalcin gene expression, and cGMP production and reduced PGE_2 production. Furthermore, the lowering effect of ALPase activity by cytokines was not caused by cytokine-induced NO, but rather by another product. ALPase is a membrane-bound enzyme that is abundant in many tissues. A high level of ALPase is found in preosteoblasts in bones. From its pattern of gene expression, ALPase is known to be an early differentiation marker during the

formation of bone (*39*). Osteocalcin, which is synthesized by osteoblasts, is present in bone matrix and osteoblasts and is known to be a differentiation marker at a later stage (*39*). Therefore, ALPase and osteocalcin are the most commonly used indexes of osteoblastic differentiation. Neither the production of O_2^- in osteoblasts nor the action of $ONOO^-$ on osteoblasts has been examined thus far. The purpose of the present chapter was to clarify the role of $ONOO^-$ in osteoblastic activity. Therefore, I have first examined the effects of $ONOO^-$ on ALPase activity as well as on osteocalcin gene expression, the most reliable indexes of osteoblastic differentiation, using both NO and O_2^- donors that produce $ONOO^-$ (*38, 39*).

The proinflammatory cytokines, which include tumor necrosis factor-α (TNF-α) and interleukin-Iß (IL-1ß), are known to enhance bone resorption (*19, 20, 40*). I have shown that the bone-resorbing effect of cytokines is not mediated via NO *per se*, despite the fact that cytokines induce the inducible nitric oxide synthase (iNOS) gene and actual NO production in mouse osteoblasts (*38*). To analyze the role of NO, O_2^-, and $ONOO^-$ in cytokine-stimulated osteoblasts, I then studied whether these cytokines actually stimulate the simultaneous generation of NO and O_2^- and whether the generated NO and O_2^- may develop an even more toxic product, $ONOO^-$, which would then modify osteoblastic differentiation.

Materials and methods

Cell culture

MC3T3-E1 mouse clonal osteogenic cells (a generous gift from Prof. S. Yamamoto, Oh-u University, Japan) were grown in αMEM (GIBCO, Grand Island, NY) containing 10% fetal bovine serum (Bioserum, Victoria, Australia), penicillin, streptomycin, and amphotericin B (Sigma, St. Louis, MO). The medium was changed every 2-3 days. Conditioned media used during the last 48 h of incubation were collected for the nitrate/nitrite assay. Cellular confluence was maintained throughout all treatment procedures.

Assays of nitrate/nitrite and ALPase in MC3T3-E1 cells

NO was measured as nitrate/nitrite products in the medium after 48 h of incubation with or without recombinant TNF-α (10 ng/ml, Dainippon Pharmaceutical, Tokyo, Japan) and/or IL-1ß (10 ng/ml, Genzyme, Cambridge, MA). Nitrate in the sample was converted to nitrite with nitrate reductase and then measured by spectrophotometry after Griess reaction (*17*). Nitrite levels were normalized by protein amount measured by Bradford's method (Bio-Rad Laboratories, Hercules, CA). The level of ALPase expression in bone tissues is closely associated with osteoblastic differentiation (*38, 39*).

Osteoblasts exposed to ethanamine, 2,2'-(hydroxynitrosohydrazono)-bis- [(dNO), Cayman Chemical, Ann Arbor, MI] or cytokines for 48 h were washed twice with PBS and then lysed in 0.1% Triton X-100. After three cycles of freezing and thawing, an aliquot of homogenate was assayed for ALPase activity using Alkaline phosphatase labeling kit (Wako Pure Chemical Industries, Osaka, Japan). Pyrogallol [(Pgl), Wako Pure Chemical Industries] was applied in the presence of 100 U/ml catalase (Sigma) to degrade the hydrogen peroxide formed from the dismutation of O_2^-.

O_2^- release assay in MC3T3-E1 cells

The amount of O_2^- released into the supernatant was assayed by measuring the reduction of ferricytochrome c, as described previously (*41*). MC3T3-E1 cells were cultured in 24-well Falcon plates (Lincoln Park, NJ). Ferricytochrome c (final concentration, 70 μM/l, Sigma) was added to the buffer (*41*) at room temperature and incubated for 60 min at 37°C in the presence or absence of superoxide dismutase [(SOD), final concentration 350 U/ml]. The reduction in ferricytochrome cwas measured by spectrophotometry (V-530, JASCO, Tokyo, Japan). The amount of O_2^- release was calculated from the difference in absorbance with or without SOD divided by the extinction coefficient for the change of ferricytochrome c to ferrocytochrome c ($E_{550\ nM}$ =

21.0 $mM^{-1} \cdot cm^{-1}$). The results are expressed as picomoles per hour per well.

Reverse transcription-polymerase chain reaction

The osteocalcin message was detected with reverse transcription-polymerase chain reaction (RT-PCR). dNO in the presence or absence of Pgl and urate (Wako Pure Chemical Industries) was applied to osteoblasts for 48 h, total RNA was extracted, and the reverse-transcribed cDNA was severed for the template of PCR (*38*). The primer sequences for the osteocalcin gene were (upper), 5 CCTCTCTCTGCTCACTCTGC (57 76) and (lower), 5'GGGCAGCACAGGTCCTAAAT (350 331). The denaturing, annealing, and elongating conditions for the PCR reaction were 94, 55, and 72°C, respectively, for a total of 35 cycles with an initial 9-min denaturation and an additional 7-min extension step at 72°C for osteocalcin. The reaction products were separated by gel electrophoresis and stained in ethidium bromide. In another experiment, TNF-α and IL-1ß in the presence or absence of Cu, Zn-SOD (100 U/ml, Sigma) were applied to the osteoblasts for 48 h. Thereafter, the same procedure was performed for RT-PCR experiments.

Nitrotyrosine immunocytochemistry

MC3T3-E1 cells were incubated on 8-well chamber slides (LAB-TEKII, Nalge Nunc International, Naperville, IL). Medium, with or without cytokines, was exchanged and cultured for another 48 h. After fixation with an ethanol-acetone mixture, the cells were treated with anti-nitrotyrosine polyclonal rabbit antibody (Upstate Biotech, Lake Placid, NY) at room temperature for 3 h. The cells were then treated with the biotinylated goat anti-rabbit and the avidin-biotin peroxidase complex (Vectastain Elite ABC kit, Vector Laboratories, Burlingame, CA). The immunoproduct was visualized by 3,3'-diaminobenzidine, as described previously (*42*), and photographed with a microscope (BH-2, Olympus, Tokyo, Japan). The level of staining intensity was measured by densitometry with a graphic software application (Adobe Photoshop, CS3, Adobe Systems, Mountain View, CA).

Statistics

All values are expressed as means ± SE. Statistical differences between the values were examined by one-way ANOVA for multiple comparisons and then Fisher's test. The unpaired *t*-test was used to examine statistical differences between two groups. p values <0.05 were considered significant.

Results

Effects of a NO donor on the expression of ALPase activity with or without C2

The NO donor dNO was used to examine the direct effect of NO on osteoblasts (*43*). MC3T3-E1 cells treated with dNO for 48 h exhibited ALPase activity that increased in a concentration-dependent manner (Fig. 1). This result indicates that NO directly facilitates osteoblastic differentiation. dNO (10^{-4} M) increased ALPase activity from the control level (308.4 ± 11.1 nmol·min^{-1}·mg protein^{-1}) to 365.0 ± 16.6 nmol·min^{-1}·mg protein^{-1} (Fig. 2). The combination of dNO (10^{-4} M) and the O_2^- donor Pgl [10^{-4} M, (*44*)] reduced ALPase activity to 216.0 ± 8.9 nmol·min^{-1}·mg protein^{-1}. The inhibitory effect of dNO plus Pgl was attenuated in the presence of the $ONOO^-$ scavenger urate [10^{-4} M, (*36, 44*)]. These results suggest that the $ONOO^-$ formed from NO and O_2^- counter-acts the effect of NO alone on ALPase activity in osteoblasts.

Effects of a NO donor on osteocalcin gene expression with or without O_2^-

Osteocalcin mRNA was constitutively expressed in untreated MC3T3-E1 cells (Fig. 3). A similar level of expression was observed in cells treated with dNO for 48 h. The gene expression was reduced when the cells were treated with a combination of dNO and Pgl (10^{-4} M). The inhibitory effect of dNO plus Pgl was reversed by urate (10^{-4} M),

indicating that the $ONOO^-$ formed from NO and O_2^- inhibited osteocalcin gene expression in osteoblasts.

Effects of cytokines on NO and O_2^- production and ALPase activity

Unstimulated MC3T3-E1 cells released a basal amount of NO detected as nitrate/nitrite (3.1 ± 0.6 nmol/mg protein, Fig. 4 A). TNF-α (10 ng/ml) and IL-1ß (10 ng/ml) increased NO production to 59.5 ± 2.7 nmol/mg protein ($p < 0.005$ vs. control) and 123.4 ± 4.5 nmol/mg protein ($p < 0.0001$ vs. control), respectively. Combined TNF-α and IL-1ß markedly enhanced NO production to 432.2 ± 29.9 nmol/mg protein ($p < 0.0001$ vs. control, TNF-α alone, or IL-1ß alone), indicating the existence of a synergistic interaction between the two cytokines. This increased NO production was attenuated by N^G-monomethyl-l-arginine (L-NMMA) (10^{-4} M) pretreatment to 259.8 ± 9.2 nmol/mg protein ($p < 0.0001$ vs. TNF-α + IL-1ß, Fig. 4A). TNF-α, IL-1ß, and combined TNF-α and IL-1ß reduced ALPase activity in osteoblasts from the control level of 300.3 ± 21.2 nmol·min^{-1}·mg $protein^{-1}$ to 77.8 ± 7.6, 73.5 ± 3.6, and 47.7 ± 2.0 nmol·min^{-1}·mg $protein^{-1}$, respectively (Fig. 4B). However, L-NMMA did not reverse the cytokine-induced ALPase reduction (52.1 ± 1.5 nmol·min^{-1}·mg $protein^{-1}$). The reduction in ALPase activity by cytokines exhibited a clear contrast with the

increase in ALPase activity by dNO (Fig. 1). Thus the decrease in ALPase activity caused by cytokines might not be due to the production of cytokine-induced NO, which is compatible with my previous findings in mouse primary osteoblasts (*38*).

O_2^- was not detected in MC3T3-E1 cells before stimulation by the cytokines (Fig. 5). Administration of TNF-α (10 ng/ml) or IL-1ß (10 ng/ml) alone did not stimulate the cells to produce O_2^-. Combined TNF-α and IL-1ß induced a significant amount of O_2^- production (293.8 ± 48.5 pmol·h^{-1}·$well^{-1}$, $p < 0.0002$). Any cytokine or NO/ O_2^- donor at the concentrations used in this study did not affect cell viability with respect to cell number, trypan blue exclusion, and the reduction of 3-(4,5-dimethylthiazol-2-yl)-2,5-diphenyltetrazolium bromide (data not shown).

Effects of SOD on cytokine-induced reduction of ALPase activity and osteocalcin gene expression

Cytokine treatment reduced ALPase activity from 301.7 ± 7.3 to 68.7 ± 1.6 nmol·min^{-1}·mg $protein^{-1}$ ($p < 0.0001$, Fig. 6). SOD partly reversed the reduction of cytokineinduced ALPase activity to 84.9 ± 3.6 nmol·min^{-1}·mg $protein^{-1}$ ($p < 0.02$, Fig. 6). Urate restored more significantly the decrease in cytokine-induced ALPase activity (205.0 ± 13.3 nmol·min^{-1}·mg $protein^{-1}$). RT-PCR demonstrated that coadministration of

TNF-α and IL-1ß reduced the gene expression of osteocalcin from the control level; SOD reversed the reduced gene expression of osteocalcin (Fig. 7).

Immunodetection of $ONOO^-$ by use of anti-nitrotyrosine antibody

The action of $ONOO^-$ can be detected by the measurement of nitrotyrosine, which represents nitrosylation of cellular protein by $ONOO^-$ (*45*). Nitrotyrosine residues on protein are stable markers of $ONOO^-$ synthesis (*36, 45*). MC3T3-E1 cells showed weak nitrotyrosine expression without the addition of any chemical (Fig. 8). The combined effect of NO and O_2^- produced by dNO and Pgl elevated the level of nitrotyrosine (Fig. 8). These results directly indicate that the administration of NO and O_2^- produced $ONOO^-$.

TNF-α (10 ng/ml) or IL-1ß (10 ng/ml) alone did not increase nitrotyrosine production (Fig. 9), whereas combined TNF-α and IL-1ß enhanced the production of nitrotyrosine. These data suggest that osteoblasts stimulated with TNF-α and IL-1ß produce more $ONOO^-$ than untreated or single cytokine-treated cells.

Discussion

NO has significant effects on bone metabolism (*46*). I have previously demonstrated that NO directly facilitated osteoblastic differentiation and that it was not responsible for the cytokine-induced inhibition of osteoblastic activity in mouse primary culture (*38*). What is the cause of the inhibition of osteoblastic activity, even though a sufficient amount of NO is formed in the presence of TNF-α and IL-1ß In addition to NO, other more reactive and toxic substances may be formed in cytokine-stimulated osteoblasts, as presented in Fig. 10. In this investigation, I found that $ONOO^-$ synthesized in cytokine-treated cells overcame the stimulatory effect of NO per se (*38*) on osteoblastic differentiation.

NO reacts with O_2^- to form the highly reactive intermediate $ONOO^-$ (*27, 37, 41*). First, I examined the effects of $ONOO^-$ on osteoblastic differentiation by use of oxygen radical donors and the specific free radical scavengers. The simultaneous administration of an NO donor (dNO) and an O_2^- donor (Pgl) was found to produce $ONOO^-$ and inhibit osteoblastic differentiation (Figs. 2 and 3) without affecting cell viability. The inhibitory effects of the NO and O_2^- donors on osteoblastic differentiation were reversed by urate, a potent and selective $ONOO^-$ scavenger (13). These results suggest that the $ONOO^-$ formed from NO and O_2^- inhibited the osteoblastic

differentiation.

Proinflammatory cytokines enhance bone resorption (*19, 20, 40*). IL-1ß and IL-1α are the most powerful stimulators of bone resorption (*47*). Two- to threefold inhibition of osteocalcin synthesis by TNF-α and IL-1ß has been reported in osteoblasts (*48, 49*). Reduced expression of the osteocalcin gene by TNF-α and IL-1ß was observed in the present study (Fig. 7). TNF-α and IL-1ß have also reduced ALPase activity in osteoblasts (*38*) (Fig. 4). Therefore, these cytokines have an inhibitory effect on osteoblastic differentiation. Because $ONOO^-$ produced from NO and O_2^- has shown a suppressive effect on the differentiation of the cytokine-treated osteoblasts, the next step to be clarified is whether cytokine-stimulated osteoblasts actually produce both NO and O_2^-. TNF-α or IL-1ß alone or their combination yielded NO production (Fig. 4). In addition, the cytokine cotreatment also enhanced the production of O_2^-, although O_2^- was not detected on application of only one cytokine (Fig. 5). Finally, I have verified that simultaneous generation of both NO and O_2^- by TNF-α and IL-1ß leads to $ONOO^-$ formation (Fig. 8). $ONOO^-$ formed from NO and O_2^- in these cells would nullify the stimulatory effect of NO and might even suppress osteoblastic differentiation.

There was no measurable restoration of ALPase activity by L-NMMA in the presence of cytokines. One reason that L-NMMA could not restore ALPase activity is that

cytokine-induced O_2^- alone suppressed the enzyme activity. This was partly ascertained by the experiment with SOD in conjunction with cytokines. SOD modestly but significantly restored both ALPase activity and osteocalcin gene expression (Fig. 6). However, the recovery of ALPase activity by SOD was not sufficient, suggesting that O_2^- synthesis alone may not fully explain cytokine-induced ALPase reduction.

The rate constant for $ONOO^-$ formation from NO and O_2^- is 6.7 X 10^9 $M^{-1}\cdot s^{-1}$ (*50*), whereas the rate constant for the scavenging of O_2^- by SOD is 2.5 X $10^{9\text{-}1}\cdot s^{-1}$ (*50*)+. Therefore, the coexistence of NO and O_2^- produced by the cytokine stimulation could form some amount of $ONOO^-$ even in the presence of SOD (*51, 52*). The produced $ONOO^-$ may participate in the reduction of ALPase activity much more than cytokine-induced O_2^-. Urate, an $ONOO^-$ scavenger, restored the cytokine-induced reduction of ALPase activity more markedly than SOD (Fig. 6). A similar argument could also be made for a continued production of NO at a low level even after L-NMMA preincubation. O_2^- produced by the cytokine stimulation may react rapidly with NO, forming $ONOO^-$ even in the presence of L-NMMA, a competitive inhibitor of NOS activity. This would explain the reason that ALPase activity remains depressed even in the supposed absence of NO (Fig. 4). Although the reduction of ALPase activity by cytokine cannot be fully explained by the action of $ONOO^-$ alone, most of the causes

may be attributed to the effects of $ONOO^-$ production. Single cytokines produced NO and did not produce O_2^- (Figs. 4 and 5). Without a superoxide source, single cytokine stimulation would not produce $ONOO^-$, yet single cytokines could inhibit ALPase activity. There may be alternate sources of O_2^-, such as mitochondrial respiration (*53*).

Damoulis and Hauschka (*54*) demonstrated that the NO donor *S*-nitroso-acetyl-penicillamine (SNAP) at a higher concentration (10^{-3} M) evoked cell death in MC3T3-E1 cells after long-term culture ≤73 h. Because SNAP has a half-life of 5 h at pH 7 and 37°C (*55*), NO produced by SNAP would affect cell viability in the first several hours of incubation. The concentration of SNAP they employed may be toxic or lethal to MC3T3-E1 cells. At the same time, dNO at a lower concentration and a longer half-life [40 h at pH 7.4 and 37°C, (*43*)] would be less harmful to the cells. In my study, NO produced from dNO at a submillimolar concentration could exert the biological effects during the entire incubation period. NO donors with a different half-life and concentration may cause the altered effects on osteoblasts. Damoulis and Hauschka have also shown that mouse TNF-α at 20 ng/ml combined with mouse IL-1ß at 5 IU/ml produced NO and reduced cell viability, although mouse TNF-α at 1 ng/ml with IL-1ß had no cytotoxic effect. As they mentioned, mouse TNF-α is more cytotoxic than human TNF-α, and mouse TNF-α at 20 ng/ml has a cytotoxic effect independent of NO. In my

investigation, human TNF-α at 10 ng/ml with human IL-1ß at 10 ng/ml produced NO and reduced ALPase activity in osteoblasts, although it had no effect on cell viability (data not shown). Thus the action of TNF-α depends on the species and the concentration in the osteoblasts.

In a previous study, I was the first to demonstrate endothelial cell nitric oxide synthase (ecNOS) expression in osteoblasts (*38*). The constitutive production of NO may regulate osteoblast growth (*46*) and contribute to bone formation by mechanical stimulation (*56*). Fox et al. (*56*) have reported that administration of L-NMMA prevented the increase in bone formation by mechanical stimulation and concluded that ecNOS was responsible for the NO production. NO produced by ecNOS would be a physiological mediator of estrogen action on bone (1, 19). Estrogen deficiency might reduce the level of NO, ALPase production, and osteocalcin gene expression. Therefore, the physiological level of NO produced by ecNOS is expected to prevent the progress of osteoporosis.

A large amount of O_2^- would not be formed under the condition where ecNOS constitutively produced NO. In contrast, under the inflammatory conditions, not only NO from iNOS but also O_2^- are produced by proinflammatory cytokines, as I demonstrated. In osteoarthritis, TNF-α, IL-1ß, and iNOS were highly expressed in

synovial cells (*57*). The collaboration of these two cytokines may lead to $ONOO^-$ production, as is shown in the present report. Accordingly, $ONOO^-$ may be one of the most effective NO metabolites in cytokine-stimulated osteoblasts. In conclusion, $ONOO^-$ produced by TNF-α and IL-1β, but not NO *per se*, would overcome the stimulatory effect of NO on osteoblastic activity and inhibit osteoblastic differentiation.

Legend

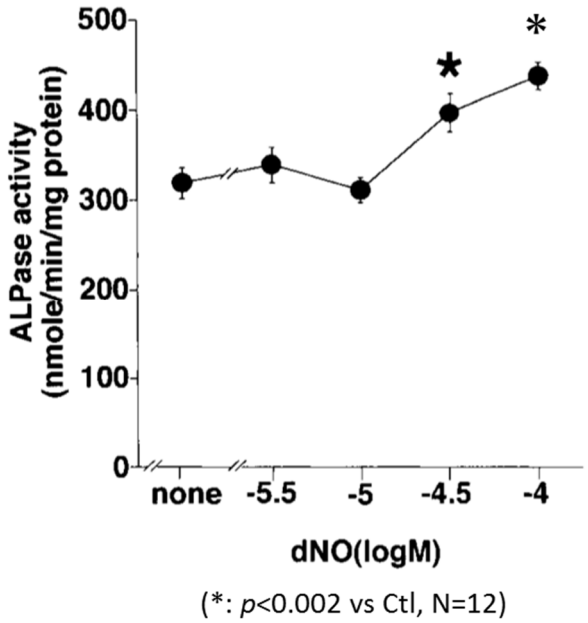

Fig. 1. Stimulatory effect of nitric oxide (NO) donor ethanamine, 2,2'-(hydroxynitrosohydrazono)bis- (dNO) on alkaline phosphatase (ALPase) activity in MC3T3 El cells. Values are means ± SE; n = 12. * Significant difference ($p < 0.002$) vs. control level.

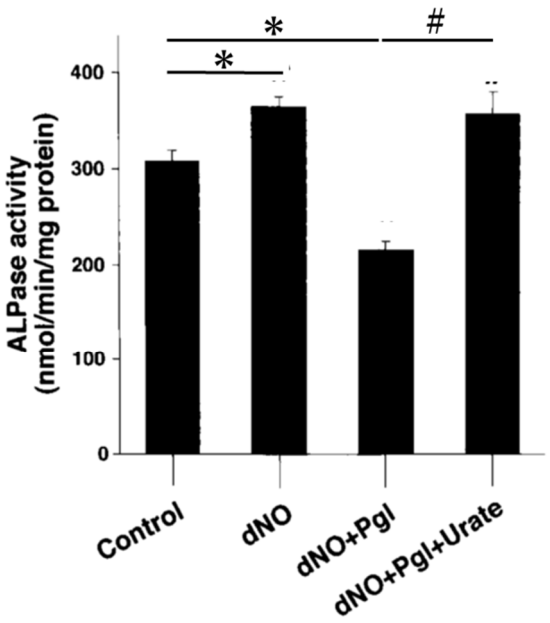

(*: p<0.01 vs Ctl, #: p<0.01 vs TNF-α+IL-1β, N=12)

Fig. 2. Effect of dNO (10^{-4} M) or combination of dNO (10^{-4} M) and pyrogallol [(Pgl), 10^{-4} M] on expression of ALPase activity. Note that urate (10^{-4} M) reversed inhibitory effects of combination of dNO and Pgl on ALPase activity. Values are means ± SE; n = 12. * Significant difference ($p < 0.01$) vs. control; #significant difference ($p < 0.01$) vs. condition inhibited by dNO plus Pgl.

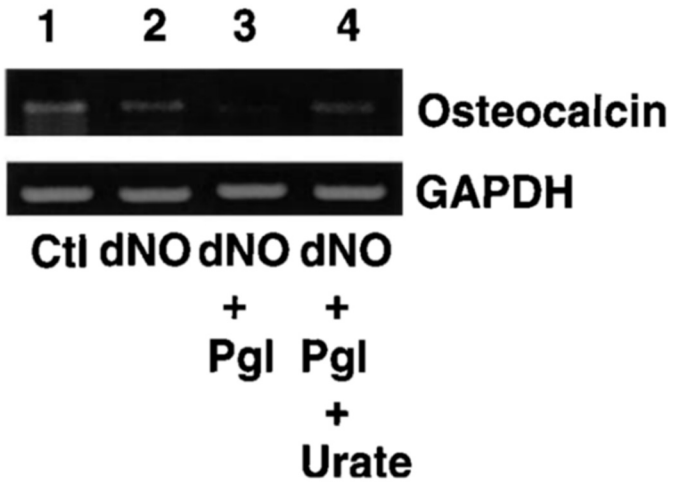

Fig. 3. Expression of osteocalcin mRNA stimulated with dNO (10^{-4} M) or combination of dNO (10^{-4} M) and Pgl (10^{-4} M). Ctl, control; GAPDH, glyceraldehyde 3 phosphate dehydrogenase. Note that urate (10^{-4} M) reversed inhibitory effect of combined dNO and Pgl. Lane 1, unstimulated osteoblasts; lane 2, dNO treated cells; lane 3, cells treated with combination of dNO and Pgl; lane 4, cells treated with dNO, Pgl, and urate.

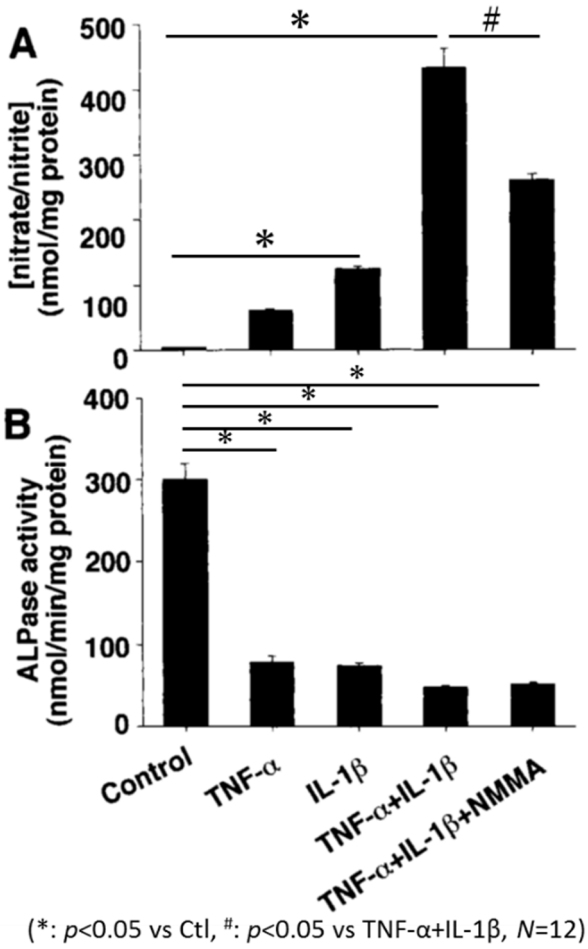

Fig. 4. A: stimulatory effects of tumor necrosis factor-α (TNF-α), interleukin-1ß (IL-1ß), combination of TNF-α plus IL-1ß, and inhibitory effect of N^G- monomethyl-l-arginine (L-NMMA) on NO production. B: inhibitory effects of TNF-α and IL-1ß on ALPase activity with or without L-NMMA in osteoblasts. Values are means ± SE; n = 12.

* Significant difference ($p < 0.005$) vs. control; # significant difference ($p < 0.005$) vs. condition stimulated by TNF-α plus IL-1ß.

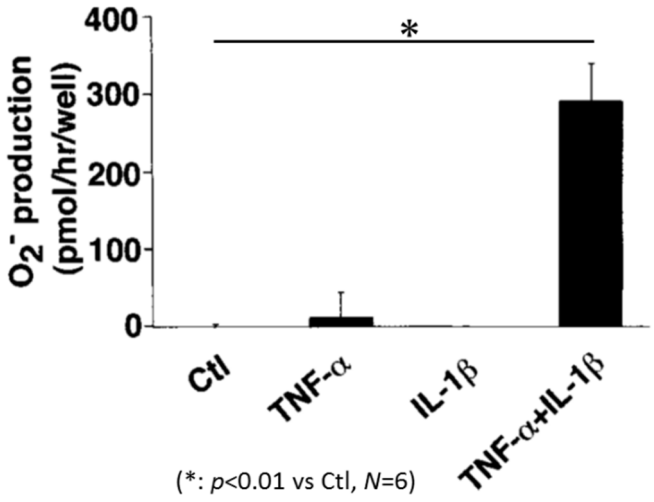

Fig. 5. Stimulatory effects of TNF-α and IL-1β on O_2^- production. Values are means ± SE; n = 6. * Significant difference ($p < 0.01$) vs. Ctl.

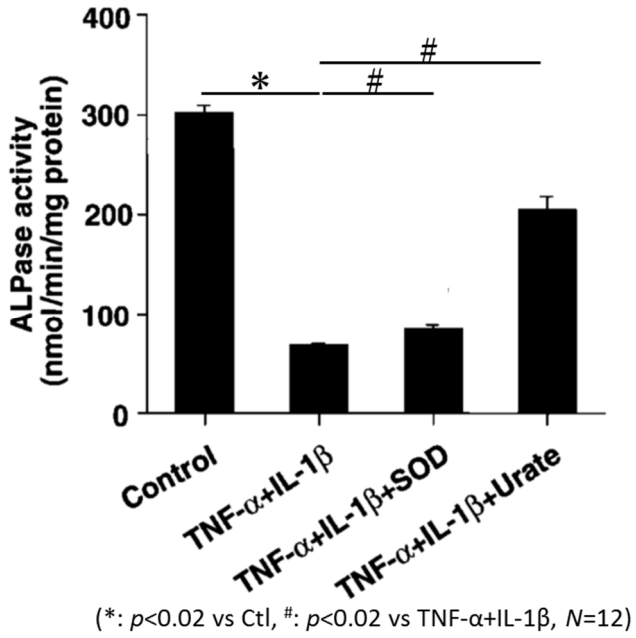

Fig. 6. Effect of superoxide dismutase (SOD, 100 U/ml) or urate (10^{-4} M) on reduction of ALPase activity induced by TNF-α and IL-1ß. Note that SOD and urate reversed inhibitory effects of combined TNF-α and IL-1ß on ALPase activity. Values are means ± SE; n = 12. * Significant difference ($p < 0.02$) vs. control; # significant difference ($p < 0.02$) vs. condition inhibited by TNF-α + IL-1ß.

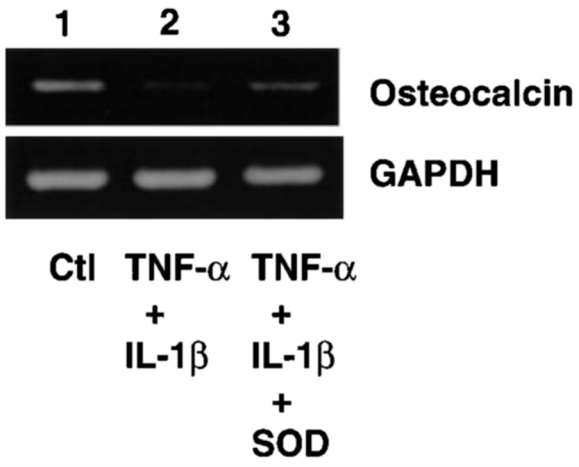

Fig. 7. Expression of osteocalcin mRNA stimulated with combination of TNF-α and IL-1ß. Note that SOD reversed inhibitory effect of combined TNF-α and IL-1ß. Lane 1, unstimulated osteoblasts; lane 2, cells treated with combination of v and IL-1ß; lane 3, cells treated with TNF-α, IL-1ß, and SOD.

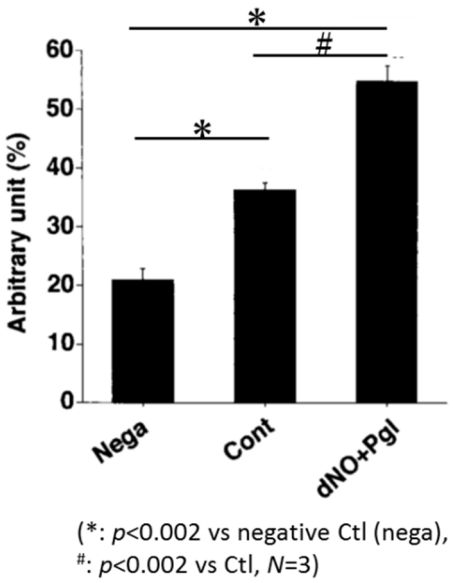

Fig. 8. Immunocytochemistry of nitrotyrosine in osteoblasts after application of NO and donors. Values are means ± SE; n = 3. * Significant difference ($p < 0.002$) vs. negative control [(Nega), without antinitrotyrosine antibody]; #significant difference ($p < 0.002$) vs. control [(Cont), without NO/O_2^- donors].

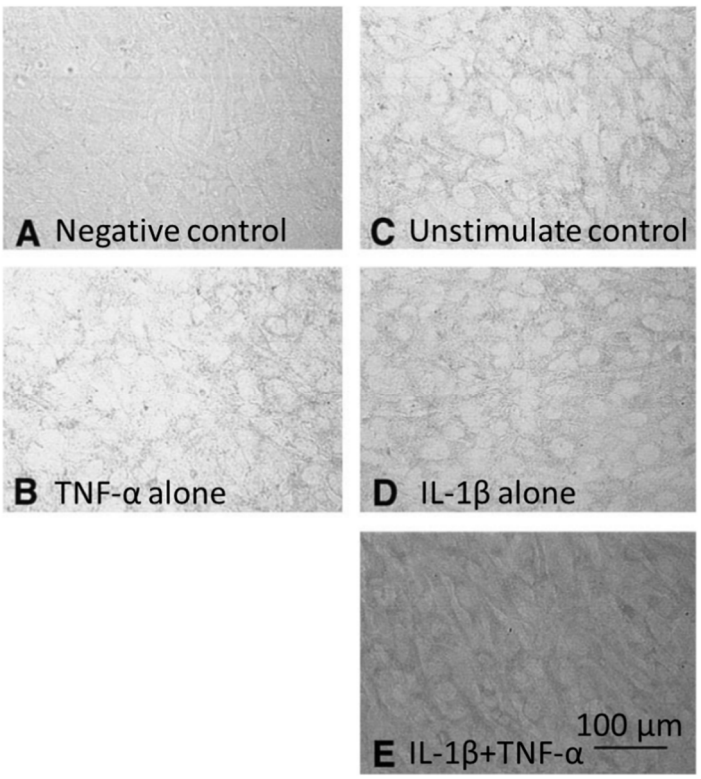

Fig. 9. Immunocytochemistry of nitrotyrosine in osteoblasts after proinflammatory cytokine application. A: negative control; B: unstimulated control; C: TNF-α alone; D. IL-1ß alone; E: TNF-α plus IL-1ß. Note that the combination of TNF-α and IL-1ß enhanced basal production of nitrotyrosine. Bar length, 100 μm.

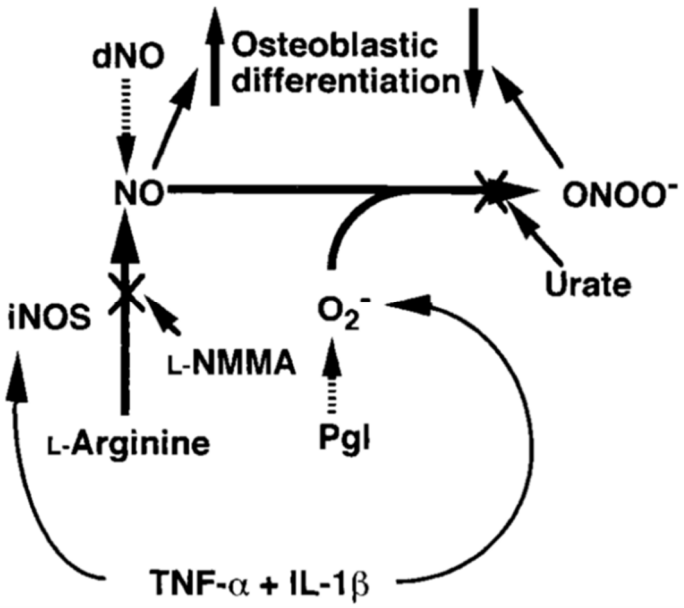

Fig. 10. Metabolic pathway of NO-related radicals. dNO and Pgl produce NO and O_2^-, respectively. NO in presence of O_2^- forms a new radical, $ONOO^-$ and $ONOO^-$ is scavenged by urate. Note that the combination of TNF-α and IL-lß has a stimulatory effect on NO and O_2^- production. L-NMMA inhibits NO production from l-arginine by inducible NO synthase (iNOS).

Chapter 2

A distinctive role of the leukotriene B_4 receptor BLT1 in osteoclastic activity during bone loss

Abstract

Although leukotriene B_4 (LTB_4) is produced in various inflammatory diseases, its functions in bone metabolism remain unknown. Using mice deficient in the high-affinity LTB_4 receptor BLT1, I evaluated the roles of BLT1 in the development of two bone resorption models, namely bone loss induced by ovariectomy and lipopolysaccharide. Through observations of bone mineral contents and bone morphometric parameters, I found that bone resorption in both models was significantly attenuated in BLT1-deficient mice. Furthermore, osteoclasts from BLT1-deficient mice showed reduced calcium resorption activities compared with wild-type osteoclasts. Osteoclasts expressed BLT1, but not the low-affinity LTB_4 receptor BLT2, and produced LTB_4. LTB_4 changed the cell morphology of osteoclasts through the BLT1-Gi protein-Rac1 signaling pathway. Given the causal relationship between osteoclast morphology and osteoclastic activity, these findings suggest that autocrine/paracrine LTB_4 increases the osteoclastic activity through the BLT1-Gi protein-Rac1 signaling pathway. Inhibition of BLT1 functions may represent a strategy for preventing bone resorption diseases.

Introduction

Leukotriene B_4 (LTB_4), a metabolite of arachidonic acid, is a potent lipid mediator with various biological activities toward neutrophils and differentiated T cells, including chemotaxis, degranulation, and production of superoxide anions (*58, 59*). These actions of LTB_4 are mediated by specific cell surface receptors (BLTs). Yokomizo et al. previously cloned two distinct BLTs, BLT1 and BLT2 (*60, 61*). BLT1 is a high-affinity receptor that mediates the inhibition of adenylate cyclase and calcium entry by coupling with the Gi- and Gq-classes of G proteins (*62*). BLT2 transduces comparable intracellular signals but has a lower affinity to LTB_4 (*62*). Although several hydroxyeicosatetraenoic acids were found to activate BLT2 (*63*), Yokomizo et al. recently identified 12(*S*)-hydroxyheptadeca-5*Z*, 8*E*, 10*E*-trienoic acid (12-HHT) as a very potent endogenous ligand for BLT2 (*64*). LTB_4 is produced in inflammatory diseases such as psoriasis (*65*), bronchial asthma (*66*), ulcerative colitis (*67*), postischemic tissue injuries (*68*), and rheumatoid arthritis (*69-72*).

Bone remodeling consists of old bone resorption by osteoclasts and new bone deposition by osteoblasts. Osteoclasts and osteoblasts participate in bone remodeling under the control of many hormones, cytokines (*73, 74*), and autacoids, including lipid mediators (*5*). The effects of LTB_4 on bone resorption were investigated using organ

cultures of mouse calvariae (*75, 76*). LTB_4 enhanced calcium efflux from the mouse calvariae, suggesting that LTB_4 stimulates bone resorption (*75*). LTB_4 increased the formation of resorption pits by osteoclasts in rat bone tissues (*76*), suggesting that LTB_4 modulates bone resorption by increasing the number and/or activity of osteoclasts.

However, few reports have provided definitive biochemical information about the mRNA/protein expression and intracellular signaling pathways of BLTs in osteoclasts as well as the in vivo roles of LTB_4/BLTs in osteoclastic bone resorption.

The clinically important hard-tissue diseases are inflammatory joint diseases and metabolic bone diseases (*5*). Inflammatory joint diseases include rheumatoid arthritis characterized by leukocyte infiltration and synovitis accompanied by erosions of cartilage and subchondral bone (*77*). In bone resorption diseases, such as osteoporosis, an imbalance of bone remodeling in which the rate of resorption exceeds the rate of formation causes the reduction in bone mass (*77*). Recently, BLT1-KO mice were shown to be resistant to inflammatory arthritis (*78, 79*). Similar phenotypes were observed with mouse strains deficient in LTB_4-synthesizing enzymes [i.e. cytosolic phospholipase A2α (cPLA2α), 5-lipoxygenase, and LTA_4 hydrolase] (*80, 81*). A pharmacological study with the BLT1 antagonist CP105696 (*82*) also revealed a critical role of BLT1 in

arthritis (*72*). Despite these important findings in this inflammatory joint disease, the roles of BLT1 in bone resorption diseases are still unknown.

In the present study, I identified critical roles for BLT1 in osteoclastic bone resorption through analyses of BLT1-KO mice affected with two bone resorption diseases, namely bone loss induced by ovariectomy and LPS. Several lines of in vitro data consistently demonstrated that LTB_4 increased osteoclastic activity through autocrine/paracrine signaling mediated by BLT1. My findings suggest that BLT1 is a potential therapeutic target for bone resorption diseases.

Materials and methods

Mice

All animal studies were conducted in accordance with the guidelines for animal research at The University of Tokyo and were approved by The University of Tokyo Ethics Committee for Animal Experiments. BLT1-KO mice were established using a gene targeting strategy (*83*). BLT1-KO mice and the corresponding WT mice have been backcrossed for >10 generations onto a C57BL/6N genetic background. Mice were given access to a standard laboratory diet and water ad libitum.

Ovariectomy-lnduced Bone Loss

BLT1-KO and WT female mice (10-week-old) underwent a bilateral ovariectomy or a sham procedure in which the bilateral ovaries were exteriorized but not removed, under anesthesia by an i.p. injection of sodium pentobarbital (Somnopentyl; 50 mg/kg body weight; Kyoritsu). Mice were killed at 4 weeks after the surgical procedure. The body weights of the BLT1-KO female mice [ovariectomized group, 21.2 ± 1.2 g (n = 8); sham-operated group, 20.9 ± 1.1 g (n = 8)] were indistinguishable from those of the WT female mice [ovariectomized group, 20.7 ± 1.2 g (n = 8); sham-operated group, 20.4 ± 1.3 g (n = 8)].

LPS-lnduced Bone Loss

BLT1-KOand WT male mice (7-to 8-week-old) were i.p. injected with LPS from *Salmonella enterica* (1.25 mg/kg of body weight; Sigma) dissolved in saline on days 0 and 2. On day 7, the femurs were collected. Mice in the control group were injected with saline only. The body weights of the BLT1-KO male mice [LPS-injected group, 23.2 ± 2.1 g (n = 9); saline-injected group, 24.7 ± 1.4g (n = 10)] were indistinguishable from those of the WT male mice [LPS-injected group, 23.5 ± 1.4g (n = 9); saline-injected group, 24.9 ± 2.0 g (n = 10)].

Analysis of Bone Phenotypes

Mouse hindlimb bones were subjected to radiographic and morphometric examinations. The femurs were dissected and stored in 70% ethanol. The BMDs of the femurs were measured by DXA (DCS-600R; Aloka). microCT (inspeXioSMX-90CT; Shimadzu) was used to assess the bone mineral content and bone mass of the trabecular bone in the distal femoral metaphysis using a 12-μm isotropic voxel size with 40 kV of tube voltage and 100 μA of tube current. Three-dimensional CT images were reconstituted and analyzed using a TRI system (Ratoc).

Osteoclast Culture

Bone marrow was flushed from the femurs and tibias of 6- to 8-week-old male mice. Osteoclasts were differentiated from hematopoietic cell lineages in bone marrow cultures by stimulation with RANKL and M-CSF (*84, 85*). Briefly, bone marrow cells were cultured in a modified Eagle's medium (αMEM; Invitrogen) containing 10% FBS (JRH) with soluble RANKL (30 ng/mL; PeproTech) and M-CSF (50 ng/mL; R&D Systems) for 5 days. Osteoclasts were stained with 0.01% naphthol AS-MX phosphate (Sigma) in the presence of 100 mM L(+/-)-tartaric acid (pH 5.0; Wako) to detect TRAP activity. TRAP-positive cells with more than three nuclei were counted as viable osteoclasts.

RT-PCR Analysis

cDNA was synthesized from 0.8 μg total RNA extracted from cultured primary osteoclasts by oligo(dT) priming using SuperScript II reverse transcriptase (Invitrogen). The resultant cDNA was amplified by PCR with the following primers: Mouse BLT1, 5'-ATGGCTGCAAACACTACATCTCCT-3' and 5'-CACTGGCATACATGCTTATTCCAC-3'; mouse BLT2, 5' -

ACAGCCTTGGCTTTCTTCAG-3' and 5'-TGCCCCATTACTTTCAGCTT-3'; mouse 5-lipoxygenase, 5'-CTGGTACCTGAAGTACATCACACTG-3' and 5'-AACAAAGTCCACTCCTTTTTCACTA-3'; mouse LTA_4 hydrolase, 5' -CAGGA AGATT TACAGATTCAACCAG-3' and 5'-GAAAATTCATTAGCAGATTTCTCCA-3'; and mouse ß-actin, 5'-GCTGTGCTATGTTGCTCTAGACTT-3' and 5'-AATTGAATGTAGTTTCATGGATGC-3'. The following protocol was used for RT-PCR: 35 cycles of 94 °C for 10 s, 56 °C for 10 s, and 72 °C for 20 s. The PCR products were electrophoresed in a 2% agarose gel and stained with ethidium bromide. For positive controls of mouse BLT1 and BLT2, plasmids including cDNAs of mouse BLT1 and BLT2 were used as templates (*86*).

Western Blot Analysis

Proteins were extracted from cultured osteoclasts using M-PER (Pierce) with IX Complete protease inhibitor mixture (Roche). The protein concentrations of the cell lysates were measured using a BCA Protein Assay kit (Pierce) with BSA (fraction V, fatty acid-free; Sigma) as a standard. Aliquots (15 µg protein) were separated by 10% polyacrylamide gel electrophoresis and transferred to a nitrocellulose membrane. After blocking with 5% skim milk, the membrane was sequentially incubated with a rabbit

polyclonal antibody against 5-lipoxygenase (1:500 dilution; Cayman Chemical) and an HRP-conjugated anti-rabbit IgG antibody (1:2,000 dilution; GE Healthcare). ß-actin was evaluated as an internal control for protein loading, by sequentially incubating the membrane with a mouse monoclonal antibody against j8-actin (1:4,000 dilution; Sigma) and an HRP-conjugated anti-mouse IgG antibody (1:2,000 dilution; Sigma). Immunoreactive proteins were visualized by the ECL chemiluminescence reaction (Amersham Biosciences) following the manufacturer's instructions.

ELISA for LTB_4

After washing with PBS, osteoclasts were stimulated with 1 μM A23187 for 15 min at 37 °C. LTB_4 production by osteoclasts was determined with a LTB_4 ELISA kit (Cayman Chemical) according to the manufacturer's instructions.

Confocal Microscopy

Bone marrow cells were seeded onto 35-mm polyD-lysine-coated glass-bottomed dishes (Iwaki) in αMEM containing 10% FBS with soluble RANKL (30 ng/mL) and M-CSF (50 ng/mL). On day 5, osteoclasts were stimulated with 100 nM LTB_4 for 30 min following pretreatment with CP105696 (1 μM for 5 min; a kind gift from Pfizer), PTX

(10 ng/mL for 2 h; List Biological Laboratories) or NSC23766 (50 μM for 10 min; Merck). Then, osteoclasts were fixed with 3.7% formaldehyde in PBS for 10 min and permeabilized with 0.1% Triton X-100 (Sigma) in PBS for 5 min. For actin labeling, osteoclasts were incubated with 0.03% rhodamine-phalloidin and 0.1% Triton X-100 in PBS for 40 min. The stained cells were observed using a confocal laser scanning microscope (LSM510; Carl Zeiss).

Calcium Resorption Assay

Bone marrow cells were cultured in αMEM containing 10% FBS with soluble RANKL (30 ng/mL) and M-CSF (50 ng/mL) for 6 days on calcium phosphate-coated dishes (BioCoat Osteologic bone culture system; BD Biosciences). The medium was changed every 2 days. In some experiments, 1 μM CP105696 or 10 ng/mL PTX were added to the replaced medium. The Rac1 inhibitor NSC23766 was supplemented to the medium at 50 μM every day. After removal of the cells with a bleach solution (6% NaOCI and 5.2% NaCI), the dishes were washed with water and photographed under a light microscope (BH-2; Olympus). The area of the calcium phosphate-resorbed pits was measured using the image-processing application software ImageJ (National Institutes of Health; NIH).

Administration of CP105696 to Ovariectomized Mice

CP-105696 at a dose of 10 mg/kg body weight or vehicle (0.5% methylcellulose) was administered orally to C57BL/6N female mice (10-week-old) daily. Treatment commenced the day before a bilateral ovariectomy. These mice were killed 10 days after the surgical procedure.

Histology

The tibias of mice after LPS or saline injection were stained with Villanueva bone stain solution (*87*) days, dehydrated in ascending grades of ethanol, and embedded in methyl methacrylate (Wako) without decalcification (*88*). The metaphyseal region of each tibia was subjected to histologic analysis using a light microscope equipped with a micrometer.

ELISA for GTP-Bound Rac

Osteoclasts were serum-starved for 15 min before exposure to 100 nM LTB_4 for 2 min. After cell lysis, a total of 12.5 μg protein was subjected to ELISA for GTP-Rac with a G-LISA Rac Activation Assay Biochem kit (Cytoskeleton).

Statistical Analysis

All values are expressed as means ± SD. The means of multiple groups were compared by ANOVA (Prism; GraphPad Software). The statistical significance of differences was determined by Tukey's multiple comparison test (for parametric analyses) or Dunnett's multiple comparison test (for nonparametric analyses). The statistical significance of differences was determined by two-tailed unpaired t test. Values of $p < 0.05$ were considered to indicate statistical significance.

Results

BLT1-KO Mice Are Resistant to Bone Loss Induced by Ovariectomy.

Bone mineral content

I examined whether mice lacking BLT1 develop ovariectomy-induced bone loss to elucidate the roles of BLT1 in bone resorption. Using dual X-ray absorptiometry (DXA), the areal bone mineral density (BMD; bone mineral content divided by the coronal area of the bone tissue measured) of the metaphyseal region of the femur from ovariectomized female mice was compared with that from sham-operated mice. The difference in BMD observed by the DXA measurements was significant between the ovariectomized and sham-operated WT mice (Fig. 1A Left). On the other hand, the DXA analysis revealed that the femoral BMD of ovariectomized BLT1-KO mice was comparable to that of sham-operated BLT1-KO mice.

Consistent results were obtained by microcomputed tomography (μCT) analysis, which selectively detects the trabecular bone mineral content. This characteristic is in contrast to the DXA analysis, which evaluates the bone mineral content of both the cortical and trabecular bones. It is of note that trabecular bone is more profoundly affected in bone resorption diseases than cortical bone (*89*). In WT mice, the trabecular bone mineral content per tissue volume (BMC/TV) in the metaphyseal region of the

femur was significantly lower in the ovariectomized mice than in the sham-operated mice (Fig. 1 B Left and C Left). "Tissue volume" means the volume of the total bone tissue including the trabecular bone and bone marrow but not the cortical bone. Furthermore, in ovariectomized mice, BMC/TV was significantly lower in WT mice than in BLT1-KO mice (Fig. 1B Left and C Left). The difference between the BMC/TV values of ovariectomized and sham-operated BLT1-KO mice was not significant (Fig. 1B Left and C Left). To confirm the role of BLT1 in the ovariectomy-induced bone loss, I examined the effect of the BLT1 antagonist CP105696 on ovariectomized mice. In accordance with the phenotypes of BLT1-KO mice, I observed that BMD and BMC/TV were significantly higher in CP105696-treated mice than vehicle-treated mice (Fig. S1 A-C).

Bone mass

The microCT analysis revealed that the trabecular bone volume per tissue volume (BV/TV) in the metaphyseal region of the femur was significantly reduced in ovariectomized WT mice, but not in ovariectomized BLT1-KO mice, compared with sham-operated mice (Fig. 2A). Two other indices related to BV/TV, the trabecular number (Tb.N; linear density of trabecular bone) and trabecular separation (Tb.Sp;

distance between the edges of trabecular bone), also indicated that the bone volume of ovariectomized BLT1-KO mice was similar to that of sham-operated BLT1-KO mice (Fig. 2A). BV/TV was significantly increased in CP105696-treated ovariectomized mice compared with vehicle-treated mice (Fig. S1D). Tb.N and Tb.Sp values also indicated the amelioration of bone volume of ovariectomized mice by treatment with CP105696 (Fig. S1D).

BLT1-KO Mice Are Resistant to Bone Loss Induced by LPS Injection.

Bone mineral content

LPS, a key component of the outer wall of Gram-negative bacteria, has been proposed to be a potent stimulator of bone resorption (*90-92*). Similar to the DXA data obtained for the female ovariectomized mice, WT male mice exhibited a significantly decreased BMD after LPS injection, while the BMD of BLT1-KO mice was unchanged (Fig. 1A Right).

A microCT analysis of the metaphyseal region of the femur consistently showed that, in WT mice, the trabecular BMC/TV was significantly lower in the LPS-injected mice than in the saline-injected mice (Fig. 1B Right and C Right). The trabecular BMC/TV value was significantly lower in WT mice than in BLT1-KO mice after LPS injection

(Fig. 1 B Right and C Right). The LPS-injected BLT1-KO mice displayed a similar BMC/TV value to the saline-injected BLT1-KO mice (Fig. 1B Right and C Right).

Bone mass

The microCT analysis also demonstrated that the trabecular BV/TV in the metaphyseal region of the femur was BV/TV, the trabecular number (Tb.N; linear density of trabecular bone) and trabecular separation (Tb.Sp; distance between the edges of trabecular bone), also indicated that the bone volume of ovariectomized BLT1-KO mice was similar to that of sham-operated BLT1-KO mice (Fig. 2A). BV/TV was significantly increased in CP105696-treated ovariectomized mice compared with vehicle-treated mice (Fig. S1D). Tb.N and Tb.Sp values also indicated the amelioration of bone volume of ovariectomized mice by treatment with CP105696 (Fig. S1D).

BLT1-KO Mice Are Resistant to Bone Loss Induced by LPS Injection.

Bone mineral content

LPS, a key component of the outer wall of Gram-negative bacteria, has been proposed to be a potent stimulator of bone resorption (*90-92*). Similar to the DXA data obtained for the female ovariectomized mice, WT male mice exhibited a significantly

decreased BMD after LPS injection, while the BMD of BLT1-KO mice was unchanged (Fig. 1A Right).

A microCT analysis of the metaphyseal region of the femur consistently showed that, in WT mice, the trabecular BMC/TV was significantly lower in the LPS-injected mice than in the saline-injected mice (Fig. 1 B Right and C Right). The trabecular BMC/TV value was significantly lower in WT mice than in BLT1-KO mice after LPS injection (Fig. 1 B Right and C Right). The LPS-injected BLT1-KO mice displayed a similar BMC/TV value to the saline-injected BLT1-KO mice (Fig. 1B Right and C Right).

Bone mass.

The microCT analysis also demonstrated that the trabecular BV/TV in the metaphyseal region of the femur was reduced in LPS-injected WT mice, but unaltered in LPS-injected BLT1-KO mice, compared with the saline-injected mice (Fig. 2B). In accordance with these observations, both the Tb.N and Tb.Sp values were similar between LPS- and saline-injected BLT1-KO mice (Fig. 2B). Histologically, deep Howship's lacunae (i.e., bone hollows) were commonly observed in LPS-injected WT mice as a result of active bone resorption (Fig.S2A). Osteoclasts lay within these distinctive Howship's lacunae (Fig. S2B). Compared with LPS-injected WT mice, the

Howship's lacunae were shallower in saline-injected WT mice. In contrast to WT mice, LPS-induced Howship's lacuna formation was unremarkable in BLT1-KO mice (Fig. S2 A and B).

mRNAs of BLT1,5-Lipoxygenase and LTA_4 Hydrolase Are Expressed and LTB_4 Is Produced in Osteoclasts.

I analyzed the mRNA expression profile of LTB_4-related genes in primary osteoclasts, which were differentiated from bone marrow cells in the presence of receptor activator of NF-κB ligand (RANKL) and macrophage colony stimulating factor (M-CSF). BLT1 mRNA was expressed in the primary osteoclasts, whereas BLT2 mRNA was not detected under my experimental conditions (Fig. 3A). These results strongly suggest that LTB_4 acts on osteoclasts mainly through BLT1. Osteoclasts also expressed mRNAs for 5-lipoxygenase and LTA_4 hydrolase (Fig. 3B). Western blot analysis further revealed that osteoclasts expressed 5-lipoxygenase protein (Fig. 3C). In accordance with these results, I observed that osteoclasts produced LTB_4 upon calcium-ionophore stimulation (Fig. 3D). These results suggest that LTB_4 represents a paracrine/autocrine factor in the regulation of osteoclasts.

LTB_4 Changes the Morphology of Osteoclasts.

WT osteoclasts changed their cell morphology from round shapes to irregular shapes after 30 min of LTB_4 treatment (Fig. 4A). In contrast, BLT1-KO osteoclasts exhibited no changes in their contours. Consistent with the data for BLT1-KO osteoclasts, pretreatment with CP105696 almost completely suppressed the LTB_4-induced morphological changes of WT osteoclasts (Fig. 4B). Furthermore, pertussis toxin (PTX), a Gi-specific inhibitor, also inhibited the morphological changes of osteoclasts (Fig. 4B). Rac proteins (Racl, 2, and 3) are a subfamily of the Rho family of small GTPases engaged in many functions such as changes in morphology and motility (*93, 94*). The Racl inhibitor NSC23766 is a cell-permeable pyrimidine compound that specifically and reversibly inhibits Racl GDP/GTP exchange activity by interfering with Racl interactions with Rac-specific guanine nucleotide exchange factors (*95*). Again, the LTB_4-induced morphological changes of osteoclasts were suppressed by this Rac1 inhibitor (Fig. 4B). Upon LTB_4 treatment, the level of active GTP-bound Rac was significantly increased in WT osteoclasts, but not in BLT1-KO osteoclasts (Fig. S3). These results support the notion that Racl is involved in LTB_4-induced osteoclast activation. Taken together, these results suggest that the BLTl-Gi protein-Racl signaling pathway is involved in the observed morphological changes of osteoclasts.

Calcium Resorption by Osteoclasts from BLT1-K0 Mice Is Impaired.

The regulation of the morphological changes of osteoclasts is deeply related to the function of osteoclasts (*96, 97*). WT osteoclasts showed more advanced calcium resorption than BLT1-KO osteoclasts in vitro (Fig. 5A). CP105696 inhibited the calcium resorption by WT osteoclasts to the levels resorbed by BLT1-KO osteoclasts in the presence or absence of CP105696 (Fig. 5A). These results suggest that BLT1 deficiency suppresses calcium resorption by osteoclasts. PTX reduced the calcium resorption by WT osteoclasts to the levels resorbed by BLT1-KO osteoclasts in the presence or absence of PTX (Fig. 5A). Therefore, the BLTl-Gi protein signaling pathway probably plays an important role in calcium resorption by osteoclasts.

BLT1 gene ablation, CP105696, and PTX had no effects on the osteoclast numbers, which were determined after the differentiation of bone marrow cells in the presence of RANKL and M-CSF (Fig. 5B). These results indicate that BLT1 regulates the osteoclastic activity without changing the number of osteoclasts. The activity of individual osteoclasts seems to be enhanced through BLT1 and Gi.

The Racl inhibitor reduced the calcium resorption by WT osteoclasts but not that by BLT1-KO osteoclasts, consistent with the results for BLT1 and Gi (Fig. 5A). However,

the Racl inhibitor NSC23766 reduced the numbers of both WT and BLT1-KO osteoclasts (Fig. 5B). Instead, this compound increased the number of preosteoclasts, which were defined as tartrate-resistant acid phosphatase (TRAP)-positive cells with less than three nuclei (Fig. S4). Since Racl lies at the convergence of various signaling pathways, this molecule probably regulates the osteoclastogenesis independently of BLT1.

Discussion

This study demonstrates the critical effects of BLT1 in murine models of bone resorption induced by ovariectomy and LPS injection. Ovariectomy, a model of postmenopausal osteoporosis, gives rise to bone resorption conditions by acute decreases in the serum estrogen levels (*89*). Estrogen deficiency increases the production of inflammatory cytokines (*98, 99*), causes a bone-remodeling imbalance in which bone resorption exceeds bone formation, and consequently induces bone resorption by activated osteoclasts (*100*). LPS injection also causes severe bone resorption (*92*). LPS activates lymphocytes and macrophages to produce inflammatory cytokines, increases osteoclastic activity, and subsequently stimulates bone resorption (*101*). Osteoclasts are the principal cells involved in bone loss (*95*) and thus appear to play important roles in these bone resorption diseases. I found that LTB_4 was produced in osteoclasts and activated BLT1 via an autocrine/paracrine mechanism and that BLT1-KO osteoclasts lost the ability to resorb calcium. These findings may account for the ameliorated bone resorption in BLT1-KO mice after ovariectomy and LPS injection.

Osteoclasts are considered to resorb bone under the control of osteoblasts or bone marrow cells (*102*). The autocrine/paracrine control of osteoclasts was unknown until I identified the stimulatory effects of platelet-activating factor (PAF) on cell survival and

bone resorption of osteoclasts (*103*). In the present study, the primary osteoclasts expressed BLT1 mRNA but not BLT2 mRNA. In addition, I detected 5-lipoxygenase and LTA_4 hydrolase mRNAs as well as 5-lipoxygenase protein in osteoclasts. LTB_4 production by osteoclasts was observed. Thus, I propose that LTB_4 is the second autocrine/paracrine factor of osteoclasts after PAF (*103*).

Among phospholipase A_2 (PLA_2) enzymes, cPLA$_2$α plays a dominant role in arachidonic acid release (*5, 104*). Arachidonic acid is metabolized to eicosanoids including LTB_4 and prostaglandin E_2 (PGE_2). By analyzing cPLA$_2$α-KO mice, my group previously revealed that this enzyme plays a key role in LPS-induced bone resorption (*92*). In that study, it was shown that LPS-induced production of the bone resorption mediator PGE_2 by osteoblasts was impaired in cPLA$_2$α-KO mice, but the effects of cPLA$_2$α deficiency on the actions of osteoclasts were not examined. Because osteoclasts express higher amounts of cPLA$_2$α than primary osteoblasts (*103*), cPLA$_2$α in osteoclasts may exert a significant effect on bone resorption by enhancing LTB_4 production.

Estrogen withdrawal after ovariectomy or natural menopause is associated with increased production of TNF-α and IL-1 (*98, 99*), both of which increase LTB_4 production in neutrophils (*105*) and macrophages (*106*). LPS was also reported to

increase LTB_4 production in both cell types (*107, 108*). Therefore, neutrophils and macrophages may be other sources of LTB_4 in the bone marrow of mice suffering from bone resorption diseases. Nevertheless, no in vivo studies have demonstrated enhanced levels of LTB_4 in the bone marrow of these mice.

In granulocytes and some cell lines, BLT1 was shown to transduce intracellular signals through the Gi- and G16-classes of G proteins, which inhibit cAMP production and raise the intracellular calcium concentration (*63*). However, the BLT1-dependent signaling pathways in osteoclasts were largely unknown. Although I did not detect a decrease in cAMP accumulation or an increase in the intracellular calcium concentration by LTB_4 in osteoclasts (data not shown), I identified critical roles for BLT1 in osteoclastic activity through PTX-sensitive Gi protein and Racl. These findings are consistent with previous reports showing that Gi and its downstream effector Racl are related to osteoclast functions (*109-111*). The number of osteoclasts was reduced by ≈75% by treatment with a Racl inhibitor (Fig. 5B), whereas only an ≈50% reduction in calcium resorption was seen under the same experimental conditions (Fig. 5A). This apparent discrepancy was probably due to impaired cell-cell fusion of preosteoclasts. Rac deficiency reportedly inhibited the fusion of preosteoclasts (*111*). Indeed, preosteoclasts have been shown to exhibit potency to resorb dentin (*112*). In the present

study, I defined osteoclasts as TRAP-positive cells with more than three nuclei. Given the significant increase in the number of preosteoclasts by a Rac inhibitor (Fig. S4), the number of osteoclasts shown in Fig. 5B may not necessarily reflect the total osteoclastic activities.

Considering the causal relationship between osteoclast morphology and osteoclastic activity (*95, 97*), it is reasonable that exogenous LTB_4 changes the shape of osteoclasts through the BLTl-Gi protein-Racl pathway. The morphological changes and migration of osteoclasts are closely related to one another (*113, 114*). The migration of osteoclasts is enhanced in a Gi-dependent manner (*110*). Racl is generally thought to play a role in cell motility (*94*) and was indeed reported to be involved in the motility of osteoclasts (*109, 111*). The functional cycle of bone resorption by osteoclasts consists of bone adherence, bone degradation, bone detachment, and movement to a new site of resorption (*95, 114*). Therefore, increased osteoclast motility is closely associated with enhanced bone resorption. LTB_4 may increase osteoclast bone resorption, at least in part, by enhancing osteoclast motility.

It has recently been reported that lipoxin and resolvin El with anti-inflammatory and proresolution activities blocked the inflammation-induced bone loss in periodontal diseases (*115, 116*). The inhibition of bone resorption by resolvin El appeared to involve

BLT1 antagonism in osteoclasts (*117*). These reports are in alignment with my current findings.

In conclusion, I propose a model for BLT1 actions in bone resorption. LTB_4 is produced in osteoclasts and activates BLT1 in an autocrine/paracrine manner. This mechanism is responsible for maintaining homeostatic bone remodeling by affecting the cell morphology and bone resorption activity of osteoclasts. In bone resorption diseases, osteoclasts are activated and enhance bone resorption with a large contribution by LTB_4/BLTI. The markedly ameliorated bone resorption observed in BLT1-KO mice after ovariectomy or LPS injection suggests comprehensive roles of BLT1 in a variety of bone resorption diseases. Many therapeutic agents are being investigated to prevent bone resorption diseases (*118*). My findings suggest that BLT1 antagonists would be one of the candidate agents for therapeutic use for bone resorption diseases.

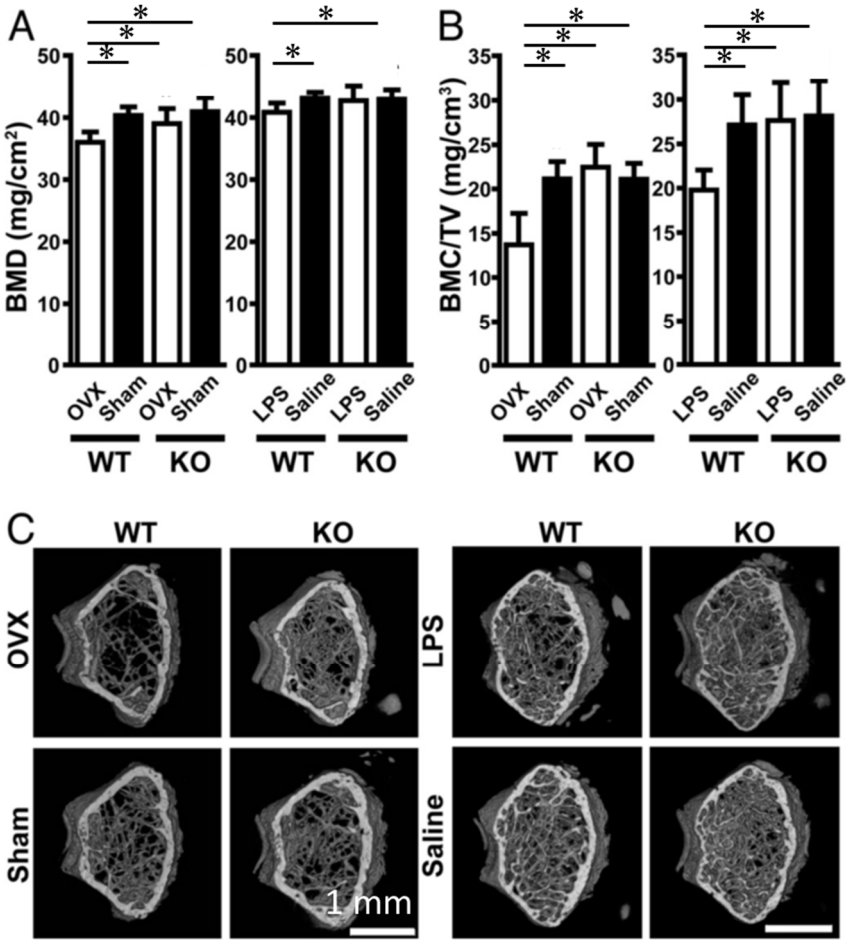

Legends

Fig. 1. Radiographic analysis of hindlimb bones. (A) Areal bone mineral density (BMD) of the metaphyseal region of the femur measured by DXA. Left graph, female mice were ovariectomized (OVX) or sham-operated (Sham). *, $p < 0.05$ vs. WT-OVX, as determined by ANOVA with Tukey's multiple comparison test (n = 8 animals per group). Right graph, male mice were injected with LPS or saline. *, $p < 0.05$ vs. WT-

LPS, as determined by ANOVA with Tukey's multiple comparison test (n = 9-10 animals per group). (B)Trabecular bone mineral content pertissue volume (BMC/TV) of the metaphyseal region of the femur measured by microCT. Data are shown as described for A. *, $p < 0.001$ vs. WT-OVX or WT-LPS, as determined by ANOVA with Tukey's multiple comparison test (n = 8 and 9-10 animals per group for ovariectomy and LPS injection, respectively). (C) Representative microCT photographs of the metaphyseal regions of femurs. Note the highly porous inside of the bone (transparent regions) in the ovariectomized and LPS-injected WT mice. (Scale bar, 1 mm.)

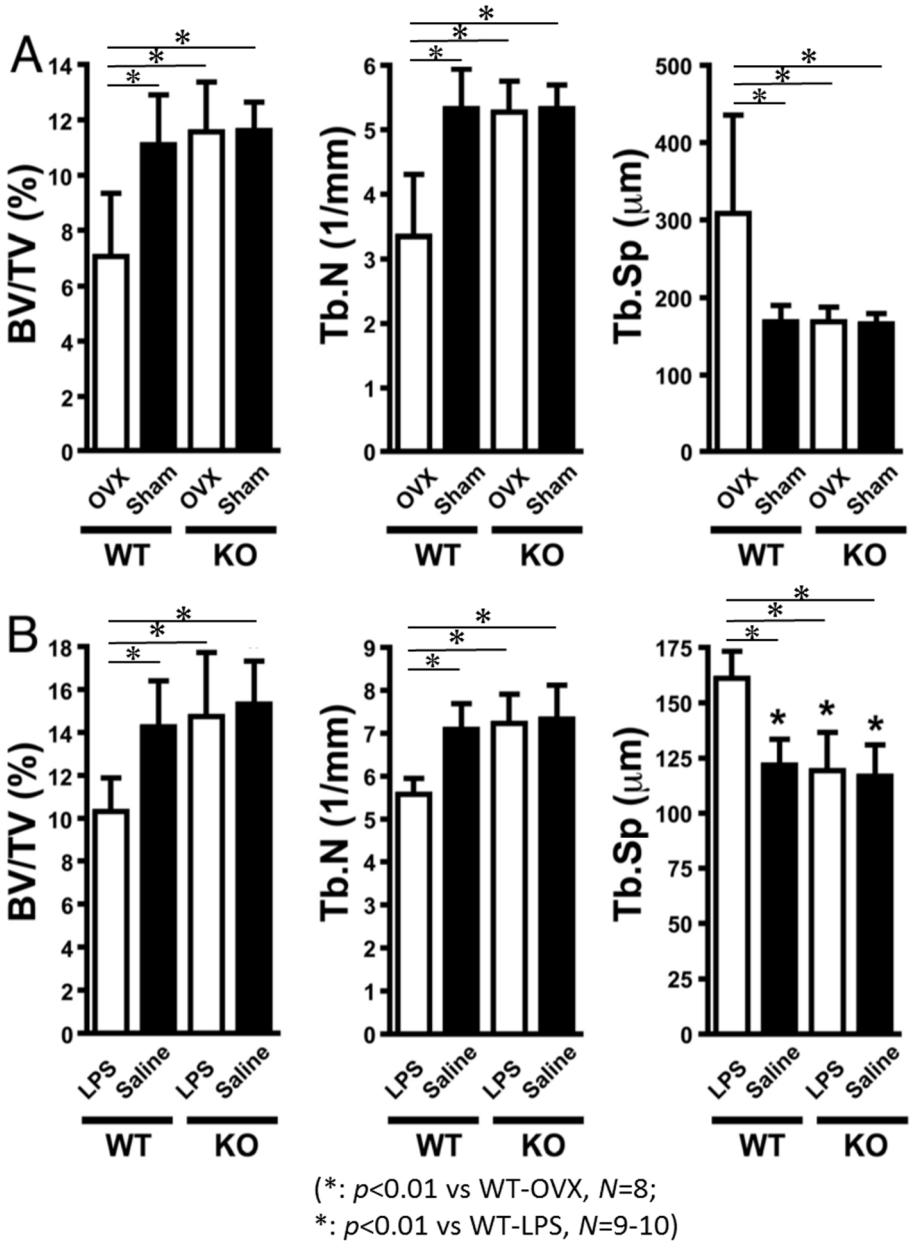

Fig. 2. Computerized morphometry of femurs. (A) Trabecular bone volume per tissue volume (BV/TV), trabecular number (Tb.N), and trabecular separation (Tb.Sp) of the metaphyseal region of the femur from ovariectomized mice. These bone mass indices were quantified based on analyses of threedimensional microCT images of the

metaphyseal region of the femur. *, p <0.01 vs. WT-OVX by ANOVA with Tukey's multiple comparison test (n = 8 animals per group). (B) Trabecular BV/TV, Tb.N, and Tb.Sp of the metaphyseal region of the femur from LPS-injected mice quantified as described for A. *, p < 0.01 vs. WT-LPS by ANOVA with Tukey's multiple comparison test (n = 9-10 animals per group).

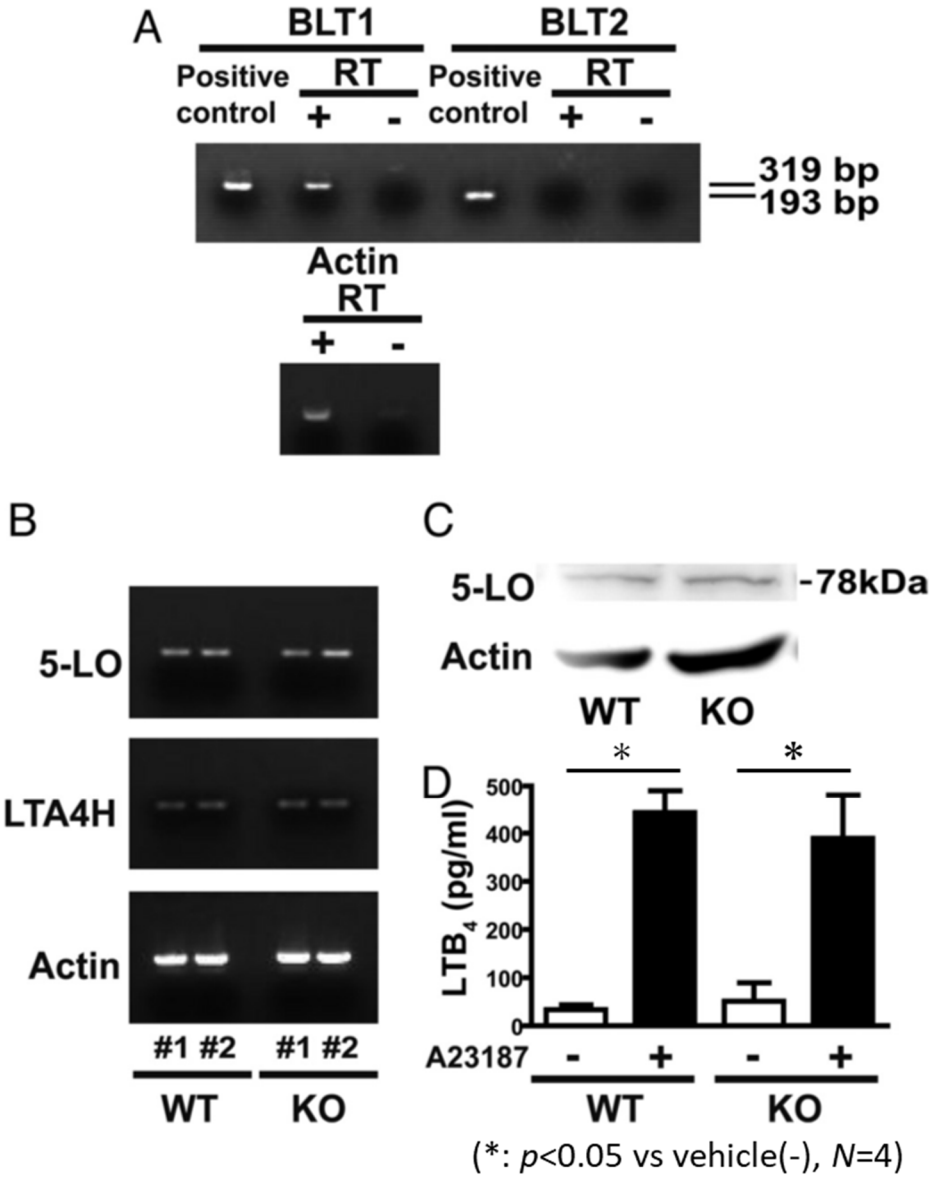

Fig. 3. Expression of LTB_4-related molecules and production of LTB_4 in primary osteoclasts. (A) mRNA expression of BLT1 and BLT2 in osteoclasts differentiated from bone marrow cells in the presence of RANKL (30 ng/ml) and M-CSF (50 ng/ml) for 5 days. RT, reverse transcription. (B) mRNA expression of 5-lipoxygenase (5-LO) and

LTA_4 hydrolase (LTA_4H) in the osteoclasts. Data from two independent primary osteoclast cultures (#1 and #2) are shown. (C) Western blot analysis for 5-lipoxygenase (5-LO) protein expression in the osteoclasts. (D) Production of LTB_4 by the osteoclasts upon stimulation with 1 μM A23187 (n = 4 per group).

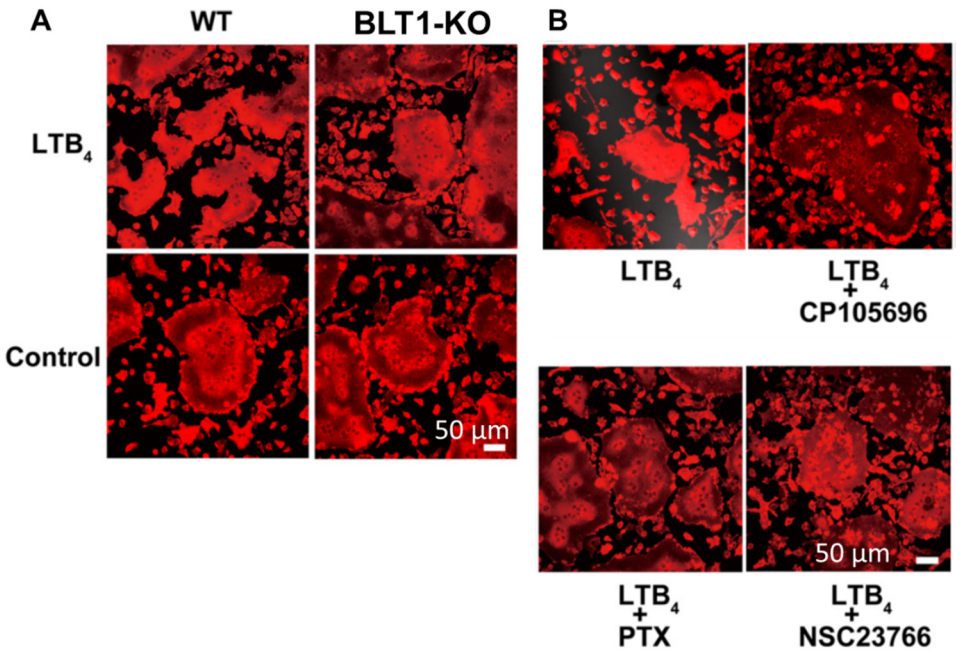

Fig. 4. Morphological changes of osteoclasts through the BLTI-Gi protein Rac1 signaling pathway. (A) Images of rhodamine-phalloidin staining of primary osteoclasts. WT osteoclasts alter their contours from round shapes to irregular shapes after 30 min of treatment with 100 nM LTB_4, while BLT1-KO osteoclasts do not change their morphology. (Scale bar, 50 μm.) (B) Inhibition of the LTB_4-induced morphological changes of WT osteoclasts by an antagonist of BLT1 and inhibitors of Gi protein and Rac1. Primary osteoclasts were incubated with 1 μM CP105696 (BLT1 antagonist) for 5 min, 10 ng/mL PTX (Gi protein inhibitor) for 2 h, or 50 μM NSC23766 (Racl inhibitor) for 10 min. The cells were then treated with 100 nM LTB_4 for 30 min. (Scale bar, 50 μm.)

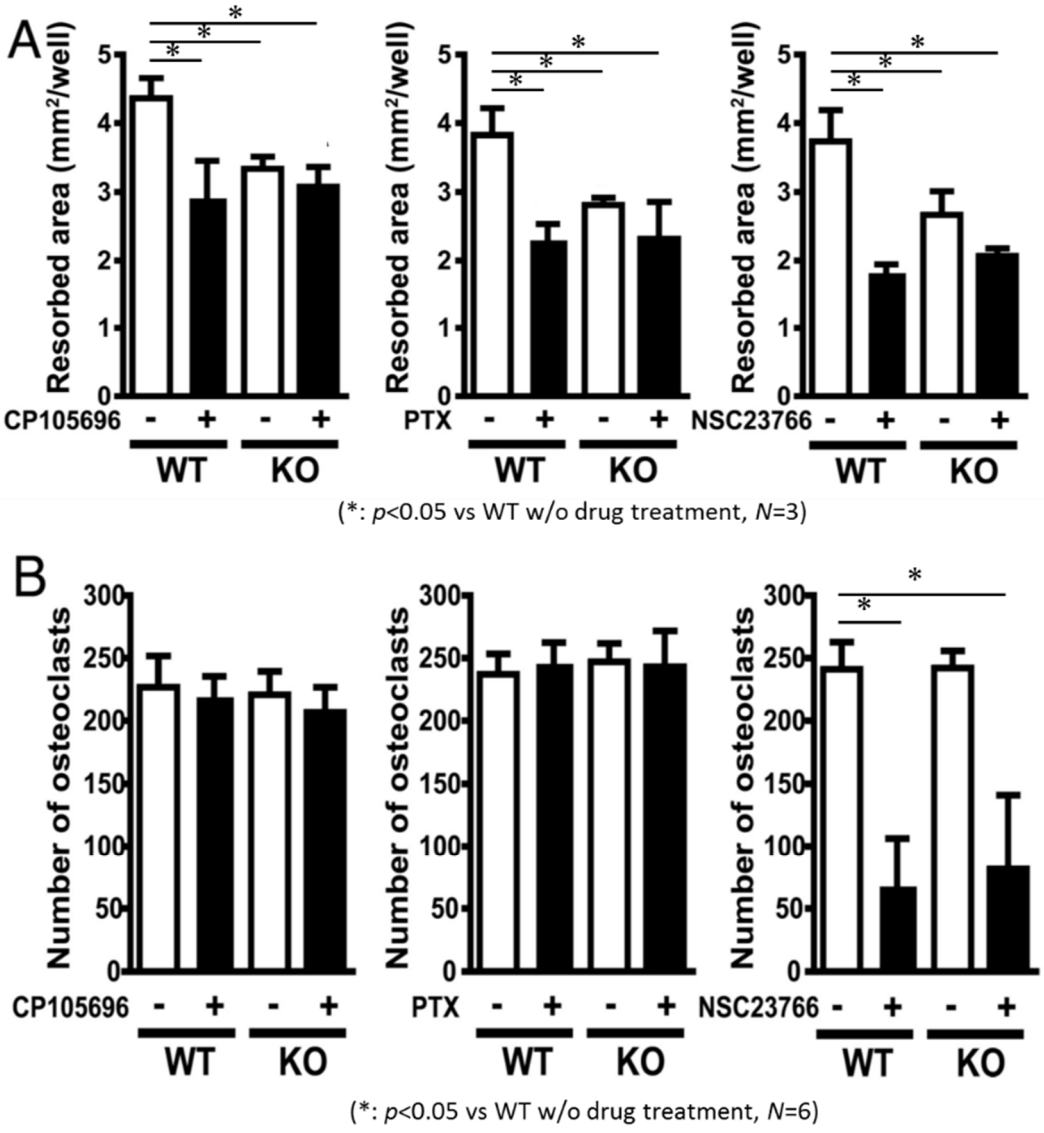

Fig. 5. Roles of BLT1, Gi and Rac1 in the calcium resorption activity and osteoclast number. (A) Calcium resorption by primary osteoclasts. Osteoclasts were cultured on calcium phosphate-coated dishes for 6 days with or without 1 μM CP105696 (BLT1 antagonist), 10 ng/mL PTX (Gi protein inhibitor), or 50 μM NSC23766 (Racl inhibitor). *, $p < 0.05$ vs. WT osteoclasts without drug treatment, as

determined by ANOVA with Dunnett's multiple comparison test (n = 3 per group). (B) Number of osteoclasts. Primary osteoclasts were cultured in 96-well dishes for 5 days. The numbers of TRAP-positive multinucleated (greater than or equal to three nuclei) cells per well were counted. *, $p < 0.05$ vs. WT osteoclasts without drug treatment, as determined by ANOVA with Tukey's multiple comparison test (n = 6 per group).

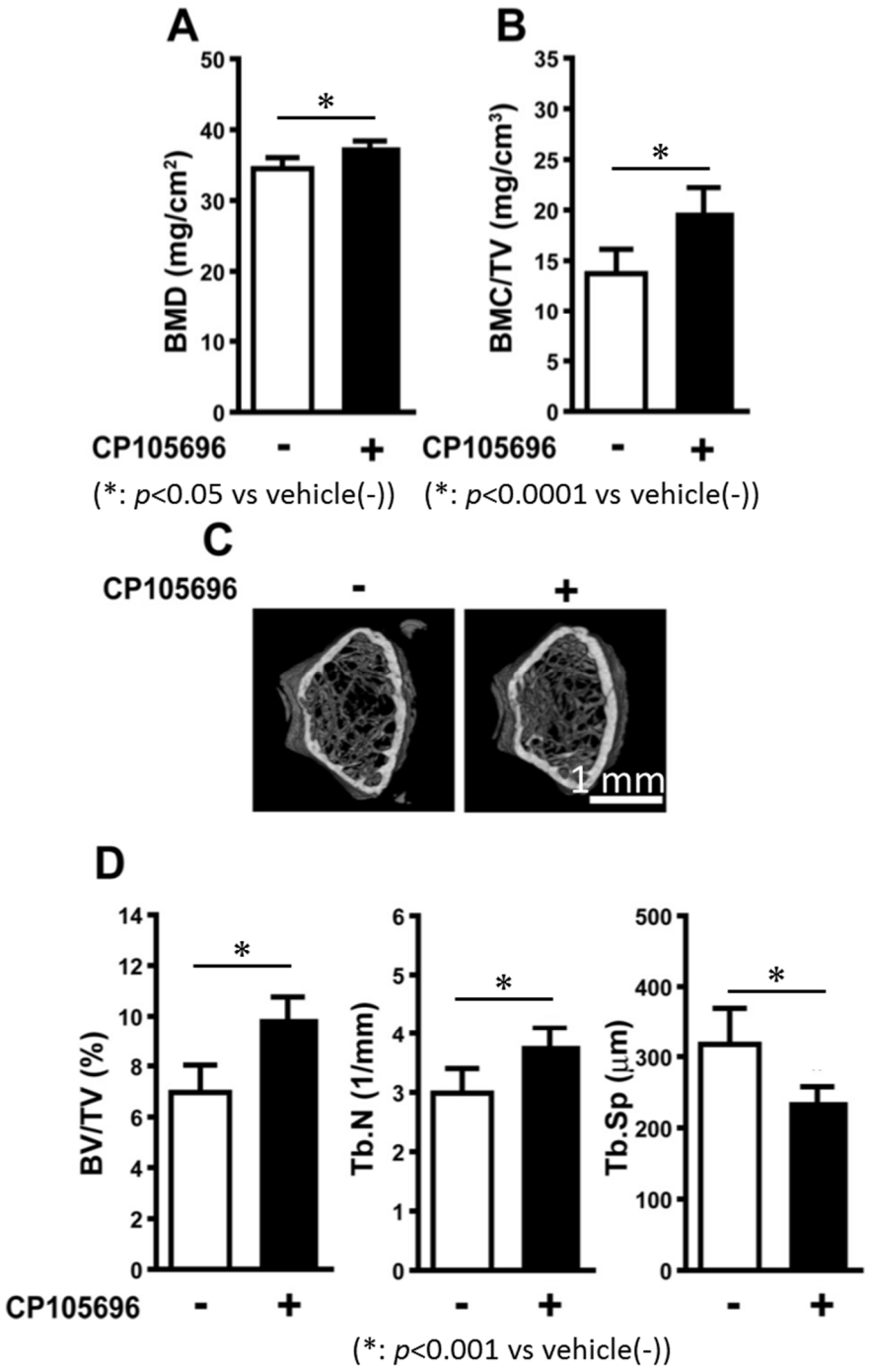

Fig. S1. Radiographic and morphometric analyses of hindlimb bones from mice treated with a BLT1 antagonist. (A) Areal bone mineral density (BMD) of the metaphyseal

region of the femur measured by DXA. Female mice treated with the BLT1 antagonist CP105696 (n = 8) or vehicle (n = 12) were ovariectomized. *, $p < 0.05$ vs. vehicle, as determined by two-tailed unpaired t test. (B) Trabecular bone mineral content per tissue volume (BMC/TV) of the metaphyseal region of the femur measured by microCT. Data are shown as described for A. *, $p < 0.0001$ vs. vehicle, as determined by two-tailed unpaired ttest (n = 8 animals in CP105696-treated group and n = 12 animals in vehicle-treated group). (C) Representative microCT photographs of the metaphyseal regions of femurs. Note the highly porous inside of the bone (transparent regions) in the vehicle-treated ovariectomized mice compared with CP105696-treated ovariectomized mice. (Scale bar, 1 mm.) (D) Trabecular bone volume per tissue volume (BV/TV), trabecular number (Tb.N), and trabecular separation (Tb.Sp) of the metaphyseal region of the femur from ovariectomized mice. These bone mass indices were quantified based on analyses of three-dimensional microCT images of the metaphyseal region of the femur. *, $p < 0.001$ vs. vehicle, as determined by two-tailed unpaired t test (n = 8 animals in CP105696-treated group and n = 12 animals in vehicle-treated group).

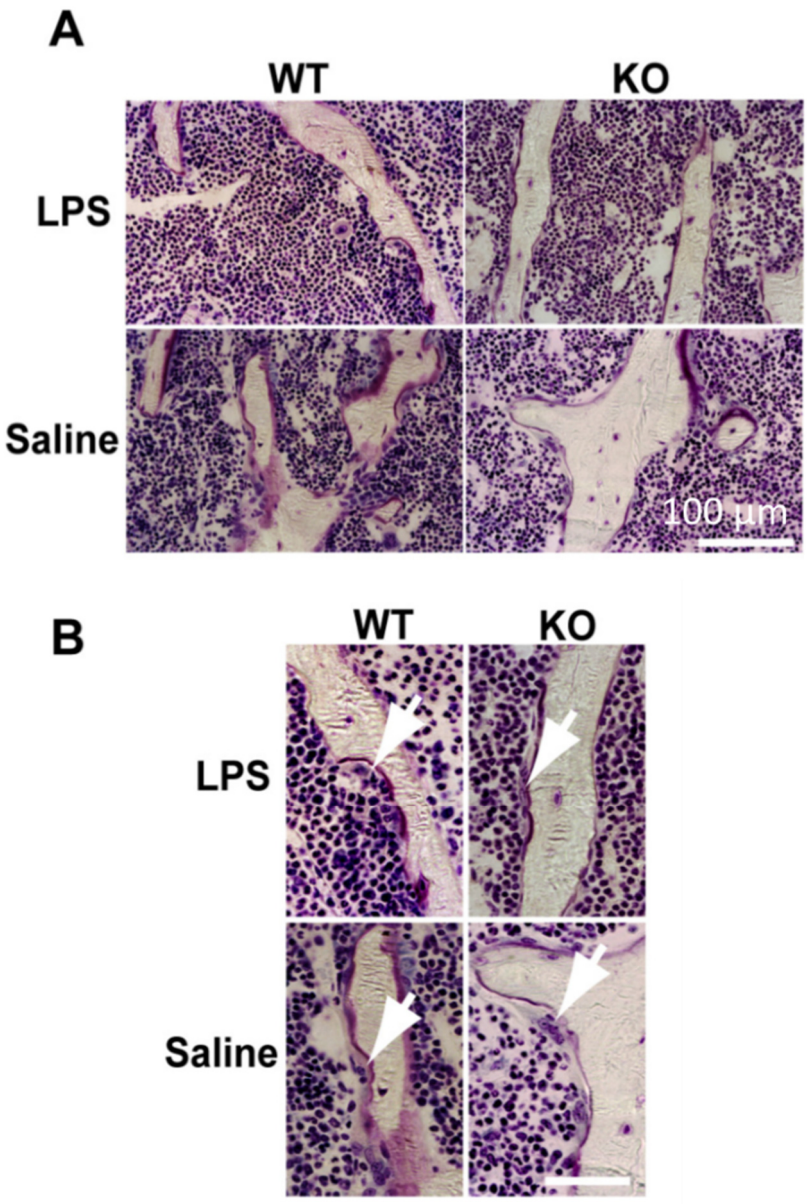

Fig. S2. Histology of tibias from LPS-injected mice. (A) Images of Villanueva bone staining of the metaphyseal region of the tibia. (Scale bar, 100 μm.) (B) High magnification images of osteoclasts. White arrows, osteoclasts. (Scale bar, 50 μm.)

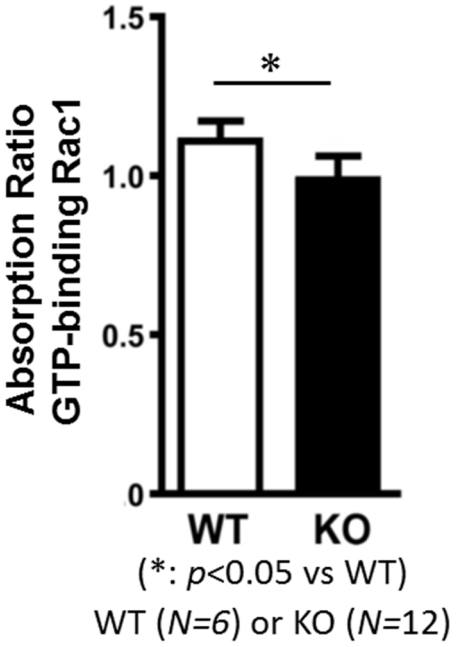

Fig. S3. Rac activation in LTB_4-treated osteoclasts. ELISA for Rac in an active GTP-bound state was performed. The absorbance ratio (LTB_4-treated cells per control cells) of WT mice was compared with that of BLT1-KO mice. *, $p < 0.05$ vs. WT osteoclasts, as determined by two-tailed unpaired ttest (n = 6 in WT group and n = 5 in BLT1-KO group).

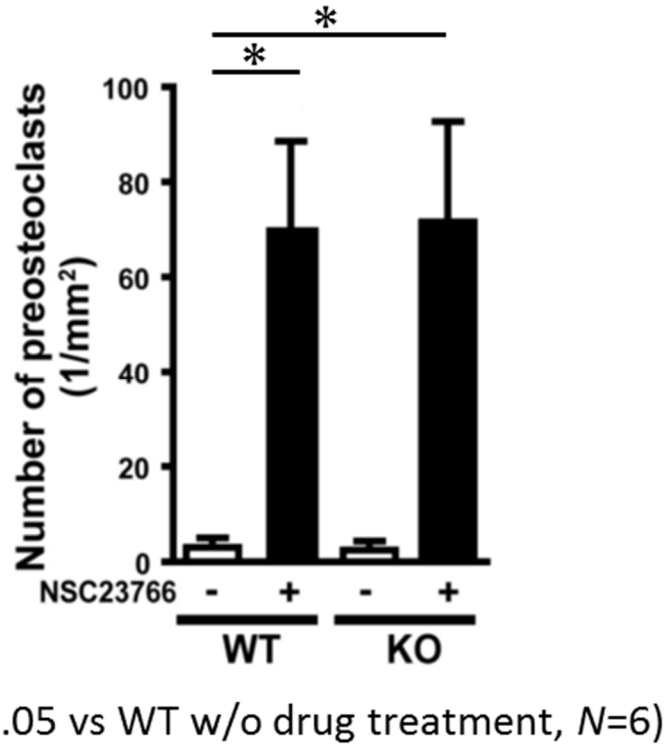

Fig. S4. Role of Rac1 in preosteoclast number. Number of preosteoclasts defined as TRAP-positive cells with less than three nuclei was measured. *, $p < 0.001$ vs. WT osteoclasts without drug treatment, as determined by ANOVA with Tukey's multiple comparison test (n = 6 each).

Chapter 3

TDAG8 activation inhibits osteoclastic bone resorption

Abstract

Although the roles of acids in bone metabolism are well characterized, the function of proton-sensing receptors in bone metabolism remains to be explored. In this study, I evaluated the role of the proton-sensing receptor T-cell death-associated gene 8 (TDAG8) in osteoclastic activity during bone loss following ovariectomy. Through observations of bone mineral content, I found that pathological bone resorption was significantly exacerbated in mice homozygous for a gene trap mutation in the *Tdag8* gene. Furthermore, osteoclasts from the homozygous mutant mice resorbed calcium in vitro more than the osteoclasts from the heterozygous mice did. Impaired osteoclast formation under acidic conditions was ameliorated in cultures of bone marrow cells by the *Tdag8* gene mutation. Extracellular acidification changed the cell morphology of osteoclasts via the TDAG8-Rho signaling pathway. These results suggest that the enhancement of the TDAG8 function represents a new strategy for preventing bone resorption diseases, such as osteoporosis.

Introduction

Bone remodeling is required for the optimal control of calcium homeostasis and is performed by the concerted actions of osteoclasts and osteoblasts (*119*). Osteoclasts are multinucleated cells that are unique in their ability to degrade bone, and osteoclastic activities are regulated by hormones such as parathyroid hormone, vitamin D3 and calcitonin (*119*). Furthermore, there are paracrine/autocrine factors, such as platelet-activating factor (*103*) and leukotriene B_4 (*5*), which affect osteoclastic activities.

Bone resorption is initiated by the secretion of protons through vacuolar-type ATPase and the passive transport of chloride through a chloride channel (*119*). To generate protons, carbonic anhydrase converts CO_2 and H_2O into protons and HCO_3^-. Osteoclast-mediated extracellular acidification enhances bone resorption, which resulted in the formation of resorbing compartments (that is, lacunae) on the bone surfaces (*120*). Although osteoclasts create the local extracellular acidic milieu around themselves, it is still unknown how osteoclasts detect and respond to this extracellular acidity.

There are two families of membrane proteins that are activated by extracellular pH: acid-sensing ion channels (*121*) and acid-sensing G-protein-coupled receptors (*122*). The latter includes the ovarian cancer G-protein-coupled receptor 1 (OGR1, also known as GPR68) (*123*), GPR4 (*123*), G2A (also known as GPR132) (*124*) and T-cell death-

associated gene 8 (TDAG8, also known as GPR65) (*125, 126*). In humans, *TDAG8* mRNA is highly expressed in peripheral blood leukocytes, lymph nodes and the spleen (*127*). Previously, Ishii et al. showed that human TDAG8 stimulates cyclic adenosine monophosphate (cAMP) formation, activates Rho and induces stress fiber formation in response to extracellular acidification in stably transfected cells (*125*). They also revealed that TDAG8 mediates the extracellular acidification-induced inhibition of pro-inflammatory cytokine production in mouse macrophages (*128*). In addition, they recently demonstrated that TDAG8 promotes tumor cell growth and survival in vivo and in vitro, strongly suggesting that TDAG8 serves as an extracellular proton sensor responsible for the adaptation of the tumor to the acidic milieu (*129*).

Ovariectomy, a model of postmenopausal osteoporosis, causes bone resorption by an acute decrease in serum estrogen levels (*130*). Estrogen deficiency results in a bone-remodeling imbalance in which bone resorption exceeds bone formation (*119*). Because osteoclasts are the major cells involved in bone loss (*96*), they play an important role in bone resorption of ovariectomized mice. In the present study, I found an inhibitory role for TDAG8 in osteoclastic bone resorption through the analysis of ovariectomized mice homozygous for a gene trap mutation in the *Tdag8* gene (*Tdag8*$^{gt/gt}$) (*131*). My in vitro data consistently demonstrated that the *Tdag8* gene mutation resulted in an increase

in osteoclastic activity, suggesting that TDAG8 in osteoclasts counteracts the increased bone resorption in osteoporosis by sensing the extracellular acidic milieu.

Materials and methods

Mice

All animal procedures were performed in accordance with the guidelines for animal research at The University of Tokyo and were approved by The University of Tokyo Ethics Committee for Animal Experiments. The *Tdag8* mutant (TM88) mouse line was generated by the gene trap strategy (*131*). The *Sleeping Beauty* transposon was inserted into the genome of a male mouse germ-line cell on a mixed (BDF1 and ICR) genetic background. The insertion site mapped to intron 1 of the *Tdag8* gene. The *Sleeping Beauty* transposon contains a splicing acceptor sequence, internal ribosome entry site, ß-galactosidase gene, polyadenylation signal, CAG promoter, GFP gene and splicing donor sequence (*131*). Therefore, this insertion mutated the *Tdag8* gene by forcing exon 1 at the 5' end of the insertion site to splice with the splice acceptor of the *Sleeping Beauty* transposon and by preventing it from splicing to exon 2 at the 3' end of the insertion site, thereby preventing the production of the mature *Tdag8* mRNA (*131*). *Tdag8*$^{+/gt}$ mice were backcrossed for nine generations with C57BL/6N mice. *Tdag8*$^{gt/gt}$ mice were then obtained by mating with *Tdag8*$^{+/gt}$ mice. The genotypes of the offspring were determined as described previously (*128*). *Tdag8*$^{+/gt}$ and/or WT littermates were used as the controls. The mice were given access to a standard laboratory diet and

water *ad libitum*.

Ovariectomy

Tdag8$^{gt/gt}$, *Tdag8*$^{+/gt}$ and WT female mice (10 weeks old) underwent either bilateral ovariectomy or a sham procedure in which the bilateral ovaries were exteriorized but not removed under anesthesia by intraperitoneal injection of sodium pentobarbital (Somnopentyl; 50 mg/kg body weight; Kyoritsu, Tokyo, Japan). The mice were euthanized 4 weeks after the surgical procedure. The body weights of *Tdag8*$^{gt/gt}$ female mice (ovariectomized group, 22.1 ± 1.4 g [n = 11]; sham-operated group, 21.7 ± 1.5 g [n = 12]) were indistinguishable from those of the WT female mice (ovariectomized group, 22.1 ± 1.1 g [n = 11]; sham-operated group, 21.3 ± 1.3 g [n = 9]) and *Tdag8*$^{+/gt}$ female mice (ovariectomized group, 22.8 ± 1.5 g [n = 11]; sham-operated group, 23.6 ± 2.2 g [n = 10]).

Analysis of bone phenotypes

Mouse hind-limb bones were subjected to radiographic examinations. The femurs were dissected and stored in 70% ethanol. MicroCT (inspeXio SMX-90CT; Shimadzu, Kyoto, Japan) was used to assess the bone mineral content and bone mass of the

trabecular bone in the distal femoral metaphysis using a 12-μm isotropic voxel size with 40 kV of tube voltage and 100 μA of tube current. Three-dimensional CT images were reconstituted and analyzed using a TRI-system (Ratoc, Tokyo, Japan).

Primary osteoclast culture

Bone marrow was flushed from the femurs and tibias of 6–8-week-old male mice. Osteoclasts were differentiated from the bone marrow cells by stimulation with RANKL and M-CSF (*85*). Briefly, the bone marrow cells from one or two mice were cultured in αMEM (Life Technologies, Rockville, MD, USA) containing 10% FBS (SAFC Biosciences, Lenexa, KS, USA) with soluble RANKL (30 ng/ml; PeproTech, Rocky Hill, NJ) and M-CSF (50 ng/ml; R&D Systems, Minneapolis, MN, USA) for 5 days. The cells were then stained with 0.01% naphthol AS-MX phosphate (Sigma-Aldrich, St. Louis, MO, USA) in the presence of 100 mM L(+)-tartaric acid (pH 5.0; Wako, Osaka, Japan) to detect tartrate-resistant acid phosphatase (TRAP) activity. TRAP-positive cells with more than three nuclei were counted as viable osteoclasts.

RT-PCR analysis

RNA was extracted from the primary osteoclasts cultured in the presence of RANKL

(30 ng/ml) and M-CSF (50 ng/ml) for 5 days with or without dexamethasone (100 nM) added for the final 24 h. cDNA was synthesized from 0.8 μg total RNA by oligo(dT) priming using Superscript II reverse transcriptase (Life Technologies). To quantify the mRNA levels of *Tdag8* and *β-actin*, the resultant cDNA was amplified by real-time PCR using the following primers: mouse *Tdag8*, 5'-GAATCTTACAGGAGATTGGAGATTG-3' and 5'-GCTGTGCTATGTTGCTCTAGACTT-3' and mouse *β-actin*, 5'-AATTGAATGTAGTTTCATGGATGC-3' and 5'-AAGAGAAGCATCCCTCCAGAAAC-3'. The following protocol was used: 40 cycles of 95°C for 15 s, 60°C for 5 s and 72°C for 5 s. The cDNA was amplified by PCR using the following primers: mouse *Gpr4*, 5'-CTCTCTACATCTTCGTCATCGG-3' and 5'-CGGTAGCACAGCAACATGAGTG-3'; mouse *Ogr1*, 5'-AGCCAACTGCCTGTCCCT-CTACTTCG-3' and 5'-CAGGCAGATGGGGAAGAGAAAGC-3'; mouse *G2a*, 5'-CTGCCTCAGGACTGGCTTGG-3' and 5'-TCACACACGCAGAAATGGTGAC-3'; and mouse *β-actin*, 5'-CACAGGCATTGTGATGGAC-3' and 5'-CTTCTGCATCCTGTCAGC-3'. The following protocol was used: 35 cycles of 94°C for 10 s, 56°C for 10 s and 72°C for 20 s. The PCR products were electrophoresed on 1% agarose gels and stained with ethidium bromide.

Osteoclast formation assay

Bone marrow cells were cultured in αMEM containing 10% FBS with soluble RANKL (30 ng/ml) and M-CSF (50 ng/ml) for 2 days. The pH of the medium was changed from 7.4 to 7.0 on day 2. The number of osteoclasts was counted on day 5.

Calcium resorption assay

Bone marrow cells were cultured in αMEM containing 10% FBS with soluble RANKL (30 ng/ml) and M-CSF (100 ng/ml) for 9 days on calcium phosphate-coated dishes (BioCoat Osteologic bone culture system; BD Biosciences, Franklin Lakes, NJ, USA). After removal of the cells with a bleach solution (6% NaOCl and 5.2% NaCl), the dishes were washed with water and photographed under a light microscope (BH-2; Olympus, Tokyo, Japan). The area of the calcium phosphate-resorbed pits was measured, using the image-processing application software ImageJ (NIH, Bethesda, MD, USA).

Confocal microscopy

Bone marrow cells were seeded onto 35-mm poly-D-lysine-coated glass-bottomed dishes (Iwaki, Tokyo, Japan) in αMEM containing 10% FBS with soluble RANKL (30 ng/ml) and M-CSF (100 ng/ml). On day 5, the osteoclasts were fixed in PBS containing 3.7% formaldehyde for 10 min and permeabilized with 0.1% Triton X-100 (Sigma-

Aldrich) in PBS for 5 min. For actin labeling, the osteoclasts were incubated with 0.03% rhodamine-phalloidin and 0.1% Triton X-100 in PBS for 40 min. The stained cells were observed using a confocal laser-scanning microscope (LSM510; Carl Zeiss, Oberkochen, Germany).

Osteoclast survival assay

Bone marrow cells were cultured in αMEM containing 10% FBS with soluble RANKL (30 ng/ml) and M-CSF (50 ng/ml) for 4 days. The pH of the medium was changed from 7.4 to 7.6, 7.4, 7.0 or 6.4 on day 4, and then the cells were cultured for an additional 18 h without soluble RANKL and M-CSF. To calculate the survival rate, the number of surviving osteoclasts was counted under a light microscope (BH-2; Olympus) before and after the additional 18-h incubation.

ELISA for GTP-Bound Rho

Osteoclasts were serum-starved for 15 min before treatment with a physiological salt solution (containing 130 mM NaCl, 0.9 mM NaH_2PO_4, 5.4 mM KCl, 0.8 mM $MgSO_4$, 1.0 mM $CaCl_2$, 25 mM glucose and 0.1% BSA) buffered with HEPES/EPPS/MES at pH 6.4 or 7.4 for 2 min (*123*). After cell lysis, a total of 12.5 μg protein was subjected to

ELISA for GTP-Rho using a G-LISA Rho Activation Assay Biochem kit (Cytoskeleton, Denver, CO, USA).

Statistical analysis

All of the values are expressed as the mean ± s.d. The mean values of multiple groups were compared by analysis of variance (Prism; GraphPad Software, La Jolla, CA, USA). The statistical significance of the differences was determined by Dunnett's multiple comparison test. The mean values of two groups were compared using the unpaired two-tailed *t*-test (Prism; GraphPad Software). Values of $p < 0.05$ were considered statistically significant.

Results

Tdag8$^{gt/gt}$ mice are susceptible to bone loss induced by ovariectomy.

Horie et al. constructed *Tdag8*$^{gt/gt}$ mice using the *Sleeping Beauty* transposon system (*131*); these mice contained a transposon insertion in the *Tdag8* gene on a C57BL/6N genetic background. I examined the role of TDAG8 in bone resorption of ovariectomized mice. Using microcomputed tomography (μCT) analysis, the trabecular bone mineral content per tissue volume (BMC/TV) of the metaphyseal region in the femurs of ovariectomized female mice was compared with that of sham-operated mice. "Tissue volume" means the volume of the total bone tissue and includes the trabecular bone and bone marrow but not the cortical bone. As expected, the BMC/TV values were significantly reduced by ovariectomy in *Tdag8*$^{gt/gt}$ mice as well as *Tdag8*$^{+/gt}$ mice and wild-type (WT) mice served as the controls (Fig. 1A, upper left). Of note, the BMC/TV value of the ovariectomized *Tdag8*$^{gt/gt}$ mice was significantly less than that of the ovariectomized *Tdag8*$^{+/gt}$ and WT mice.

The μCT analysis also revealed that the trabecular bone volume per tissue volume (BV/TV) in the metaphyseal region of the femurs was significantly reduced in the ovariectomized *Tdag8*$^{gt/gt}$ mice, *Tdag8*$^{+/gt}$ mice and WT mice, compared with individual sham-operated mice (Fig. 1A, upper right). Similar to the BMC/TV value, the

ovariectomized *Tdag8*$^{gt/gt}$ mice displayed a greater reduction in the femoral BV/TV than the ovariectomized *Tdag8*$^{+/gt}$ mice or WT mice. Two other parameters related to BV/TV, the trabecular number (the linear density of the trabecular bone, Fig. 1A, lower left) and trabecular separation (the distance between the edges of the trabecular bone, Fig. 1A, lower right), also indicated that the bone volume of the ovariectomized *Tdag8*$^{gt/gt}$ mice significantly decreased compared with that of the ovariectomized *Tdag8*$^{+/gt}$ or WT mice (Fig. 1B). Taken together, *Tdag8*$^{gt/gt}$ mice developed more severe bone resorption than the *Tdag8*$^{+/gt}$ or WT mice did. Therefore, TDAG8 appears to protect bone from aberrant resorption following ovariectomy.

Tdag8 mRNA is expressed in primary osteoclasts.

Given that local acidic milieu is created only by osteoclasts, it is reasonable to assume that TDAG8 is activated by protons on the cell surface of osteoclasts in an autocrine manner. Thus, I focused on osteoclasts in the following studies. To elucidate the role of *Tdag8* gene in osteoclastic activity, the expression of *Tdag8* mRNA was investigated in the primary osteoclasts. As shown in Figure 2A, *Tdag8* mRNA expression was detected in the primary osteoclasts that were differentiated from the bone marrow cells in the presence of the receptor activator of NF-κB ligand (RANKL)

and macrophage colony-stimulating factor (M-CSF). In the thymus, glucocorticoid (dexamethasone) has been shown to increase the expression of *Tdag8* gene (*131-133*), and I consistently observed that dexamethasone enhanced the expression of *Tdag8* mRNA in the osteoclast cultures (Fig. 2A). Among the three other proton-sensing G-protein-coupled receptor tested, both *Ogr1* and *G2a* mRNAs were expressed in the primary osteoclasts, whereas *Gpr4* mRNA was not detected (Fig. 2B).

TDAG8 deficiency enhances osteoclast formation and osteoclastic calcium resorption.

Under the more acidic culture conditions at pH 7.0 compared with the physiological culture conditions at pH 7.4, osteoclast formation was inhibited in the bone marrow cell cultures derived from *Tdag8*$^{+/gt}$ mice (Fig. 3A). Furthermore, the resulting *Tdag8*$^{+/gt}$ osteoclasts were rather small (Fig. 3B). However, the observed inhibition was ameliorated in *Tdag8*$^{gt/gt}$ osteoclasts (Fig. 3A), which were larger than *Tdag8*$^{+/gt}$ osteoclasts at acidic pH (Fig. 3B). These results show that *Tdag8*$^{gt/gt}$ osteoclast formation is resistant to acidic pH. Although osteoclast formation in *Tdag8*$^{gt/gt}$ mice was not significantly different from that in *Tdag8*$^{+/gt}$ mice at pH 7.4, *Tdag8*$^{gt/gt}$ osteoclasts resorbed more calcium than *Tdag8*$^{+/gt}$ osteoclasts in vitro (Fig. 3C, D). This result indicates that the calcium-resorbing activity of individual *Tdag8*$^{gt/gt}$ osteoclasts is

enhanced compared with *Tdag8*$^{+/gt}$ osteoclasts in the medium even at normal pH.

I also observed that the survival rate of the osteoclasts increased under acidic conditions. The survival rate of the *Tdag8*$^{gt/gt}$ osteoclasts under acidic conditions was similar to that of the *Tdag8*$^{+/gt}$ osteoclasts (Fig. 3E), suggesting that the increased survival of osteoclasts under acidic conditions is independent of TDAG8.

TDAG8 changes the morphology of osteoclasts.

The regulation of morphological changes in osteoclasts is highly related to their functions (*96, 134*). Because the *Tdag8*$^{+/gt}$ and *Tdag8*$^{gt/gt}$ osteoclasts expressed green fluorescent protein (GFP) under the control of the constitutive CAG promoter (*135*), I was able to visualize the cells under a laser-scanning confocal microscope without staining (Fig. 4A, green). The actin was stained with rhodamine-phalloidin. The "actin ring" of osteoclasts is the actin-rich peripheral sealing zone characteristic of mature osteoclasts (Fig. 4A, red) (*136*). After 40 min of stimulation with an acidic buffer at pH 6.4, the *Tdag8*$^{+/gt}$ osteoclasts looked abnormally shrunken (Fig. 4A middle left, green), and the actin ring was deformed to several small open actin circles (Fig. 4A middle left, red). In contrast, the *Tdag8*$^{gt/gt}$ osteoclasts did not alter their morphology at pH 6.4 (Fig. 4A middle right, green), although the deformation of the actin ring did occur (Fig.

4A middle right, red). Rho has been implicated in the modulation of the F-actin cytoskeleton and cell shape (*137*) and the formation of stress fibers in osteoclasts (*138*). Y-27632 is a cell-permeable and selective inhibitor of Rho-associated protein kinases (*139*). The acidic pH-induced retraction of osteoclasts was suppressed by Y-27632 (Fig. 4A lower left, green), whereas the deformation of the actin ring was not inhibited (Fig. 4A lower left, red). Upon the acid treatment, the level of active guanosine triphosphate (GTP)-bound Rho was significantly increased in the *Tdag8*$^{+/gt}$ osteoclasts but not in the *Tdag8*$^{gt/gt}$ osteoclasts (Fig. 4B). These results indicate that acidic pH stimulates the actin stress fiber-related retraction of osteoclasts through the TDAG8-Rho signaling pathway, although the deformation of the actin ring is independent of this pathway. An increase in cAMP accumulation by acidic pH was not observed in the osteoclasts, probably due to the resulting cAMP level too low to detect under my experimental conditions (*125*).

Discussion

This study is the first to demonstrate the inhibitory effects of TDAG8 on bone resorption induced by ovariectomy. An increased ability of osteoclasts to resorb calcium in vitro probably accounts for the enhanced bone resorption in ovariectomized *Tdag8*$^{gt/gt}$ mice. TDAG8 in osteoclasts is likely to counteract the enhanced bone resorption in osteoporosis by sensing the extracellular acidic milieu generated by the osteoclasts themselves.

I found the phenotypes of *Tdag8*$^{gt/gt}$ mice only after ovariectomy, that is, under estrogen-deficient conditions. Estrogen deficiency leads to increased osteoclast number and osteoclastic activity, probably due to decreasing osteoprotegerin expression and also by increasing RANKL expression in osteoblasts (*140*). In addition, the RANKL-activated osteoclasts are reported to be rich in vacuolar type-ATPase, a key molecule for extracellular acidification (*141, 142*), which is necessary for bone resorption. Thus, it is plausible that the intensely activated TDAG8 under estrogen-deficient conditions becomes involved in the regulation of osteoclastic activity in vivo.

In my in vitro culture experiments, osteoclasts were differentiated from bone marrow cells in the medium containing RANKL as well as M-CSF. Thus, I assume that the differentiated osteoclasts have already been in a state of activation, recapitulating the

estrogen-deficient conditions in vivo. Given the accelerated formation and enhanced calcium resorption of the *Tdag8*$^{gt/gt}$ osteoclasts in vitro, the proton-sensing signaling through TDAG8 appears to negatively regulate the formation and function of osteoclasts in the pathological state.

It is interesting that the *Tdag8*$^{gt/gt}$ osteoclasts showed enhanced calcium resorption even under a regular pH condition. This observation strongly suggests that TDAG8 actually senses the local acidic milieu beneath osteoclasts, leading to the regulation of osteoclastic calcium resorption under the in vitro culture conditions.

There are four proton-sensing G-protein-coupled receptors: OGR1 (*123*), GPR4 (*123*), G2A (*124*) and TDAG8 (*125, 126*). I detected mRNA expression of all of these genes, except *Gpr4*, in primary mouse osteoclasts. Among these proton sensors, OGR1 has been considered to enhance osteoclast formation and bone resorption (*143-145*). Activation of OGR1 in RAW 264.7 osteoclast-like cells was shown to mediate calcium influx by acid stimulation (*144*), which is consistent with the report of Ludwig *et al.* (*123*). Meanwhile, acid-stimulated TDAG8 elicited cAMP production, Rho activation and stress fiber formation (*125, 126*). Thus, there may be a balance between these two proton-sensing G protein-coupled receptor s to maintain normal osteoclast formation and function under acidic conditions.

The actin ring is located within the podosomes, which are small cell processes and serve as adhesion structures in the marginal zone of osteoclasts (*136, 146, 147*). The podosomes contain F-actin filaments and numerous other proteins; cortactin, gelsolin, Wiskott-Aldrich syndrome protein and actin-related protein 2/3 complex are present within the podosome core, whereas integrins and the integrin-associated proteins paxillin, talin and vinculin are localized around the podosome core (*147*). These podosome-related proteins are involved in podosome organization (*136, 147*). Because acidic pH would destroy the structure of these molecules independently of TDAG8, this may explain the comparable deformation of the actin ring observed in the *Tdag8*$^{+/gt}$ and *Tdag8*$^{gt/gt}$ osteoclasts.

In conclusion, I propose that TDAG8 functions in inhibiting bone resorption; this mechanism is possibly responsible for maintaining bone homeostasis. Many therapeutic agents are currently being investigated to prevent bone resorptive disease (*118*). My findings suggest that chemical compounds with agonist and/or potentiator activity at TDAG8 can act as therapeutic agents for bone resorptive diseases such as osteoporosis.

Legends

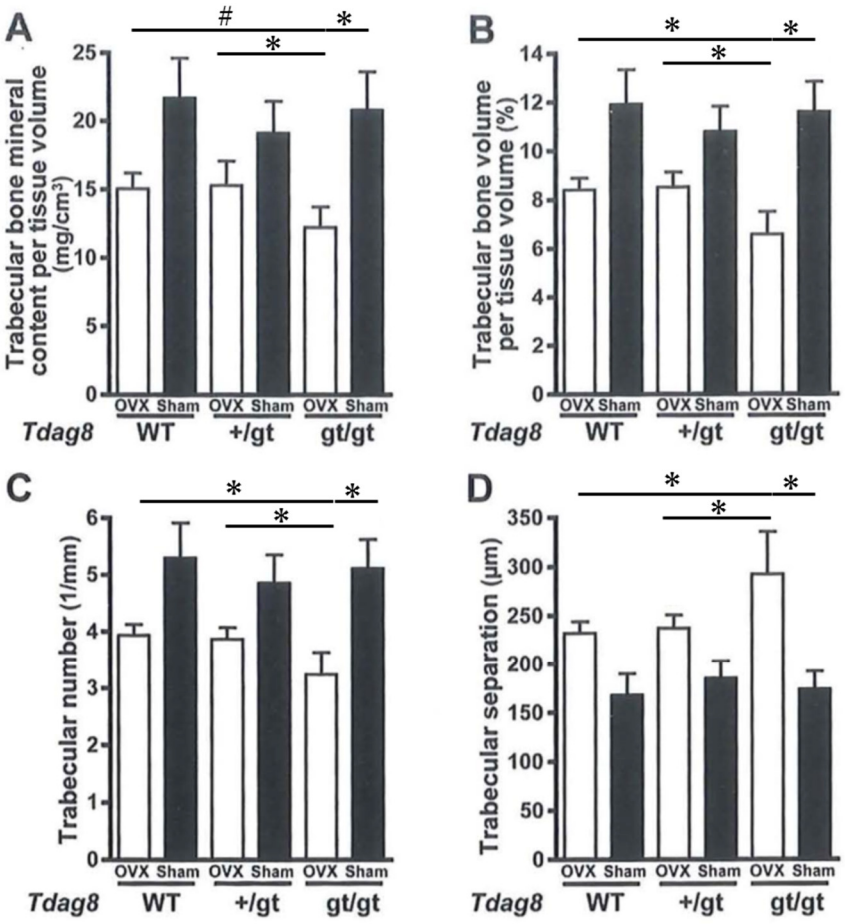

(*: p<0.05 vs ovariectomized *TDAG8* $^{gt/gt}$, N=9-12)

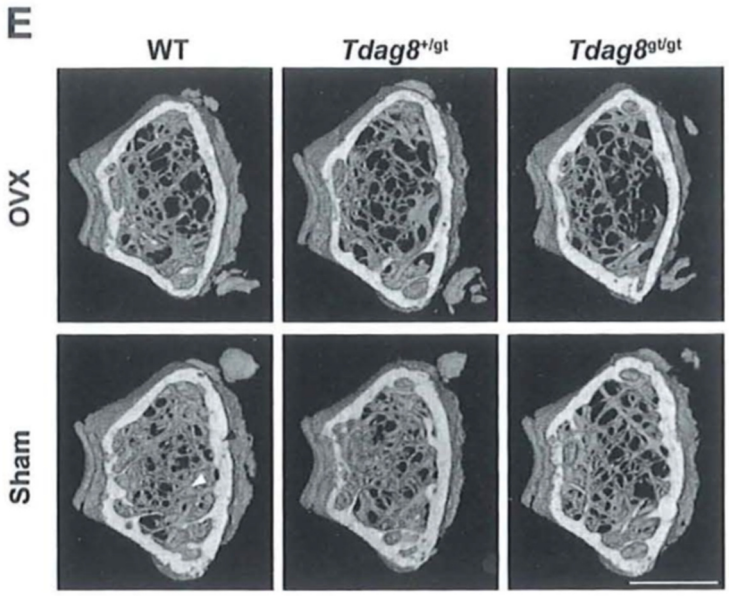

Fig 1. Radiographic analysis of the hind-limb bones. (A-D) Morphometric analysis of the metaphyseal region of the femur from ovariectomized mice using microcomputed tomography (μCT). *$p < 0.01$, #$p < 0.01$ and !$p < 0.05$ *vs.* ovariectomized *Tdag8*$^{gt/gt}$ mice (n = 9–12 animals from at least 5 independent experiments). (E) Representative μCT photographs of the metaphyseal region of the femurs. Black and white arrowheads indicate cortical and trabecular bone, respectively. Note the highly porous inside of the bone in the ovariectomized *Tdag8*$^{gt/gt}$ mice. Bar, 2 mm. OVX, ovariectomized; Sham, sham-operated.

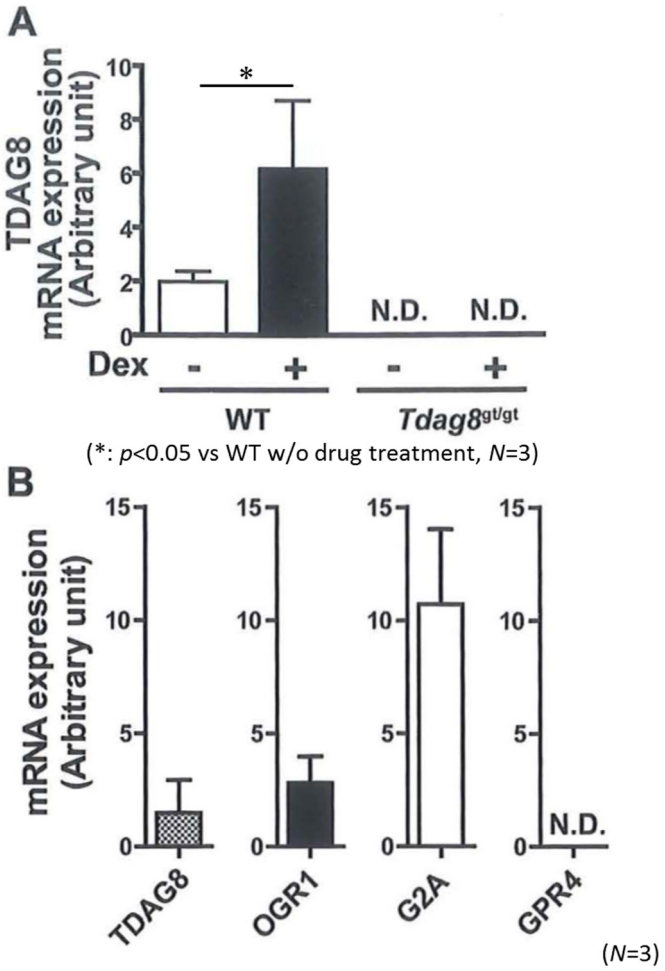

Fig 2. Expression of proton-sensing G-protein-coupled receptors in the primary osteoclasts. (A) Quantitative analysis of *Tdag8* mRNA expression in osteoclasts differentiated from bone marrow cells in the presence of RANKL (30 ng/ml) and M-CSF (50 ng/ml) for 5 days with or without dexamethasone (Dex; 100 nM) for the final 24 h. *$p < 0.05$ *vs.* WT osteoclasts without drug-treatment ($n = 3$ independent cultures). Similar results were obtained in three independent experiments. (B) Detection of the mRNA expression of *Gpr4*, *Ogr1*, *G2a* and *β-actin* in osteoclasts. Data from three independent primary osteoclast cultures (#1–#3) are shown. RT, reverse transcriptase.

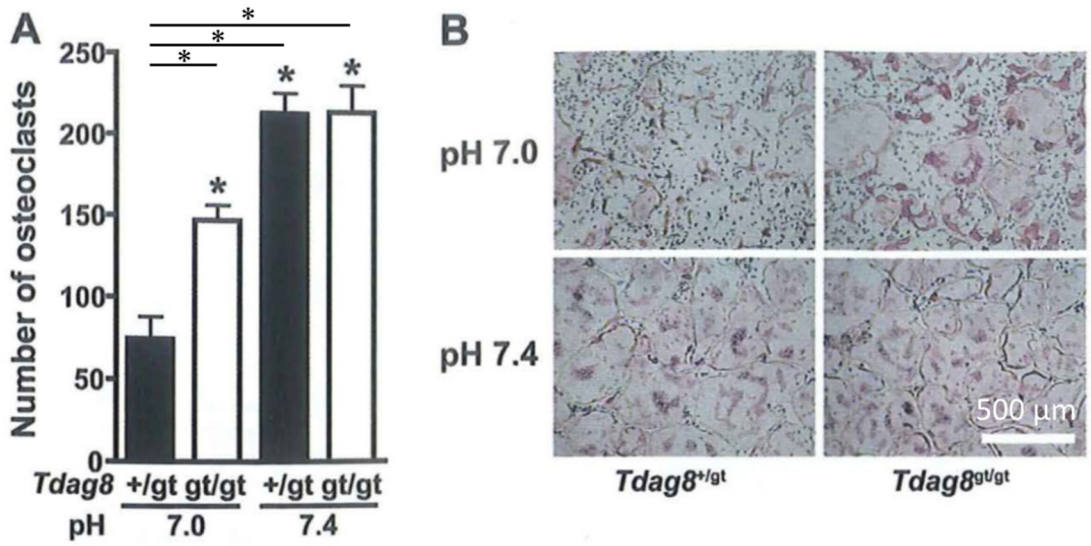

(*: p<0.001 vs *TDAG8* $^{gt/gt}$ at pH 7.0, N=3)

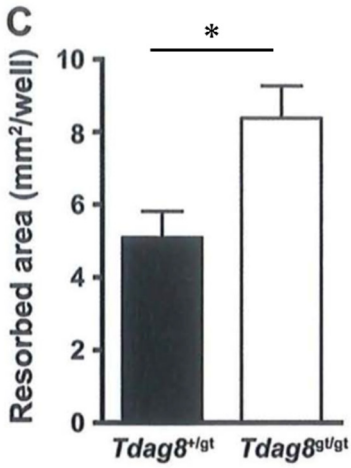

(*: p<0.075 vs *TDAG8* $^{+/gt}$, N=3)

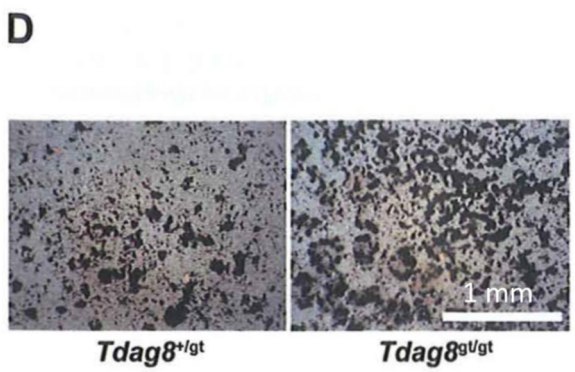

(*: p<0.05 vs *TDAG8* $^{gt/gt}$ at pH 7.6, N=6)

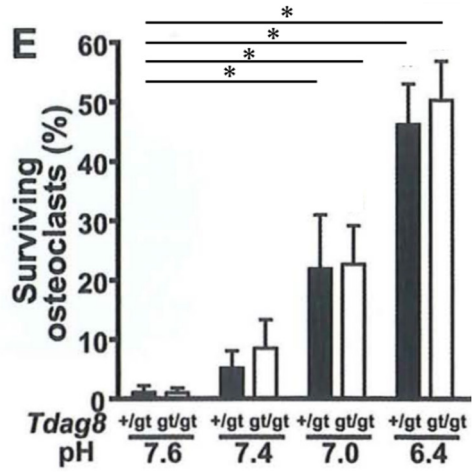

Fig 3. Role of TDAG8 in the formation, calcium resorption activity and survival rate of osteoclasts. (A) Osteoclast formation from bone marrow cells. *$p < 0.001$ *vs.* *Tdag8*$^{+/gt}$ osteoclasts cultured at pH 7.0 ($n = 6$ wells). (B) Tartrate-resistant acid phosphatase (TRAP)-stained images of the primary osteoclasts. The number of *Tdag8*$^{+/gt}$ osteoclasts was lower than that of the *Tdag8*$^{gt/gt}$ osteoclasts at pH 7.0. Bar, 500 μm. (C) Calcium resorption by the primary osteoclasts. Osteoclasts were cultured on calcium phosphate-coated dishes at pH 7.4. *$p = 0.0075$ *vs.* *Tdag8*$^{+/gt}$ osteoclasts ($n = 3$ wells). (D) Representative images of calcium resorption by primary osteoclasts. Bar, 1 mm. (E) Survival rate of osteoclasts under acidic conditions. The increased survival rate of the osteoclasts under acidic conditions was independent of TDAG8 ($n = 6$ wells). *$p < 0.05$ *vs.* *Tdag8*$^{+/gt}$ osteoclasts cultured at pH 7.6 ($n = 6$ wells). Similar results were obtained in three independent experiments (a, c, and e).

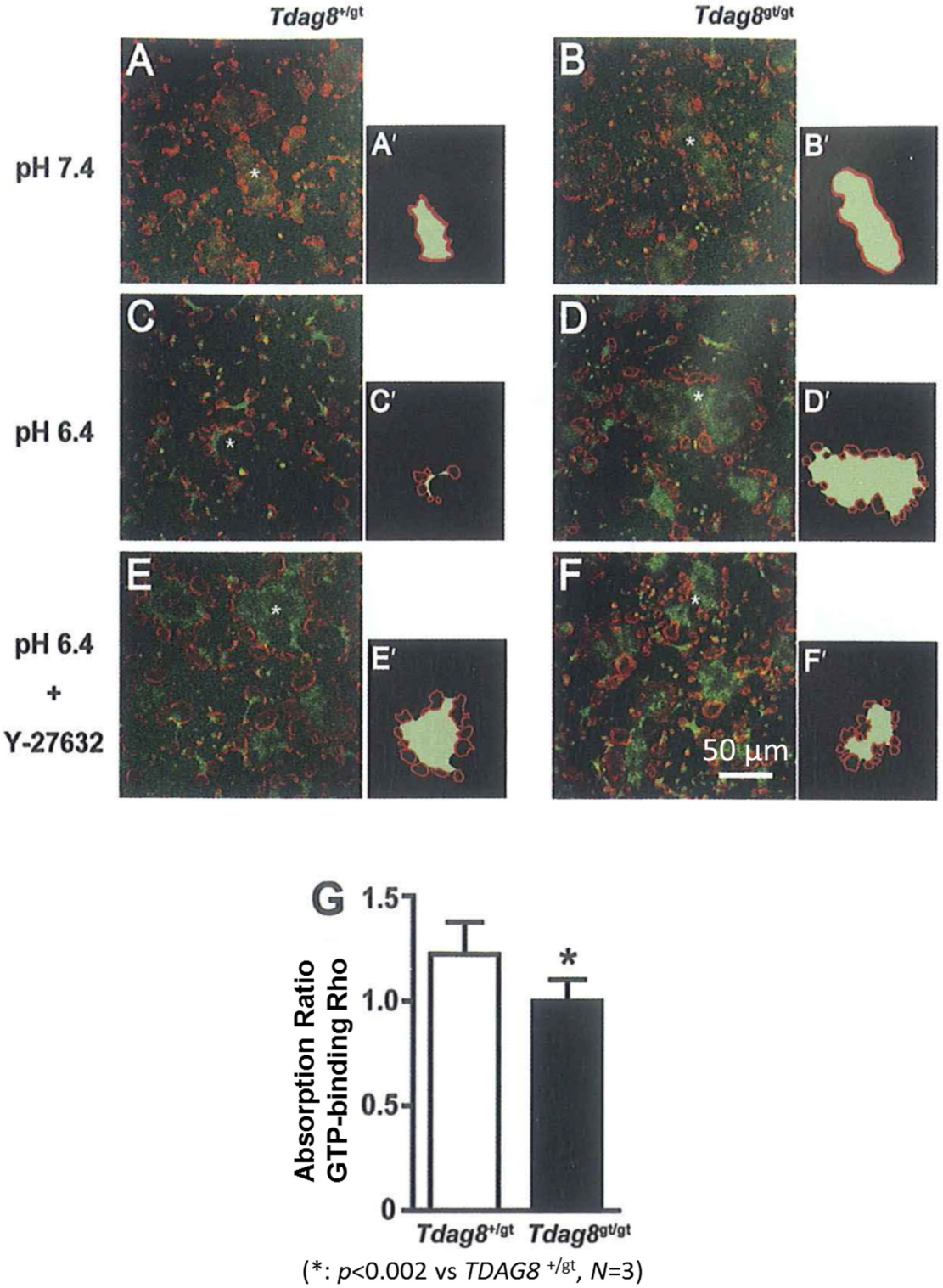

Fig 4. Morphological changes in osteoclasts mediated through the TDAG8-Rho signaling pathway. (A-F) Images of the rhodamine-phalloidin staining of the primary

osteoclasts. The *Tdag8*$^{+/gt}$ osteoclasts, which originally had a round shape, were markedly shrunken 40 min after the pH was decreased to 6.4, whereas the *Tdag8*$^{gt/gt}$ osteoclasts were unchanged. In parallel, the actin ring was comparably deformed to several small open circles after 40 min under the acidic conditions (at pH 6.4) in the *Tdag8*$^{+/gt}$ and *Tdag8*$^{gt/gt}$ osteoclasts. Bar, 50 μm. Similar results were obtained in three independent experiments. (G) Rho activation in the acid-treated osteoclasts. ELISA for Rho in an active GTP-bound state was performed in triplicate. The absorbance ratio (acid-treated cells to control cells) of *Tdag8*$^{+/gt}$ mice was compared with that of *Tdag8*$^{gt/gt}$ mice. $*p = 0.002$ *vs. Tdag8*$^{+/gt}$ osteoclasts ($n = 3$ independent experiments).

General discussion

In this dissertation, I investigated the roles of bioactive molecules associated with inflammation in bone metabolism and found that they contribute to bone remodeling and inflammation.

In Chapter 1, I demonstrated that NO directly enhances osteoblastic differentiation, but does not directly enhance cytokine-induced bone resorption. I also showed that $ONOO^-$, generated by NO and superoxide, but not NO *per se,* surpassed the stimulatory effect of NO on osteoblastic activity and inhibited osteoblastic differentiation. In Chapter 2, I showed that LTB_4 produced in osteoclasts activates BLT1 in an autocrine/paracrine manner and enhances osteoclastic bone resorption by altering cell morphology. In Chapter 3, I showed that TDAG8, a proton-sensing G-protein-coupled receptor, inhibits bone resorption.

Many inflammatory diseases including bacterial infection, such as periodontitis, cause bone destruction (*148*). Bone-forming osteoblasts and bone-resorbing osteoclasts play roles in bone remodeling and bone inflammation. Bone remodeling is a process maintained by crosstalk between these cells. The inflammation-caused uncoupling between these cells would lead to unbalanced bone resorption. Therefore, it is important to study cross-talk cell function in bone remodeling as well as to investigate

cell differentiation and function in each cell type, respectively. I have investigated roles of some bioactive molecules on osteoblastic differentiation as well as osteoclastic bone resorption in *in vitro* study. Furthermore, in *in vivo* study with bone resorption models, I have shown that the control of these molecules would rescue the bone resorptive process.

As shown in Figure 1 of the general discussion, I have demonstrated the roles of several bioactive substances in bone metabolism. I have shown that NO plays diverse roles during osteoblastic differentiation and resorption, depending on the inflammatory state. I have also demonstrated that NO directly facilitates osteoblastic differentiation, and it is not responsible for cytokine-induced bone resorption. This is the first study to show that NO has morphogenetic effects in bone. I have also demonstrated that osteoblasts have ecNOS, which may control the basal level of osteoblastic differentiation.

PG and NO are bioactive molecules, and the synthetases of these molecules are COX and NOS, respectively. NOS regulates the expression of COX by producing NO. However, lipid mediators other than PGE_2, one of the most active PGs, have not been studied in the context of bone metabolism. I have shown that LTB_4, a well-known lipid

mediator, increases bone resorption through BLT1, the LTB_4 receptor. This study is the first step toward further investigations of lipid mediators related to bone metabolism.

Most bioactive lipid receptors are GPCRs. Using phylogenetic analysis of GPCRs, I found that TDAG8, a proton-sensing GPCR, inhibits bone resorption caused by inflammation. Acids produced by osteoclasts release calcium from bone. However, to date, the role of proton-sensing receptors has not been investigated. To our knowledge, this is the first study to show that proton-sensing GPCRs play a role in bone metabolism.

The molecules discussed above have not typically been familiar to the researchers of bone biology. I have demonstrated in this dissertation that molecules involved in inflammation in other tissues, also play a role in bone remodeling. I hope that the research findings in this dissertation will serve as a stepping stone to novel developments in the study of bone biology, in particular, bone inflammation. I also hope that these findings will be applied to the treatment of bone-resorptive diseases.

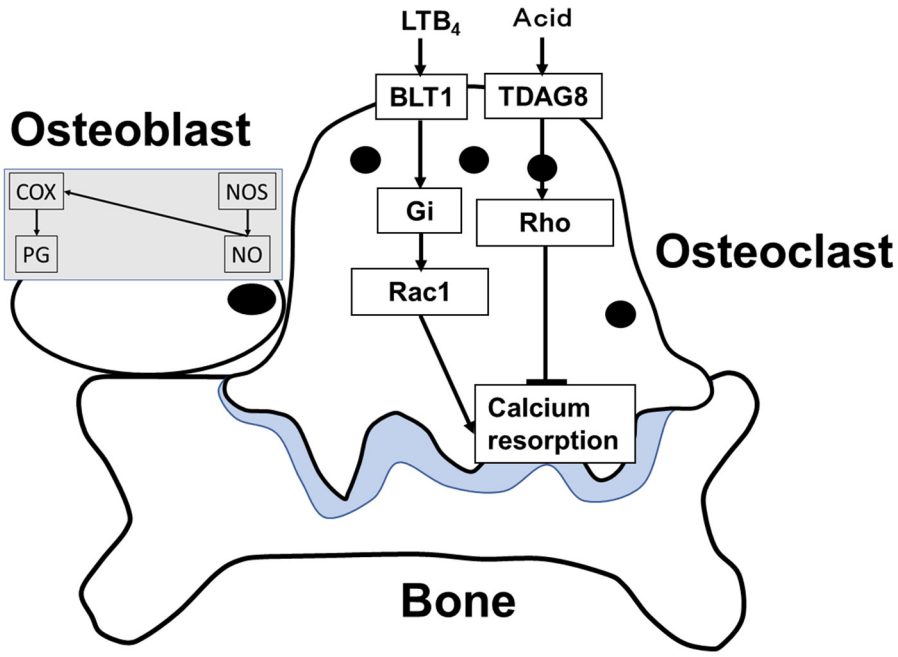

Figure 1. Schematic representation of bioactive substances related to bone inflammation.

The bioactive molecules nitric oxide (NO), leukotriene B_4 (LTB_4), and acid(s) interact with osteoblasts and osteoclasts in the bone. The receptors, intracellular signaling molecules, and enzymes related to NO, LTB_4, and acid(s) are also shown. The blue space indicates resorbed bone. COX, cyclooxygenase; NOS, nitric oxide synthase; PG, prostaglandin.

Acknowledgments

Chapter 1

Part 1

I appreciate Dr. K. Hosoi (Department of Gerontology, University of Tokyo) for kind advice to primary murine osteoblast culture and Dr. Y. Nunokawa (Suntory Institute for Biomedical Research) for designing of inducible NOS primer. A part of this work was financially supported by a grant from Grant-in-Aid for Scientific Research (No. 07557082) from the Ministry of Education, Science and Culture of Japan; the Ministry of Health and Welfare; the Fugaku Trust; Study group of Molecular Cardiology; and the Mochida Memorial Foundation for Medical and Pharmacological Research.

Part 2

I appreciate Chieko Hemmi for skillful assistance. Part of this work was financially supported by a grand in aid for scientific research from the Ministry of Education, Science, and Culture and the Ministry of Health and Welfare, the Japan Foundation for Osteoporosis, and the Sankyo Foundation for Life Sciences and Sharyo Zaidan.

Chapter 2

I thank Ms. K. Ohori and C. Kanokoda for their technical assistance and all members in my group's laboratory (Department of Biochemistry and Molecular

Biology) for their support and valuable suggestions. I am also grateful to Drs. D. W. Owens, E. Pagani, and H. Showell (Pfizer Inc.) for the BLT1 antagonist CP105696. This work was supported, in part, by Grants-in-Aid for Scientific Research from the Ministry of Education, Science, Culture, Sports, and Technology of Japan (to T.S., T.T., S.I., and H.H.), Health and Labour Sciences Research Grants for the Comprehensive Research on Aging and Health (to S.I.) and the Research on Allergic Disease and Immunology (to S.I.) from the Ministry of Health, Labour, and Welfare of Japan, a grant to the Respiratory Failure Research Group from the Ministry of Health, Labour, and Welfare of Japan (to S.I.), and grants from the 0N0 Medical Research Foundation (to S.I.) and the Takeda Science Foundation (to S.I.).

Chapter 3

I would like to thank Ms. K. Ohori and Ms. C. Kanokoda for their technical assistance. I am also grateful to all of the members of my group's laboratory (Department of Biochemistry and Molecular Biology, the University of Tokyo) for their support and valuable suggestions. This work was supported in part by Grants-in-Aid for Scientific Research from the Ministry of Education, Culture, Sports, Science and Technology of Japan (to T.S., S.I. and H.H.), Health and Labour Sciences Research

Grant for the Research on Allergic Disease and Immunology from the Ministry of Health, Labour and Welfare of Japan (to S.I.) and a grant to the Respiratory Failure Research Group from the Ministry of Health, Labour and Welfare of Japan (to S.I.).

I declare that I have no conflict of interest.

References

1. J. A. Siddiqui, N. C. Partridge, Physiological Bone Remodeling: Systemic Regulation and Growth Factor Involvement. *Physiology (Bethesda, Md.)* **31**, 233-245 (2016).
2. E. Hsu, R. Pacifici, From Osteoimmunology to Osteomicrobiology: How the Microbiota and the Immune System Regulate Bone. *Calcif Tissue Int* **102**, 512-521 (2018).
3. K. Okamoto, H. Takayanagi, Osteoimmunology. *Cold Spring Harbor perspectives in medicine* **9**, (2019).
4. T. J. Guzik, R. Korbut, T. Adamek-Guzik, Nitric oxide and superoxide in inflammation and immune regulation. *J Physiol Pharmacol : an official journal of the Polish Physiological Society* **54**, 469-487 (2003).
5. H. Hikiji, T. Takato, T. Shimizu, S. Ishii, The roles of prostanoids, leukotrienes, and platelet-activating factor in bone metabolism and disease. *Prog Lipid Res* **47**, 107-126 (2008).
6. K. Ghimire, H. M. Altmann, A. C. Straub, J. S. Isenberg, Nitric oxide: what's new to NO? *Am J Physiol Cell Physiol* **312**, C254-c262 (2017).
7. S. Moncada, R. M. Palmer, E. A. Higgs, Nitric oxide: physiology, pathophysiology, and pharmacology. *Pharmacological Reviews* **43**, 109 (1991).
8. T. Okuno, T. Yokomizo, T. Hori, M. Miyano, T. Shimizu, Leukotriene B4 receptor and the function of its helix 8. *J Biol Chem* **280**, 32049-32052 (2005).
9. T. R. Arnett, I. R. Orriss, Metabolic properties of the osteoclast. *Bone* **115**, 25-30 (2018).
10. M. Hukkanen *et al.*, Cytokine-stimulated expression of inducible nitric oxide synthase by mouse, rat, and human osteoblast-like cells and its functional role in osteoblast metabolic activity. *Endocrinology* **136**, 5445-5453 (1995).
11. C. W. Löwik, P. H. Nibbering, M. van de Ruit, S. E. Papapoulos, Inducible production of nitric oxide in osteoblast-like cells and in fetal mouse bone explants is associated with suppression of osteoclastic bone resorption. *J Clin Invest* **93**, 1465-1472 (1994).
12. I. MacIntyre *et al.*, Osteoclastic inhibition: an action of nitric oxide not mediated by cyclic GMP. *Proc Natl Acad Sci U S A* **88**, 2936-2940 (1991).
13. N. Takahashi *et al.*, Osteoblastic cells are involved in osteoclast formation. *Endocrinology* **123**, 2600-2602 (1988).
14. J. K. Liao, W. S. Shin, W. Y. Lee, S. L. Clark, Oxidized low-density lipoprotein decreases the expression of endothelial nitric oxide synthase. *J Biol Chem* **270**, 319-324 (1995).
15. C. R. Lyons, G. J. Orloff, J. M. Cunningham, Molecular cloning and functional expression of an inducible nitric oxide synthase from a murine macrophage cell line. *J*

Biol Chem **267**, 6370-6374 (1992).

16. A. J. Celeste *et al.*, Isolation of the human gene for bone gla protein utilizing mouse and rat cDNA clones. *The EMBO journal* **5**, 1885-1890 (1986).
17. L. C. Green *et al.*, Analysis of nitrate, nitrite, and [15N]nitrate in biological fluids. *Analytical biochemistry* **126**, 131-138 (1982).
18. M. Noda *et al.*, cDNA cloning of alkaline phosphatase from rat osteosarcoma (ROS 17/2.8) cells. *J Bone Miner Res* **2**, 161-164 (1987).
19. M. Gowen, D. D. Wood, E. J. Ihrie, M. K. McGuire, R. G. Russell, An interleukin 1 like factor stimulates bone resorption in vitro. *Nature* **306**, 378-380 (1983).
20. D. R. Bertolini, G. E. Nedwin, T. S. Bringman, D. D. Smith, G. R. Mundy, Stimulation of bone resorption and inhibition of bone formation in vitro by human tumour necrosis factors. *Nature* **319**, 516-518 (1986).
21. C. M. Maragos *et al.*, Complexes of .NO with nucleophiles as agents for the controlled biological release of nitric oxide. Vasorelaxant effects. *J Med Chem* **34**, 3242-3247 (1991).
22. W. S. Shin *et al.*, Autocrine and paracrine effects of endothelium-derived relaxing factor on intracellular Ca2+ of endothelial cells and vascular smooth muscle cells. Identification by two-dimensional image analysis in coculture. *J Biol Chem* **267**, 20377-20382 (1992).
23. Y. Wang *et al.*, Contribution of sustained Ca^{2+} elevation for nitric oxide production in endothelial cells and subsequent modulation of Ca2+ transient in vascular smooth muscle cells in coculture. *J Biol Chem* **271**, 5647-5655 (1996).
24. J. A. Riancho *et al.*, Expression and functional role of nitric oxide synthase in osteoblast-like cells. *J Bone Miner Res* **10**, 439-446 (1995).
25. E. Bornefalk, S. Ljunghall, A. G. Johansson, K. Nilsson, O. Ljunggren, Interleukin-1 beta induces cyclic AMP formation in isolated human osteoblasts: a signalling mechanism that is not related to enhanced prostaglandin formation. *Bone and mineral* **27**, 97-107 (1994).
26. A. J. de Brum-Fernandes *et al.*, Expression of prostaglandin endoperoxide synthase-1 and prostaglandin endoperoxide synthase-2 in human osteoblasts. *Biochem Biophys Res Commun* **198**, 955-960 (1994).
27. J. S. Beckman, T. W. Beckman, J. Chen, P. A. Marshall, B. A. Freeman, Apparent hydroxyl radical production by peroxynitrite: implications for endothelial injury from nitric oxide and superoxide. *Proc Natl Acad Sci U S A* **87**, 1620-1624 (1990).
28. A. Inoue, Y. Hiruma, S. Hirose, A. Yamaguchi, H. Hagiwara, Reciprocal regulation by cyclic nucleotides of the differentiation of rat osteoblast-like cells and mineralization of nodules. *Biochem Biophys Res Commun* **215**, 1104-1110 (1995).

29. H. Hagiwara *et al.*, cGMP produced in response to ANP and CNP regulates proliferation and differentiation of osteoblastic cells. *Am J Physiol* **270**, C1311-1318 (1996).
30. J. Lian *et al.*, Structure of the rat osteocalcin gene and regulation of vitamin D-dependent expression. *Proc Natl Acad Sci U S A* **86**, 1143-1147 (1989).
31. G. S. Stein, J. B. Lian, *Molecular Mechanisms Mediating Developmental and Hormone Regulated Expression of Genes in Osteoblasts*. (Academic Press, New York, NY, ed. 1st, 1993).
32. H. Kawaguchi, C. C. Pilbeam, J. R. Harrison, L. G. Raisz, The role of prostaglandins in the regulation of bone metabolism. *Clin Orthop Relat Res* 36-46 (1995).
33. H. Ozawa *et al.*, Effect of a continuously applied compressive pressure on mouse osteoblast-like cells (MC3T3-E1) in vitro. *J Cell Physiol* **142**, 177-185 (1990).
34. B. Brüne, E. G. Lapetina, Activation of a cytosolic ADP-ribosyltransferase by nitric oxide-generating agents. *J Biol Chem* **264**, 8455-8458 (1989).
35. U. C. Garg, A. Hassid, Nitric oxide decreases cytosolic free calcium in Balb/c 3T3 fibroblasts by a cyclic GMP-independent mechanism. *J Biol Chem* **266**, 9-12 (1991).
36. D. C. Hooper *et al.*, Uric acid, a natural scavenger of peroxynitrite, in experimental allergic encephalomyelitis and multiple sclerosis. *Proc Natl Acad Sci U S A* **95**, 675-680 (1998).
37. H. Ischiropoulos, L. Zhu, J. S. Beckman, Peroxynitrite formation from macrophage-derived nitric oxide. *Arch Biochem Biophys* **298**, 446-451 (1992).
38. H. Hikiji *et al.*, Direct action of nitric oxide on osteoblastic differentiation. *FEBS letters* **410**, 238-242 (1997).
39. M. Weinreb, D. Shinar, G. A. Rodan, Different pattern of alkaline phosphatase, osteopontin, and osteocalcin expression in developing rat bone visualized by in situ hybridization. *J Bone Miner Res* **5**, 831-842 (1990).
40. C. S. Lader, A. M. Flanagan, Prostaglandin E2, interleukin 1alpha, and tumor necrosis factor-alpha increase human osteoclast formation and bone resorption in vitro. *Endocrinology* **139**, 3157-3164 (1998).
41. C. Szabó, B. Zingarelli, A. L. Salzman, Role of poly-ADP ribosyltransferase activation in the vascular contractile and energetic failure elicited by exogenous and endogenous nitric oxide and peroxynitrite. *Circ Res* **78**, 1051-1063 (1996).
42. H. Kawaguchi *et al.*, In vivo gene transfection of human endothelial cell nitric oxide synthase in cardiomyocytes causes apoptosis-like cell death. Identification using Sendai virus-coated liposomes. *Circulation* **95**, 2441-2447 (1997).
43. A. G. Estévez *et al.*, Examining apoptosis in cultured cells after exposure to nitric oxide and peroxynitrite. *Methods in enzymology* **301**, 393-402 (1999).

44. Y. W. Xie, M. S. Wolin, Role of nitric oxide and its interaction with superoxide in the suppression of cardiac muscle mitochondrial respiration. Involvement in response to hypoxia/reoxygenation. *Circulation* **94**, 2580-2586 (1996).
45. J. S. Beckmann *et al.*, Extensive nitration of protein tyrosines in human atherosclerosis detected by immunohistochemistry. *Biol Chem Hoppe Seyler* **375**, 81-88 (1994).
46. D. M. Evans, S. H. Ralston, Nitric oxide and bone. *J Bone Miner Res* **11**, 300-305 (1996).
47. H. MC, L. JA, *Local regulators of bone: IL-1, TNF, lymphotoxin, interferon 7, IL-8, IL-10, IL-4, the LIF/IL-6 family, and additional cytokines.*, Principles of Bone Biology (Academic Press, San Diego, CA, 1996).
48. D. B. Evans, M. Thavarajah, J. A. Kanis, Involvement of prostaglandin E2 in the inhibition of osteocalcin synthesis by human osteoblast-like cells in response to cytokines and systemic hormones. *Biochem Biophys Res Commun* **167**, 194-202 (1990).
49. R. S. Taichman, P. V. Hauschka, Effects of interleukin-1 beta and tumor necrosis factor-alpha on osteoblastic expression of osteocalcin and mineralized extracellular matrix in vitro. *Inflammation* **16**, 587-601 (1992).
50. R. S. Lewis, S. Tamir, S. R. Tannenbaum, W. M. Deen, Kinetic analysis of the fate of nitric oxide synthesized by macrophages in vitro. *J Biol Chem* **270**, 29350-29355 (1995).
51. H. Ischiropoulos *et al.*, Peroxynitrite-mediated tyrosine nitration catalyzed by superoxide dismutase. *Arch Biochem Biophys* **298**, 431-437 (1992).
52. C. R. White *et al.*, Superoxide and peroxynitrite in atherosclerosis. *Proc Natl Acad Sci U S A* **91**, 1044-1048 (1994).
53. J. J. Poderoso *et al.*, Nitric oxide regulates oxygen uptake and hydrogen peroxide release by the isolated beating rat heart. *Am J Physiol* **274**, C112-119 (1998).
54. P. D. Damoulis, P. V. Hauschka, Nitric oxide acts in conjunction with proinflammatory cytokines to promote cell death in osteoblasts. *J Bone Miner Res* **12**, 412-422 (1997).
55. Y. Hou, J. Wang, J. Ramirez, P. G. Wang, in *Methods in Enzymology.* (Academic Press, San Diego, CA, 1999), vol. 301, pp. 242-249.
56. S. W. Fox, T. J. Chambers, J. W. Chow, Nitric oxide is an early mediator of the increase in bone formation by mechanical stimulation. *Am J Physiol* **270**, E955-960 (1996).
57. C. Melchiorri *et al.*, Enhanced and coordinated in vivo expression of inflammatory cytokines and nitric oxide synthase by chondrocytes from patients with osteoarthritis. *Arthritis Rheum* **41**, 2165-2174 (1998).
58. A. W. Ford-Hutchinson, M. A. Bray, M. V. Doig, M. E. Shipley, M. J. Smith, Leukotriene B, a potent chemokinetic and aggregating substance released from polymorphonuclear leukocytes. *Nature* **286**, 264-265 (1980).

59. B. Samuelsson, S. E. Dahlén, J. A. Lindgren, C. A. Rouzer, C. N. Serhan, Leukotrienes and lipoxins: structures, biosynthesis, and biological effects. *Science (New York, N.Y.)* **237**, 1171-1176 (1987).
60. T. Yokomizo, T. Izumi, K. Chang, Y. Takuwa, T. Shimizu, A G-protein-coupled receptor for leukotriene B4 that mediates chemotaxis. *Nature* **387**, 620-624 (1997).
61. T. Yokomizo, K. Kato, K. Terawaki, T. Izumi, T. Shimizu, A second leukotriene B(4) receptor, BLT2. A new therapeutic target in inflammation and immunological disorders. *The J Exp Med* **192**, 421-432 (2000).
62. T. Yokomizo, T. Izumi, T. Shimizu, Leukotriene B4: metabolism and signal transduction. *Arch Biochem Biophys* **385**, 231-241 (2001).
63. T. Yokomizo, K. Kato, H. Hagiya, T. Izumi, T. Shimizu, Hydroxyeicosanoids bind to and activate the low affinity leukotriene B4 receptor, BLT2. *J Biol Chem* **276**, 12454-12459 (2001).
64. T. Okuno *et al.*, 12(S)-Hydroxyheptadeca-5Z, 8E, 10E-trienoic acid is a natural ligand for leukotriene B4 receptor 2. *Journal Exp Med* **205**, 759-766 (2008).
65. L. Iversen, K. Kragballe, V. A. Ziboh, Significance of leukotriene-A4 hydrolase in the pathogenesis of psoriasis. *Skin pharmacol : the official journal of the Skin Pharmacology Society* **10**, 169-177 (1997).
66. Z. Csoma *et al.*, Increased leukotrienes in exhaled breath condensate in childhood asthma. *Am J Respir Crit Care Me*d **166**, 1345-1349 (2002).
67. A. T. Cole *et al.*, Mucosal factors inducing neutrophil movement in ulcerative colitis: the role of interleukin 8 and leukotriene B4. *Gut* **39**, 248-254 (1996).
68. B. J. Zimmerman, D. J. Guillory, M. B. Grisham, T. S. Gaginella, D. N. Granger, Role of leukotriene B4 in granulocyte infiltration into the postischemic feline intestine. *Gastroenterol* **99**, 1358-1363 (1990).
69. L. B. Klickstein, C. Shapleigh, E. J. Goetzl, Lipoxygenation of arachidonic acid as a source of polymorphonuclear leukocyte chemotactic factors in synovial fluid and tissue in rheumatoid arthritis and spondyloarthritis. *J Clin Invest* **66**, 1166-1170 (1980).
70. E. M. Davidson, S. A. Rae, M. J. Smith, Leukotriene B4, a mediator of inflammation present in synovial fluid in rheumatoid arthritis. *Ann Rheum Dis* **42**, 677-679 (1983).
71. N. Ahmadzadeh, M. Shingu, M. Nobunaga, T. Tawara, Relationship between leukotriene B4 and immunological parameters in rheumatoid synovial fluids. *Inflammation* **15**, 497-503 (1991).
72. R. J. Griffiths *et al.*, Leukotriene B4 plays a critical role in the progression of collagen-induced arthritis. *Proc Natl Acad Sci U S A* **92**, 517-521 (1995).
73. H. Yasuda *et al.*, A novel molecular mechanism modulating osteoclast differentiation and

function. *Bone* **25**, 109-113 (1999).

74. T. Suda, Y. Ueno, K. Fujii, T. Shinki, Vitamin D and bone. *J Cell Biochem* **88**, 259-266 (2003).

75. S. Meghji, J. R. Sandy, A. M. Scutt, W. Harvey, M. Harris, Stimulation of bone resorption by lipoxygenase metabolites of arachidonic acid. *Prostaglandins* **36**, 139-149 (1988).

76. C. Garcia *et al.*, Leukotriene B4 stimulates osteoclastic bone resorption both in vitro and in vivo. *J Bone Miner Res* **11**, 1619-1627 (1996).

77. J. B. Smith, M. K. Haynes, Rheumatoid arthritis--a molecular understanding. *Ann Intern Med* **136**, 908-922 (2002).

78. N. D. Kim, R. C. Chou, E. Seung, A. M. Tager, A. D. Luster, A unique requirement for the leukotriene B4 receptor BLT1 for neutrophil recruitment in inflammatory arthritis. *J Exp Med* **203**, 829-835 (2006).

79. W. H. Shao, A. Del Prete, C. B. Bock, B. Haribabu, Targeted disruption of leukotriene B4 receptors BLT1 and BLT2: a critical role for BLT1 in collagen-induced arthritis in mice. *J Immunol* **176**, 6254-6261 (2006).

80. M. Hegen *et al.*, Cytosolic phospholipase A2alpha-deficient mice are resistant to collagen-induced arthritis. *J Exp Med* **197**, 1297-1302 (2003).

81. M. Chen *et al.*, Neutrophil-derived leukotriene B4 is required for inflammatory arthritis. *J Exp Med* **203**, 837-842 (2006).

82. H. J. Showell, R. Breslow, M. J. Conklyn, G. P. Hingorani, K. Koch, Characterization of the pharmacological profile of the potent LTB4 antagonist CP-105,696 on murine LTB4 receptors in vitro. *Br J Pharmacol* **117**, 1127-1132 (1996).

83. K. Terawaki *et al.*, Absence of leukotriene B4 receptor 1 confers resistance to airway hyperresponsiveness and Th2-type immune responses. *J Immunol* **175**, 4217-4225 (2005).

84. R. J. Sells Galvin, C. L. Gatlin, J. W. Horn, T. R. Fuson, TGF-beta enhances osteoclast differentiation in hematopoietic cell cultures stimulated with RANKL and M-CSF. *Biochem Biophys Res Commun* **265**, 233-239 (1999).

85. Y. Okada *et al.*, Prostaglandin G/H synthase-2 is required for maximal formation of osteoclast-like cells in culture. *J Clin Invest* **105**, 823-832 (2000).

86. Y. Iizuka *et al.*, Characterization of a mouse second leukotriene B4 receptor, mBLT2: BLT2-dependent ERK activation and cell migration of primary mouse keratinocytes. *J Biol Chem* **280**, 24816-24823 (2005).

87. A. R. Villanueva, L. Ilnicki, H. M. Frost, R. Arnstein, Measurement of the bone formation rate in a case of familial hypophosphatemic vitamin D-resistant rickets. *J Lab*

Clin Med **67**, 973-982 (1966).

88. H. M. Frost, Preparation of thin undecalcified bone sections by rapid manual method. *Stain technol* **33**, 273-277 (1958).
89. D. Rickard, A. Harris, R. Turner, S. Khosla, T. C. Spelsberg, in *Principals of Bone Biology,* J. P. Bilesikian, L. G. Raisz, G. A. Rodan, Eds. (Academic Press, San Diego, CA, 2002), vol. 2, pp. 655-676.
90. H. Takayanagi *et al.*, T-cell-mediated regulation of osteoclastogenesis by signalling cross-talk between RANKL and IFN-gamma. *Nature* **408**, 600-605 (2000).
91. L. Li, A. Khansari, L. Shapira, D. T. Graves, S. Amar, Contribution of interleukin-11 and prostaglandin(s) in lipopolysaccharide-induced bone resorption in vivo. *Infect Immun* **70**, 3915-3922 (2002).
92. C. Miyaura *et al.*, An essential role of cytosolic phospholipase A2alpha in prostaglandin E2-mediated bone resorption associated with inflammation. *J Exp Med* **197**, 1303-1310 (2003).
93. N. Tapon, A. Hall, Rho, Rac and Cdc42 GTPases regulate the organization of the actin cytoskeleton. *Curr Opin Cell Biol* **9**, 86-92 (1997).
94. V. Kölsch, P. G. Charest, R. A. Firtel, The regulation of cell motility and chemotaxis by phospholipid signaling. *J Cell Sci* **121**, 551-559 (2008).
95. K. Väänanen, H. Zhao, in *Principals of Bone Biology,* J. P. Bilesikian, L. G. Raisz, G. A. Rodan, Eds. (Academic Press, San Diego, CA, 2002), vol. 1, chap. 127-140.
96. H. K. Väänänen, H. Zhao, in *Principals of Bone Biology,* J. P. Bilesikian, L. G. Raisz, T. J. Martin, Eds. (Academic Press, San Diego, 2008), vol. 1, pp. 193-210.
97. L. T. Duong, A. Sanjay, W. Home, R. Baron, G. A. Rodan, in *Principals of Bone Biology,* J. P. Bilesikian, L. G. Raisz, G. A. Rodan, Eds. (Academic Press, San Diego, CA, 2002), vol. 1, pp. 141-150.
98. R. Pacifici *et al.*, Spontaneous release of interleukin 1 from human blood monocytes reflects bone formation in idiopathic osteoporosis. *Proc Natl Acad Sci U S A* **84**, 4616-4620 (1987).
99. R. Pacifici *et al.*, Effect of surgical menopause and estrogen replacement on cytokine release from human blood mononuclear cells. *Proc Natl Acad Sci U S A* **88**, 5134-5138 (1991).
100. R. T. Turner, B. L. Riggs, T. C. Spelsberg, Skeletal effects of estrogen. *Endocr Rev* **15**, 275-300 (1994).
101. J. Ciampolini, K. G. Harding, Pathophysiology of chronic bacterial osteomyelitis. Why do antibiotics fail so often? *Postgrad Med J* **76**, 479-483 (2000).
102. L. Duplomb, M. Dagouassat, P. Jourdon, D. Heymann, Concise review: embryonic stem

cells: a new tool to study osteoblast and osteoclast differentiation. *Stem cells (Dayton, Ohio)* **25**, 544-552 (2007).

103. H. Hikiji, S. Ishii, H. Shindou, T. Takato, T. Shimizu, Absence of platelet-activating factor receptor protects mice from osteoporosis following ovariectomy. *J Clin Invest* **114**, 85-93 (2004).

104. N. Uozumi *et al.*, Role of cytosolic phospholipase A2 in allergic response and parturition. *Nature* **390**, 618-622 (1997).

105. G. Camussi, C. Tetta, F. Bussolino, C. Baglioni, Tumor necrosis factor stimulates human neutrophils to release leukotriene B4 and platelet-activating factor. Induction of phospholipase A2 and acetyl-CoA:1-alkyl-sn-glycero-3-phosphocholine O2-acetyltransferase activity and inhibition by antiproteinase. *Europ J Biochem* **182**, 661-666 (1989).

106. P. Conti *et al.*, The combination of interleukin 1 plus tumor necrosis factor causes greater generation of LTB4, thromboxanes and aggregation on human macrophages than these compounds alone. *Prog Cinic Biol Res* **301**, 541-545 (1989).

107. M. E. Surette, N. Dallaire, N. Jean, S. Picard, P. Borgeat, Mechanisms of the priming effect of lipopolysaccharides on the biosynthesis of leukotriene B4 in chemotactic peptide-stimulated human neutrophils. *Faseb J* **12**, 1521-1531 (1998).

108. J. A. Rankin, I. Sylvester, S. Smith, T. Yoshimura, E. J. Leonard, Macrophages cultured in vitro release leukotriene B4 and neutrophil attractant/activation protein (interleukin 8) sequentially in response to stimulation with lipopolysaccharide and zymosan. *J Clin Invest* **86**, 1556-1564 (1990).

109. A. Fukuda *et al.*, Regulation of osteoclast apoptosis and motility by small GTPase binding protein Rac1. *J Bone Miner Res* **20**, 2245-2253 (2005).

110. N. Ishida *et al.*, CCR1 acts downstream of NFAT2 in osteoclastogenesis and enhances cell migration. *J Bone Miner Res* **21**, 48-57 (2006).

111. Y. Wang *et al.*, Identifying the relative contributions of Rac1 and Rac2 to osteoclastogenesis. *J Bone Miner Res* **23**, 260-270 (2008).

112. M. Yagi *et al.*, DC-STAMP is essential for cell-cell fusion in osteoclasts and foreign body giant cells. *J Expb Med* **202**, 345-351 (2005).

113. A. Sanjay *et al.*, Cbl associates with Pyk2 and Src to regulate Src kinase activity, alpha(v)beta(3) integrin-mediated signaling, cell adhesion, and osteoclast motility. *J Cell Biol* **152**, 181-195 (2001).

114. S. L. Teitelbaum, Bone resorption by osteoclasts. *Science (New York, N.Y.)* **289**, 1504-1508 (2000).

115. C. N. Serhan *et al.*, Reduced inflammation and tissue damage in transgenic rabbits

overexpressing 15-lipoxygenase and endogenous anti-inflammatory lipid mediators. *J Immunol* **171**, 6856-6865 (2003).

116. H. Hasturk *et al.*, Resolvin E1 regulates inflammation at the cellular and tissue level and restores tissue homeostasis in vivo. *J Immunol* **179**, 7021-7029 (2007).
117. B. S. Herrera *et al.*, An endogenous regulator of inflammation, resolvin E1, modulates osteoclast differentiation and bone resorption. *Br J Pharmacol* **155**, 1214-1223 (2008).
118. C. MacLean *et al.*, Systematic review: comparative effectiveness of treatments to prevent fractures in men and women with low bone density or osteoporosis. *Ann Intern Med* **148**, 197-213 (2008).
119. K. Henriksen, J. Bollerslev, V. Everts, M. A. Karsdal, Osteoclast activity and subtypes as a function of physiology and pathology--implications for future treatments of osteoporosis. *Endocr Rev* **32**, 31-63 (2011).
120. R. Baron, L. Neff, D. Louvard, P. J. Courtoy, Cell-mediated extracellular acidification and bone resorption: evidence for a low pH in resorbing lacunae and localization of a 100-kD lysosomal membrane protein at the osteoclast ruffled border. *J Cell Biol* **101**, 2210-2222 (1985).
121. J. A. Wemmie, M. P. Price, M. J. Welsh, Acid-sensing ion channels: advances, questions and therapeutic opportunities. *Trends Neurosci* **29**, 578-586 (2006).
122. K. Seuwen, M. G. Ludwig, R. M. Wolf, Receptors for protons or lipid messengers or both? *J Recept Signal Transduct Res* **26**, 599-610 (2006).
123. M. G. Ludwig *et al.*, Proton-sensing G-protein-coupled receptors. *Nature* **425**, 93-98 (2003).
124. N. Murakami, T. Yokomizo, T. Okuno, T. Shimizu, G2A is a proton-sensing G-protein-coupled receptor antagonized by lysophosphatidylcholine. *J Biol Chem* **279**, 42484-42491 (2004).
125. S. Ishii, Y. Kihara, T. Shimizu, Identification of T cell death-associated gene 8 (TDAG8) as a novel acid sensing G-protein-coupled receptor. *J Biol Chem* **280**, 9083-9087 (2005).
126. J. Q. Wang *et al.*, TDAG8 is a proton-sensing and psychosine-sensitive G-protein-coupled receptor. *J Biol Chem* **279**, 45626-45633 (2004).
127. D. S. Im, C. E. Heise, T. Nguyen, B. F. O'Dowd, K. R. Lynch, Identification of a molecular target of psychosine and its role in globoid cell formation. *J Cell Biol* **153**, 429-434 (2001).
128. C. Mogi *et al.*, Involvement of proton-sensing TDAG8 in extracellular acidification-induced inhibition of proinflammatory cytokine production in peritoneal macrophages. *J Immunol* **182**, 3243-3251 (2009).
129. Y. Ihara *et al.*, The G protein-coupled receptor T-cell death-associated gene 8 (TDAG8)

facilitates tumor development by serving as an extracellular pH sensor. *Proc Natl Acad Sci U S A* **107**, 17309-17314 (2010).

130. R. Turner, D. Rickard, U. T. Iwaniec, T. C. Spelsberg, in *Principals of Bone Biology,* J. P. Bilesikian, L. G. Raisz, T. J. Martin, Eds. (Academic Press, San Diego, 2008), vol. 1, pp. 855-886.
131. K. Horie *et al.*, Characterization of Sleeping Beauty transposition and its application to genetic screening in mice. *Mol Cell Biol* **23**, 9189-9207 (2003).
132. C. G. Radu *et al.*, Normal immune development and glucocorticoid-induced thymocyte apoptosis in mice deficient for the T-cell death-associated gene 8 receptor. *Mol Cell Biol* **26**, 668-677 (2006).
133. N. Tosa *et al.*, Critical function of T cell death-associated gene 8 in glucocorticoid-induced thymocyte apoptosis. *Int Immunol* **15**, 741-749 (2003).
134. W. C. Horne, L. T. Duong, A. Sanjay, R. Baron, in *Principals of Bone Biology,* J. P. Bilesikian, L. G. Raisz, T. J. Martin, Eds. (Academic Press, San Diego, 2008), vol. 1, pp. 221-236.
135. H. Niwa, K. Yamamura, J. Miyazaki, Efficient selection for high-expression transfectants with a novel eukaryotic vector. *Gene* **108**, 193-199 (1991).
136. A. Bruzzaniti *et al.*, Dynamin forms a Src kinase-sensitive complex with Cbl and regulates podosomes and osteoclast activity. *Mol Biol Cell* **16**, 3301-3313 (2005).
137. A. J. Ridley, A. Hall, The small GTP-binding protein rho regulates the assembly of focal adhesions and actin stress fibers in response to growth factors. *Cell* **70**, 389-399 (1992).
138. M. A. Chellaiah *et al.*, Rho-A is critical for osteoclast podosome organization, motility, and bone resorption. *J Biol Chem* **275**, 11993-12002 (2000).
139. M. Uehata *et al.*, Calcium sensitization of smooth muscle mediated by a Rho-associated protein kinase in hypertension. *Nature* **389**, 990-994 (1997).
140. M. K. Osako *et al.*, Estrogen inhibits vascular calcification via vascular RANKL system: common mechanism of osteoporosis and vascular calcification. *Circ Res* **107**, 466-475 (2010).
141. H. Feng *et al.*, Myocyte enhancer factor 2 and microphthalmia-associated transcription factor cooperate with NFATc1 to transactivate the V-ATPase d2 promoter during RANKL-induced osteoclastogenesis. *J Biol Chem* **284**, 14667-14676 (2009).
142. D. Q. Yang *et al.*, V-ATPase subunit ATP6AP1 (Ac45) regulates osteoclast differentiation, extracellular acidification, lysosomal trafficking, and protease exocytosis in osteoclast-mediated bone resorption. *J Bone Miner Res* **27**, 1695-1707 (2012).
143. K. Iwai *et al.*, RGS18 acts as a negative regulator of osteoclastogenesis by modulating the acid-sensing OGR1/NFAT signaling pathway. *J* Bone *Miner Res* **22**, 1612-1620 (2007).

144. A. Pereverzev *et al.*, Extracellular acidification enhances osteoclast survival through an NFAT-independent, protein kinase C-dependent pathway. *Bone* **42**, 150-161 (2008).
145. M. Yang *et al.*, Expression of and role for ovarian cancer G-protein-coupled receptor 1 (OGR1) during osteoclastogenesis. *J Biol Chem* **281**, 23598-23605 (2006).
146. M. Chellaiah *et al.*, Gelsolin deficiency blocks podosome assembly and produces increased bone mass and strength. *J Cell Biol* **148**, 665-678 (2000).
147. S. Linder, P. Kopp, Podosomes at a glance. *J Cell Sci* **118**, 2079-2082 (2005).
148. B. Zhao, TNF and Bone Remodeling. *Current osteoporosis reports* **15**, 126-134 (2017).